Investigation of Lamb Wave Propagation in Pre-stressed Plates with Applications to Structural Health Monitoring

By

Munawwar Mohabuth

B.Eng. (Mechanical)

A thesis submitted for the degree of Doctor of Philosophy at the

School of Mechanical Engineering

The University of Adelaide

Australia

Submitted: 17th December 2018

Accepted: 19th February 2019

Abstract

The evaluation of applied, residual and thermally-induced stresses, along with the non-destructive detection of damage, plays a critical role in the assessment of the integrity and residual life of engineering structures. There is currently a growing demand from many industries to develop and incorporate on-line stress monitoring capabilities into existing as well as future Structural Health Monitoring (SHM) systems. These capabilities would allow for a significant improvement to failure risk management and life forecasting, which currently largely rely on stress values obtained at the design or testing stage. It is also very attractive from cost considerations to share the same network of sensors for both damage detection and stress evaluation. Guided wave based techniques are among the most promising options to meet these demands and expectations. Although SHM systems utilising guided waves are already in operation in a number of applications, the design, integration and implementation of in situ stress monitoring techniques are still under development.

The overall aim of this thesis is to develop a better understanding of the phenomena associated with the propagation of Lamb waves in pre-stressed plates. Such an understanding is of paramount importance in the development of in situ stress monitoring procedures based on Lamb waves and the operation of existing and future guided wave based SHM systems. The specific objectives of this thesis include the extension of the classical theory of acoustoelasticity to guided waves propagating in pre-stressed plates, the development of a new experimental procedure for the evaluation of third-order elastic constants and the analysis of the residual noise due to the effect of applied or thermally-induced stress after baseline signal subtraction. In particular, it was demonstrated that this residual noise is not negligible and has a similar impact on the operation of SHM systems as ambient temperature variations.

The main body of this thesis is comprised of a combination of ‘published’ and ‘accepted for publication’ journal articles. These articles are united by the same framework, the theory of acoustoelasticity, which is applied to a range of problems, each representing a separate chapter of this thesis (Chapters 3 - 6). In

addition, Chapter 1 provides brief introduction to the research area, along with a broad literature review which is not intended to duplicate the specific literature reviews incorporated as part of the journal articles. Chapter 2 presents the mathematical background, including the basic equations of nonlinear elasticity, relevant to the theoretical developments in Chapters 3 – 6. The thesis is concluded with Chapter 7 which summarises the main outcomes of the research undertaken and outlines the future work. The main outcomes of the thesis include the development of: (1) a new analytical model to study the propagation of Lamb waves in pre-stressed compressible plates, (2) a new approach to analyse the effect of a large pre-deformation on the propagation of Lamb waves in incompressible plates, (3) a new analytical model to estimate the effect of stress induced variations on damage detection with Lamb waves, and (4) a new method to evaluate third-order elastic constants utilising Rayleigh waves.

Declaration

I certify that this work contains no material which has been accepted for the award of any other degree or diploma in my name, in any university or other tertiary institution and, to the best of my knowledge and belief, contains no material previously published or written by another person, except where due reference has been made in the text. In addition, I certify that no part of this work will, in the future, be used in a submission in my name, for any other degree or diploma in any university or other tertiary institution without the prior approval of the University of Adelaide and where applicable, any partner institution responsible for the joint-award of this degree.

I acknowledge that copyright of published works contained within this thesis resides with the copyright holder(s) of those works. I also give permission for the digital version of my thesis to be made available on the web, via the University's digital research repository, the Library Search and also through web search engines, unless permission has been granted by the University to restrict access for a period of time. I acknowledge the support I have received for my research through the provision of an Australian Government Research Training Program Scholarship.

15th May 2019

Munawwar Mohabuth — Date

Acknowledgements

First and foremost, I would like to express my sincere gratitude to my principal supervisor, Prof. Andrei Kotousov, for his mentorship and continuous support during the course of my candidature. His passion, ambition and work ethic have been a strong source of inspiration to me.

I would also like to thank my co-supervisor, A/Prof. Ching-Tai (Alex) Ng, for his technical advice and support. A very special thank you goes to Dr. Aditya Khanna for his invaluable contributions and friendship. I would also like to thank my fellow colleagues, James Hughes and James Vidler, for their assistance and encouragement.

I would like to acknowledge the financial support provided by the university through the provision of an Australian Government Research Training Program Scholarship. I am also very grateful to the School of Mechanical Engineering for the additional financial support in the form of casual tutoring and lecturing positions.

Last but not least, I would like to thank my family for their continued support and encouragement. This journey would not have been possible without them.

List of Publications

This thesis consists of a combination of 'published' and 'accepted for publication' journal articles in accordance with the Academic Program Rules 2018 of The University of Adelaide. A complete list of articles authored by the candidate is presented here.

The main body of this thesis is based on the following journal articles:

(i) **M. Mohabuth**, A. Kotousov and C.T. Ng (2016), Effect of uniaxial stress on the propagation of higher-order Lamb wave modes, *Int. J. Non-Linear Mech.*, 86, 104-11, doi: 10.1016/j.ijnonlinmec.2016.08.006.

(ii) **M. Mohabuth**, A. Kotousov and C.T. Ng (2019), Large acoustoelastic effect for Lamb waves propagating in an incompressible elastic plate, *J. Acoust. Soc. Am.*, 145, 1221-1229, doi: 10.1121/1.5092604.

(iii) **M. Mohabuth**, A. Kotousov, C.T. Ng and L.R.F. Rose (2018), Implication of changing loading conditions on structural health monitoring utilising guided waves, *Smart Mater. Struct.*, 27, 1-12, doi: 10.1088/1361-665X/aa9f89.

(iv) **M. Mohabuth**, A. Khanna, J. Hughes, J. Vidler, A. Kotousov and C.T. Ng (2018), On the determination of the third-order elastic constants of homogeneous isotropic materials utilising Rayleigh waves, *Ultrasonics*, article in press, doi: 10.1016/j.ultras.2019.02.006.

The following journal articles and refereed conference papers are of close relevance to the main research topic but are not included as part of this thesis:

(v) **M. Mohabuth**, A. Kotousov and C.T. Ng (2015), Lamb waves in plates subjected to uniaxial stresses, Proceedings of the 17th International Conference on Applied Mechanics and Mechanical Engineering (ICAMME 2015), 13-14 July 2015, Stockholm, Sweden.

(vi) C.T. Ng, **M. Mohabuth** and A. Kotousov (2016), Analysis of stress effect on Lamb wave propagation in isotropic plates, Proceedings of the 24th Australasian Conference on the Mechanics of Structures and Materials (ACMSM24), 6-9 December 2016, Perth, Australia.

(vii) J.M. Hughes, J. Howie, J. Vidler and **M. Mohabuth** (2017), Stress monitoring using the change in velocity of Rayleigh waves, Proceedings of the 9th Australasian Congress on Applied Mechanics (ACAM 9), 27-29 November 2017, Sydney, Australia.

(viii) **M. Mohabuth**, A. Kotousov, A., C.T. Ng and L.R.F. Rose (2017), Effect of changing stress on damage diagnostic with guided waves, Proceedings of the 8th International Conference on Structural Health Monitoring of Intelligent Infrastructure (SHMII-8), 5-8 December, Brisbane, Australia.

(ix) J.M. Hughes, J. Vidler, C.T. Ng, A. Khanna, **M. Mohabuth**, L.R.F. Rose and A. Kotousov (2018), Comparative evaluation of in situ stress monitoring with Rayleigh waves, *Struc. Health Monit.*, 1-11, doi: 10.1177/1475921718798146.

The remaining articles written by the candidate are not directly related to the main topic of the thesis. These are listed below for the sake of completeness:

(x) **M. Mohabuth**, D. Chang and A. Khanna, Experimental study on local plastic collapse in a plate weakened by two collinear cracks, Proceedings of the 4th International Conference on Advances in Mechanics Engineering (ICAME 2015), 20-21 July 2015, Madrid, Spain, doi: 10.1051/matecconf/20152801002.

(xi) J.M. Hughes, J. Howie, J. Vidler and **M. Mohabuth** (2017), Non-contact measurement of nonlinear Rayleigh waves using the scanning laser vibrometer, Proceedings of the 9th Australasian Congress on Applied Mechanics (ACAM 9), 27-29 November 2017, Sydney, Australia.

(xii) A. Khanna, A. Kotousov, **M. Mohabuth** and S. Bun (2018), Three-dimensional analysis of an edge crack in a plate of finite thickness with the first-order plate theory, *Theor. Appl. Fract. Mech.*, 95, 155-163, doi: 10.1016/j.tafmec.2018.02.017.

Table of Contents

Chapter 1

Introduction

Chapter 1

Introduction

This chapter provides a brief introduction to the research area and discusses the motivation behind the current study. A broad review of literature is also presented as part of this chapter. The review is not intended to duplicate the introduction, background and literature review sections of the journal articles, which form the main body of this thesis, Chapters 3 - 6. The current review presents the past studies from a historical perspective without much technical details, which will be discussed in the next chapter. The overall aim and specific objectives of the current study are formulated after the literature review, along with an outline of the structure of the thesis.

1.1 Background and Motivation

The study of small wave motions in solids subjected to stresses is of interest in a number of fields, including engineering, science and medicine. Indeed, residual and applied stresses are ubiquitous in structural components as well as in natural or biological systems (Destrade and Ogden, 2012). Elastic waves may be utilised to evaluate the residual stress fields and mechanical properties of different types of materials, such as geo-materials and soft tissues (in fact, this is the only way to evaluate the properties of living tissues in vivo) (Ensminger and Bond, 2011; Cheeke, 2012). Elastic waves guided by boundaries, or the so-called guided waves, are now widely utilised to detect structural defects and damage (Mitra and Gopalakrishnan, 2016; Raghavan and Cesnik, 2007). Therefore, an understanding of the mathematics and mechanics of wave propagation in pre-stressed solids is of paramount importance in many research areas and practical applications.

This thesis is focused on the investigation of Lamb waves, which are a particular type of elastic guided waves propagating in flat plates (Rose, 2014). Plate components represent one of the most common structural elements in

mechanical and civil engineering. The overall aim of the present study is to develop a better understanding of the effect of stress on Lamb wave propagation in order to facilitate the development of experimental techniques and practical methods for the detection of structural defects and the evaluation of applied, residual or thermally-induced stresses in situ, which is an integral part of the Structural Health Monitoring (SHM) field (Farrar and Worden, 2007).

The derived theoretical solutions, and the experimental and computational results presented in this thesis are all obtained within the framework of the theory of acoustoelasticity (Pao et al., 1984; Kim and Sachse, 2001). It is well-known that if both the pre-deformation (pre-stress) and the wave amplitude are of infinitesimal magnitudes, then the governing equations can be linearised, such that the corresponding problems can be relatively easily treated using a range of analytical approaches. When the wave amplitude is large, the governing equations become highly non-linear, and their resolution for non-trivial problems is extremely difficult (Bland, 1969; Norris, 1998; Saccomandi, 2007). The acoustoelastic theory lies between these two limiting situations. This theory, which is also known as the "theory of small-on-large", considers the propagation of small amplitude elastic waves in infinite media and in waveguides subjected to a finite deformation (Norris, 2007). In this way, the term acoustoelasticity essentially refers the interplay between the static deformation of a solid body and the wave motion.

1.2 Literature Review

1.2.1 Acoustoelasticity: Historical Perspective

An elastic wave propagating in a stressed solid has a different wave speed as compared to a wave propagating in the same solid in a stress free state. The wave speed depends on the type of wave, stress magnitude and direction of wave propagation with respect to the applied stress (Toupin and Bernstein, 1961). The change in the wave speed from the unstressed state is, however, very small. For example, in metals the change is typically of the order of 10^{-5} m/s per 1 MPa of the applied or residual stress (Pao and Gamer, 1985). These experimentally

observed phenomena largely motivated the development of the acoustoelastic theory in the mid-twentieth century as the classical linear theory of elasticity, which is based on the concept of infinitesimal deformations, cannot describe the change in the wave speed with applied stress (Bergman and Shahbender, 1958; Smith, 1963; Crecraft, 1962) or the change in compressibility with pressure (Bridgman, 1929a, 1929b; Birch, 1937). The linear theory postulates that the deformations are functions of the stress and temperature only and as a result, the wave speed is independent of the applied stress or pre-deformation (Achenbach, 1984; Spencer, 2004).

Many attempts have been made to develop a general theory, which does not rely on the assumption of infinitesimally small deformations and is capable of describing the change in the wave speed with applied stress. Léon Brillouin was the first to derive the governing equations of such a theory in an invariant (tensorial) form (Brillouin, 1925). He found that hydrostatic pressure (or hydrostatic stress) causes a decrease in the wave speeds of both the longitudinal and shear waves. Brillouin's theory eventually led to the conclusion that at sufficiently high pressures the wave speeds should reduce to zero. It was later demonstrated that his paradoxical results were due to incorrect assumptions (Tang, 1967).

Cauchy (1829) and Love (1926) were among the first researchers to have made significant contributions towards the development of the theory of wave motions in the presence of a finite deformation. In particular, Love derived the correct wave equations in the case of an incompressible material subjected to hydrostatic pressure. These equations were shown to be a particular case of the more general theory developed later by Murnaghan (1951).

In 1937, Murnaghan developed the finite deformation theory and incorporated the so-called third-order elastic constants, which he denoted as l, m and n, into the governing equations to describe the nonlinear stress-strain behaviour. A year later, in 1938, F. Birch demonstrated that the experimentally observed change in the wave speed with an applied hydrostatic pressure can be

accurately described by Murnaghan's theory, and the hydrostatic pressure itself has no effect on the wave propagation.

In 1940, Biot derived the governing equations for solids subjected to initial stresses. These equations found immediate applications in problems related to geo-mechanics. For example, the theoretically predicted coupling between different wave modes in the presence of an initial pressure gradient, which was also suspected by Love (1926), was shown to be quite significant for tidal waves or the modes of oscillation of the Earth.

In 1953, Hughes and Kelly conducted pioneering experimental measurements of the longitudinal and shear wave speeds under hydrostatic pressure as well as under pure compression in order to evaluate the values of the third-order elastic constants l, m and n for different materials, including Polystyrene, Armco Iron and Pyrex. They demonstrated that the second-order elastic constants change linearly with the applied stress and this change could be described by the third-order elastic constants. They also noted that the third-order constants appeared to be negative, as suggested by Brillouin (1946) and an order of magnitude larger than the second-order constants. This fundamental work has since become the commonly accepted framework for the analysis of wave motions in pre-stressed solids and is now referred to as the theory of acoustoelasticity.

The acoustoelastic theory involves two departures from the classical linear elastic (or infinitesimal) theory. First, since the deformations are considered to be finite, the final coordinates of a point are not interchangeable with the original coordinates and second, the relationship between the stress and strain components is not linear anymore. Because the initial and final coordinates are not interchangeable, either may be taken as the independent variables (Hughes and Kelly, 1953). The initial coordinates are called Lagrangian coordinates and the final coordinates are called Eulerian coordinates. The acoustoelastic theory was formulated in both coordinate systems by Brillouin (1946) and Murnaghan (1937, 1951) but later Murnaghan only used the Lagrangian coordinates.

The classical (second-order) elastic constants, such as the Lamé constants λ and μ, can be considered as a first-order approximation of the stress-strain relationship of real materials. The physical basis for third- as well as higher-order elastic constants is that the force-displacement dependence between atoms does not follow a linear behaviour. The dependence is much more complicated, and it can be described by microscopic theories, which incorporate anharmonic terms in the interatomic potential (Hiki, 1981; Landau and Liftshitz, 1986). From a mathematical point of view, the third-order elastic constants represent a second-order expansion of the actual stress-strain relationship. For an isotropic material, there are three independent third-order elastic constants in addition to the two second-order elastic constants (Destrade and Ogden, 2013). Several definitions and notations for the third-order constants have been introduced by different researchers: Murnaghan (1937, 1951), Biot (1940, 1965), Bland (1969), Eringen and Suhubi (1974) and Landau and Lifshitz (1986). The relationships between these different definitions and notations can be found in many textbooks (see, for example, Norris, 1998).

It was not until the early 1970s that researchers and engineers began to realise the potential of the acoustoelastic theory for practical applications, in particular for the measurement of residual and applied stresses in structures subjected to a homogeneous stress state, e.g. rails, pipelines or wires. Several experimental techniques for the evaluation of applied or residual stresses were hence developed, specifically for relatively short wavelengths or ultrasonic frequencies in the MHz range (Crecraft, 1967, 1968; Smith et al., 1966; Egle and Bray, 1976). This frequency range allows a good spatial resolution to be achieved; however, a further increase of the wave frequency leads to a significant attenuation of the signal due to the interaction of the elastic waves with surface asperities and material texture (Rose, 2014). Ultrasonic bulk waves and the acoustoelastic effect have been successfully used over the past sixty years in the measurement and control of residual stresses in welded structures and railroad rails, the tightening of bolts and the assessment of stress levels in bars as well as in multi-wire strands (Chaki and Bourse, 2009).

The methodology behind the evaluation of stresses is quite straightforward: one needs to measure the differences in bulk wave speeds propagating in different directions of the loaded and unloaded structure. These differences can be linked to the stress state using known third-order constants or by calibrating the wave speed changes under controlled loading. For example, a state of uniaxial stress can be characterised by one of five waves traveling along or perpendicular to the applied stress direction (Hughes and Kelly, 1953). However, the relative change in the wave speed, which is directly proportional to the applied stress, is relatively small (Pao and Gamer, 1985) and therefore, measurements must be performed with very high accuracy. Nevertheless, the main obstacles in ultrasonic pulse techniques are the influences of the microstructure and composition gradients as well as plastic deformations, which can all cause changes to the bulk wave speeds comparable to those due to applied or residual stresses (Pao et al., 1984; Pao, 1987).

Further developments of the theory of acoustoelasticity largely split into two directions; the first is aimed at studying the propagation of large or finite amplitude waves in pre-stressed media while the second is focused on the investigation of the acoustoelastic effect for different types of waves, such as guided waves. The first direction was found to have limited potential for practical applications as the existence of limiting stress for real materials, which is the stress beyond which the material ceases to behave elastically, largely restricts the amplitudes of the elastic waves as well as the associated nonlinear effects (Norris, 1998; Saccomandi, 2007). Previous studies on the acoustoelastic effect for guided waves will be discussed in the following section. The remainder of this sub-section focuses on recent studies on the propagation of large amplitude elastic waves in pre-stressed media.

The studies on finite amplitude elastic waves were usually restricted to specific hyperelastic strain energy functions such as the Mooney-Rivlin and Hadamard models (Currie and Hayes, 1969; Boulanger and Hayes, 1992; Boulanger et al., 1994; Destrade and Saccomandi, 2004). The focus of these studies was largely on the mathematical aspects of the theory, for example to determine the conditions for the existence of particular types of propagating

waves such as solitons or to obtain exact solutions for specific boundary and initial conditions. These solutions sometimes help to shed light on highly complex phenomena in nonlinear dynamics, which incorporate dissipative and dispersive mechanisms (Saccomandi, 2007). However, this research direction is not within the scope of the present thesis.

1.2.2 Guided Waves in Pre-Stressed Plates

Lamb waves are a type of guided waves, which propagate in elastic plates. In 1917, the English mathematician Horace Lamb was the first to provide a description of the possible modes of infinitesimal wave motions in linearly elastic plates as well as their characteristic equations (or dispersion equations). In an infinite body, only two types of non-dispersive wave motions are possible, namely longitudinal and shear (transverse) waves. However, in plates there is an infinite number of wave modes which can propagate (Rose, 2014). The two main types of Lamb wave modes are the symmetric and antisymmetric modes, which are characterised by wave motions in the in-plane directions (along the direction of wave propagation and normal to the plate). Lamb waves are dispersive in nature, which means that the wave speeds depend on the relationship between the frequency (or wavelength) and the plate thickness (Rose, 2014).

Another type of guided waves, propagating near the free surface of thick plates, is Rayleigh waves. The existence of Rayleigh waves, which are also known as surface waves, was discovered in 1885 by Lord Rayleigh. In isotropic solids, these waves cause the surface particles to move along an elliptical curve in planes normal to the surface and parallel to the direction of wave propagation. The displacements due to the wave motion are minimal below a depth of two wavelengths (Achenbach, 1984); so Rayleigh waves are insensitive to changes in plates of thicknesses greater than two wavelengths. These waves are also non-dispersive and propagate with the same wave speed, independent of the frequency (Achenbach, 1984).

The acoustoelasticity of Rayleigh waves has been quite thoroughly investigated but there are significantly fewer studies published on the acoustoelasticity of Lamb waves. One of the first theoretical studies on the

acoustoelastic effect for Rayleigh and Lamb waves propagating in non-uniformly stressed plates was conducted by Husson (1985). These authors found that Rayleigh waves become weakly dispersive under bending and that Lamb waves are only affected by the membrane stress but are not sensitive to bending stress.

In recent years, there have been several important contributions related to the behaviour of small amplitude waves in pre-stressed layers, albeit in a different context to acoustoelasticity, specifically, on the derivation of asymptotic relationships describing the wave motion in the long and short wave limits. In particular, Kaplunov et al. (2000, 2002a, 2002b) developed asymptotic equations for the long-wave low-frequency, long-wave high-frequency and short-wave motions along a principal direction in pre-stressed incompressible elastic layers. These equations were then extended by Pichugin and Rogerson (2001, 2002a, 2002b) who considered wave propagation along non-principal directions. The dynamic response of pre-stressed compressible layers was also studied with asymptotic approaches, e.g. Nolde et al. (2004), Rogerson and Prikazchikova (2009) and Kayestha et al. (2011). The derivation of such asymptotic equations is important for the validation of numerical and analytical methods as such equations provide benchmark results for the fundamental as well as higher-order Lamb wave modes. A detailed analysis of the asymptotic approaches is beyond the scope of this thesis but the reader is referred to the books by Berdichevsky (2009) and Kaplunov et al. (1998) for a comprehensive discussion.

Recently, a number of researchers have investigated wave propagation in pre-stressed plates and other waveguides with semi-analytical and purely computational approaches (Chen and Wilcox, 2007; Loveday, 2009; Bartoli et al., 2010; Peddeti and Santhanam, 2018). In general, the outcomes of these numerical studies confirm the theoretical findings that the pre-deformation leads to strain-induced anisotropy in an initially isotropic material, thereby causing a change in the wave speeds of the different guided wave modes. From a practical point of view, the change in the wave speeds could be utilised for the non-destructive and in situ evaluation of the stress state of elongated structures, such

as bars, rails, wires, plate- and shell-like components. The measurement of stress in such structures currently represents a significant challenge for industry, as highlighted in the Introduction.

The above mentioned numerical and semi-analytical methods are beyond the scope of the current thesis, which is focused on analytical methods for the analysis of Rayleigh and Lamb wave propagation in pre-stressed plates. The current thesis utilises the theoretical framework developed by Ogden (2007) for incremental motions superimposed on a large deformation. In this framework, the wave propagation is considered as an infinitesimal deformation which is superimposed onto a finite static homogeneous deformation. The dispersion relations in the case of a pre-stressed compressible finite plate was previously derived by Roxburgh and Ogden (1994) but these authors focused on the vibration and stability phenomena rather than on the analysis of the propagation of Lamb waves. The effect of applied stress on Lamb wave propagation was considered by Gandhi et al. (2012); however, their work was restricted to small initial strains only such that the elasticity tensor was obtained to the first-order in the infinitesimal strain tensor. One of the objectives of the current thesis is to investigate the effect of the stress state on the propagation of the fundamental and higher-order Lamb wave modes, using the general framework developed by Ogden. Another objective is to implement the research outcomes for the improvement of existing and future Structural Health Monitoring systems.

1.2.3 Structural Health Monitoring

Damage monitoring is often required for the safe and efficient operation of machine and structures. Structural health monitoring (SHM) refers to the process of monitoring the integrity of structures in situ using real-time data obtained from a permanently attached or embedded sensor network (Farrar and Worden, 2007). In this way, there is no need for shutdown and disassembly of the structures to be inspected as the sensors are an inherent part of these structures. SHM systems represent an alternative to traditional non-destructing evaluation procedures, which are normally time consuming and labour intensive (Maalej et al., 2002; Su and Ye, 2009; Staszewski et al., 2004).

In recent years, significant progress has been made in the development of SHM techniques utilising guided waves (Raghavan and Cesnik, 2007; Mitra and Gopalakrishnan, 2016; Giurgiutiu, 2016). In particular, it was found that Rayleigh and Lamb waves are able to propagate over large distances without significant attenuation, thereby providing the possibility of interrogating large areas of such components with a limited number of sensors (Staszewski, 2005; Diamanti and Soutis, 2010; Schmidt et al. 2013). A typical guided wave based SHM system incorporates a grid of permanently bonded or embedded transducers. One of the transducers is excited with a tone burst of a few cycles, generating a stress wave that propagates along the structure. The time-domain responses from the transmitter and the receiving transducers (sensors) are then recorded. This process is repeated using different transducers as transmitters and sensors. The signal remaining after subtraction from damage-free reference data which exceeds the background noise is assumed to be linked to a defect or mechanical damage (Croxford et al., 2007).

As discussed in the previous sections, it is not only possible to detect damage with Rayleigh and Lamb waves but it is also possible to evaluate the stress state of structures using these two types of waves. Therefore, the same sensor network can potentially be utilised to assess the factors affecting both the structural integrity, which is related to accumulated damage or defects, and the applied stress. The extension of SHM systems to stress monitoring can dramatically improve the evaluation of the current condition of structures as well as the residual life forecasts. The future development of systems monitoring both damage and stress is very important in the context of changing the current maintenance paradigm from schedule-driven inspections to condition-based maintenance procedures.

One of the main contributions to the background noise in real-world situations arises from variations in environmental and operational conditions, such as the ambient temperature (Konstantinidis et al., 2006; Lanza di Scalea and Salamone, 2008; Raghavan and Cesnik, 2008; Dodson and Inman, 2013) or applied loading (Chen and Wilcox, 2007; Lee et al. 2011; Sohn, 2007; Michaels et al. 2011; Roy et al., 2015). Background noise is arguably the main reason why

SHM systems, which have been developed and successfully demonstrated in the last two decades in laboratory conditions, often fail to prove their efficiency in the real-world environment. The background noise can interfere with the operation of SHM systems leading to false alarms or the prevention of critical damage from being detected in service. One way to address this problem is to increase the number of sensors, which can however adversely affect the cost, weight and power efficiency of the SHM systems. Another way is to develop different compensation methods, which would negate the effects of environmental conditions on damage detection. Several such methods have been developed to compensate for ambient temperature variations (Lu and Michaels, 2005; Croxford et al., 2010; Dao and Staszewski, 2013); however, it seems that no methods for the evaluation or compensation of the effect of stress variations on damage detection have been proposed so far. The current thesis addresses this issue and develops a mathematical framework for the evaluation of the background noise due to changing stress conditions.

A relatively recent research direction in the area of structural integrity and damage monitoring is the evaluation of the so-called early damage (or damage accumulated prior to the formation of a propagating crack) with ultrasonic techniques (Jhang, 2009; Matlack et al., 2015; Kim et al., 2019). In structural materials, early fatigue damage stages can occupy from 20% to 60% of the total fatigue life in the high cycle fatigue regime and almost 100% of the total fatigue life in the ultrahigh cycle fatigue regime. Thus, accurate evaluation of early damage can be crucial for safety and in the scheduling of effective maintenance procedures.

It was demonstrated in a number of studies (Hikata et al., 1965; Na et al., 1996; Cantrell and Yost, 1994) that third-order constants are quite sensitive to damage associated with dislocation mechanisms, e.g. fatigue, creep and radiation damage. Therefore, accurate measurements of third-order elastic constants is important in the context of current developments focusing on early damage evaluation techniques. This thesis addresses this challenge and suggests a new experimental method, which has many advantages in comparison with current techniques.

1.3 Objectives

The overall aim of this thesis is to develop a better understanding of the phenomena associated with the propagation of Lamb waves in pre-stressed plates. Such an understanding is required for the development of in situ stress monitoring procedures based on Lamb waves and the operation of existing as well as future Lamb wave based SHM systems. The specific objectives of the current study are:

1. to investigate the effect of uniaxial applied stress on the propagation of Lamb waves in compressible materials along the direction of the applied stress and provide a detailed analysis of the behaviour of the fundamental (S_0 , A_0) and first two higher-order modes ($S_{1,2}$, $A_{1,2}$). These wave modes are often utilised for the purposes of damage detection in plate- and shell-like structures;
2. to generalise the outcomes of the first objective for multi-axial applied stress and arbitrary wave propagation direction with respect to the stress orientation;
3. to explore the linear and nonlinear effects, also referred to as the classical and large acoustoelastic effects respectively, of a large pre-strain on the propagation of Lamb waves in incompressible materials, which have broad applications in engineering and medical science;
4. to undertake the analysis of the residual noise due to changing loading conditions in guided wave based SHM systems utilising a baseline subtraction method for defect and damage detection and compare it with the noise due to ambient temperature variations. This particular objective has important implications for the operation of existing SHM systems and the development of future SHM systems;
5. to develop and validate a new experimental procedure based on Rayleigh waves for the evaluation of third-order elastic constants. This new technique has several potential applications, including the monitoring of stress and early damage in mechanical and civil engineering structures.

1.4 Structure of the Thesis

This thesis is comprised of a combination of 'published' and 'accepted for publication' research articles in leading high-impact journals, such as the journal of *Smart Materials and Structures* and the *Journal of the Acoustical Society of America*. These articles are united by the same framework, the theory of acoustoelasticity, which is applied to a range of problems, each representing a separate chapter in the main body of this thesis. The thesis contains seven main chapters, which are briefly outlined below:

Chapter 1: Introduction

This chapter provides a brief background to the research area, along with the motivation behind the current study. A broad review of literature is then presented, beginning with a historical perspective on the theory of acoustoelasticity. This is followed by an overview of guided wave acoustoelasticity as well as its applications to Structural Health Monitoring. The overall aim and specific objectives of the current study are then formulated and a brief outline of the thesis is provided.

Chapter 2: Mathematical Preliminaries

In this chapter, the framework used in the study of guided wave acoustoelasticity is presented. This framework relies on the theory of incremental motions superimposed on a finite deformation (*theory of small-on-large*), which is described within the theory of nonlinear elasticity (Ogden, 1984, 2007; Norris, 2007). First, the basic equations describing the mechanics of an elastic body subjected to a static finite deformation are reviewed. This includes a discussion of the equilibrium and constitutive equations for both compressible and incompressible materials. The incremental equations describing the mechanical response of the finitely deformed body to a small dynamic displacement are then presented. The resulting incremental equations of motions form the basis of the

theory of acoustoelasticity, which is utilised in the theoretical developments in the subsequent chapters.

Chapter 3: Effect of uniaxial stress on the propagation of higher-order Lamb wave modes

This chapter is concerned with the development of a new acoustoelastic formulation to study the propagation of Lamb waves in a compressible elastic plate subjected to a homogeneous pre-stress. The governing equations are derived based on the theory of incremental motions superimposed on a large deformation and a new invariant based formulation is utilised for the strain energy function (Destrade and Ogden, 2013; Shams et al., 2011). The analysis is here restricted to the plane strain incremental problem of wave propagation along a principal direction and the dispersion equations are obtained for a general form of the strain energy function, which can incorporate large pre-deformations. The dispersion equations are subsequently specialised to the case of weakly nonlinear elasticity by considering the Murnaghan form of the strain energy function, which is expanded to the third-order in the strain (Murnaghan, 1951). The acoustoelastic effect associated with Lamb waves propagating along the direction of an applied uniaxial load is then investigated by considering the change in the phase velocity of the different Lamb wave modes with the applied stress.

Chapter 4: Large Acoustoelastic effect for Lamb waves propagating in an incompressible elastic plate

In this chapter, the problem of Lamb wave propagation in a pre-stressed incompressible elastic plate is considered. The motivation behind this work stems from the increasing use of rubber-like materials in a number of practical applications, such as in engine mountings and seismic isolators (Destrade and Ogden, 2005). Rubber-like materials differ from ordinary stiff materials such as metals as they are amenable to large deformations (with strains up to hundreds of percent) but are constrained to undergo volume preserving deformations

(incompressibility constraint). An understanding of the wave propagation characteristics in such materials is thus of paramount importance.

The acoustoelastic formulation developed previously (Chapter 3) is here extended to the incompressible case. The analysis is set within the theory of weakly nonlinear elasticity, whereby the strain energy function is expanded as a power series in terms of some measure of strain (Abiza et al., 2012; Destrade et al., 2010c). Previous works in this area have mainly considered third-order expanded strain energy functions. The tacit assumption was that the pre-stress or pre-strain is small and the correction to the wave speeds is obtained implicitly to the first-order in the strain and depends on the second- and third- order elastic constants (Gandhi et al., 2012; Pei and Bond, 2016, 2017). Motivated by the applications of rubber-like solids and soft materials with large elastic strain limits, the analysis is here extended to fourth-order expanded strain energy functions (Hamilton et al., 2004; Destrade et al., 2010a, 2010b). The correction to the wave speeds is then obtained implicitly to the second-order in the strain and involves second-, third- and fourth-order elastic constants. Numerical results based on the new acoustoelastic formulation, termed as the large acoustoelastic formulation, are then compared to the prediction of the classical acoustoelastic formulation for different Lamb wave modes propagating in a pre-stressed Silicone-Rubber plate.

Chapter 5: Implication of changing loading conditions on structural health monitoring utilising guided waves

This chapter is related to the effect of variations in the stress state of a structure on the operation of Structural Health Monitoring systems based on Lamb waves. First, the effect of stress variations on the propagation of Lamb waves is investigated using the previously developed acoustoelastic formulation (Chapter 3). This formulation is extended to consider the more general problem of Lamb wave propagation along an arbitrary (non-principal) direction in a compressible elastic plate subjected to biaxial loading. Dispersion results are then presented to demonstrate the effect of the applied stress, propagation direction and

frequency on the change in the phase velocity of the fundamental Lamb wave modes. Based on these results, an analytical model is developed to quantify the residual signal obtained after reference (baseline) signal subtraction (Konstantinidis et al., 2006; Croxford et al., 2007) due to the effect of the applied stress. The results from the analytical model are also compared to the residual noise levels due to temperature variations. Stress mitigation techniques are also proposed using key features identified from the dispersion results to minimize the effect of stress in Lamb wave based SHM systems.

Chapter 6: On the determination of the third-order elastic constants of homogeneous isotropic materials utilising Rayleigh waves

In this chapter, a new method for the evaluation of the third-order elastic constants of homogeneous isotropic materials is presented. The new method is based on the acoustoelastic effect associated with Rayleigh and bulk waves and it involves the measurement of the change in the speeds of these waves with the applied stress. As described previously, Rayleigh waves and Lamb waves are both guided waves which propagate in elastic plates. Rayleigh waves are essentially a special type of Lamb waves which propagate near the free surface of thick plates (Pitts et al., 1976). In fact, the fundamental symmetric and anti-symmetric Lamb wave modes converge to Rayleigh waves at high frequency-thickness products. The main motivation for using Rayleigh waves in the determination of third-order elastic constants is the non-dispersive nature of this type of wave, which makes signal analysis relatively simple. Comparatively, Lamb waves are multi-modal and dispersive in nature, and as a result, the signal analysis is much more complex.

The theoretical foundation for the new method relies on the classical equations of acoustoelasticity for bulk waves (Hughes and Kelly, 1953) as well as the nonlinear characteristic equation governing the acoustoelastic effect for Rayleigh waves. The latter equation is obtained using the previously developed acoustoelastic formulation for Lamb waves propagating in a pre-stressed plate (Chapter 3) and considering the limit of the frequency-thickness product tending

to infinity. The accuracy of the new method is investigated numerically using Monte-Carlo simulations (Hammersley and Handscomb, 1964; Madras, 2002), and the effect of different types of probabilistic distributions of the wave speed measurements is considered.

Chapter 7: Summary and Recommendations

The summary of the main outcomes of this thesis are presented in this concluding chapter, along with a brief discussion of the possible future research directions.

1.5 Concluding Remarks

In this introductory chapter, the background and motivation behind the current study was provided. A brief literature review was also presented, along with the specific objectives of the research undertaken. The theoretical framework employed to address these objectives is elaborated upon in the next chapter, in which the fundamentals of the theory of incremental motions superimposed on a finite deformation are presented.

References

Abiza, Z., Destrade, M. and Ogden, R.W. (2012), Large acoustoelastic effect, *Wave Motion*, 49, 364–374, doi: 10.1016/j.wavemoti.2011.12.002.

Achenbach, J. (1984), Wave Propagation in Elastic Solids, Elsevier, Amsterdam.

Bartoli, I., Phillips, R., Coccia, S., Srivastava, A., di Scalea, F.L., Fateh, M. and Carr, G. (2010), Stress dependence of ultrasonic guided waves in rails, *Transportation Research Record: Journal of the Transportation Research Board*, 2159, 91–97, doi: 10.3141/2159-12.

Berdichevsky, V.L. (2009), Variational Principles of Continuum Mechanics, in Interaction of Mechanics and Mathematics, edited by L. Truskinovsky, Springer-Verlag, Berlin Heidelberg.

Bergman, R.H. and Shahbender, R.A. (1958), Effect of statically applied stresses on the velocity of propagation of ultrasonic waves, *Journal of Applied Physics*, 29, 1736-1738, doi: 10.1063/1.1723035.

Biot, M.A. (1940), The influence of initial stress on elastic waves, *Journal of Applied Physics*, 11, 522–530, doi: 10.1063/1.1712807.

Biot, M.A. (1965), Mechanics of Incremental Deformations, John Wiley & Sons, New York.

Birch, F. (1937), The effect of pressure on the modulus of rigidity of several metals and glasses, *Journal of Applied Physics*, 8, 129-133, doi: 10.1063/1.1710264.

Birch, F. (1938), The effect of pressure upon the elastic parameters of isotropic solids, according to Murnaghan's theory of finite strain, *Journal of Applied Physics*, 9, 279–288, doi: 10.1063/1.1710417.

Bland, D.R. (1969), Nonlinear dynamic elasticity, Blaisdell, Waltham.

Boulanger, Ph. and Hayes, M. (1992), Finite-amplitude waves in deformed Mooney-Rivlin materials, *Quarterly Journal of Mechanics and Applied Mathematics*, 45, 575-593, doi: 10.1093/qjmam/45.4.575.

Boulanger, Ph., Hayes, M. and Trimarco, C. (1994), Finite-amplitude plane waves in deformed Hadamard elastic materials, *Geophysics Journal International*, 118, 447-458, doi: j.1365-246X.1994.tb03976.x.

Bridgman, P.W. (1929a), The effect of pressure on the rigidity of steel and several varieties of glass, *Proceedings of the American Academy of Arts and Sciences*, 63, 401-420, doi: 10.2307/20026225.

Bridgman, P.W. (1929b), The effect of pressure on the rigidity of several metals, *Proceedings of the American Academy of Arts and Sciences*, 64, 39-49, doi: 10.2307/20026251.

Brillouin, L. (1925), Sur les tensions de radiation, *Annales de Physique*, 10, 528-586, doi: 10.1051/anphys/192510040528.

Brillouin, L. (1946), Les Tenseurs en Mécanique et en Élasticité, Dover Publications, New York.

Cantrell, J.H. and Yost, W.T. (1994), Acoustic harmonic generation from fatigue-induced dislocation dipoles, *Philosophical Magazine A*, 69, 315-326, doi: 10.1080/01418619408244346.

Cauchy, A.-L. (1829), Sur l'équilibre et le mouvement intérieur des corps considérés comme des masses continues, Exercices de Mathématiques, 4, 293–319.

Chaki, S. and Bourse, G. (2009), Guided ultrasonic waves for non-destructive monitoring of the stress levels in prestressed steel strands, *Ultrasonics*, 49, 162–171, doi: 10.1016/j.ultras.2008.07.009.

Cheeke, J. (2012), Fundamentals and Applications of Ultrasonic Waves, CRC Press, Boca Raton.

Chen, F. and Wilcox, P.D. (2007), The effect of load on guided wave propagation, *Ultrasonics*, 47, 111–122, doi: 10.1016/j.ultras.2007.08.003.

Crecraft, D.I. (1962), Ultrasonic wave velocities in stressed nickel steel, *Nature*, 195, 1193–1194, doi: 10.1038/1951193a0.

Crecraft, D.I. (1967), The measurement of applied and residual stresses in metals using ultrasonic waves, *Journal of Sound and Vibration*, 5, 173–192, doi: 10.1016/0022-460X(67)90186-1.

Crecraft, D.I. (1968), Ultrasonic measurement of stresses, *Ultrasonics*, 6, 117–121, doi: 10.1016/0041-624X(68)90205-9.

Croxford, A.J., Moll, J., Wilcox, P.D. and Michaels, J.E. (2010), Efficient temperature compensation strategies for guided wave structural health monitoring, *Ultrasonics*, 50, 517-528, doi: 10.1016/j.ultras.2009.11.002.

Croxford, A.J., Wilcox, P.D, Drinkwater, B.W and Konstantinidis, G. (2007), Strategies for guided-wave structural health monitoring, *Proceedings of the Royal Society A: Mathematical, Physical and Engineering Sciences*, 463, 2691-2981, doi: 10.1098/rspa.2007.0048.

Currie, P. and Hayes, M. (1969), Longitudinal and transverse waves in finite elastic strain. Hadamard and Green Materials, *IMA Journal of Applied Mathematics*, 5, 140–161, doi: 10.1093/imamat/5.2.140.

Dao, P.B. and Staszewski, W.J. (2013), Cointegration approach for temperature effect compensation in Lamb-wave based damage detection, *Smart Materials and Structures*, 22, 1-20, doi: 10.1088/0964-1726/22/9/095002.

Destrade, M. and Ogden, R.W. (2005), Surface waves in a stretched and sheared incompressible elastic material, *International Journal of Non-Linear Mechanics*, 40, 241-253, doi: 10.1016/j.ijnonlinmec.2004.05.008.

Destrade, M. and Ogden, R.W. (2013), On stress-dependent elastic moduli and wave speeds, *IMA Journal of Applied Mathematics*, 78, 965-997, doi: 10.1093/imamat/hxs003.

Destrade, M. and Saccomandi, G. (2004), Finite-amplitude inhomogeneous waves in Mooney-Rivlin viscoelastic solids, *Wave Motion*, 40, 251-262, doi: 10.1016/j.wavemoti.2004.04.001.

Destrade, M., Gilchrist, M.D. and Murphy, J.G. (2010c), Onset of nonlinearity in the elastic bending of blocks, *Journal of Applied Mechanics*, 77, 061015-061020, doi: 10.1115/1.4001282.

Destrade, M., Gilchrist, M.D. and Ogden, R.W. (2010b), Third- and fourth-order elasticities of biological soft tissues, *Journal of the Acoustical Society of America*, 127, 2103-2106, doi: 10.1121/1.3337232.

Destrade, M., Gilchrist, M.D. and Saccomandi, G. (2010a), Third- and fourth-order constants of incompressible soft solids and the acousto-elastic effect, *Journal of the Acoustical Society of America*, 127, 2759-2763, doi: 10.1121/1.3372624.

Diamanti, K. and Soutis, C. (2010), Structural health monitoring techniques for aircraft composite structures, *Progress in Aerospace Sciences*, 46, 342-352, doi: 10.1016/j.paerosci.2010.05.001.

Dodson, J.C. and Inman, D.J. (2013), Thermal sensitivity of Lamb waves for structural health monitoring applications, *Ultrasonics*, 53, 677-685, doi: 10.1016/j.ultras.2012.10.007.

Egle, D.M. and Bray, D.E. (1976), Measurement of acoustoelastic and third-order elastic constants for rail steel, *Journal of the Acoustical Society of America*, 60, 741–744, doi: 10.1121/1.381146.

Ensminger, D., Bond, L. (2011), Ultrasonics, CRC Press, Boca Raton.

Eringen, A.C. and Suhubi, E.S. (1974), Elastodynamics, Academic press, New York.

Farrar, C. and Worden, K. (2007), An introduction to structural health monitoring, *Philosophical Transactions of the Royal Society A: Mathematical, Physical and Engineering Sciences*, 365, 303–315, doi: 10.1098/rsta.2006.1928.

Gandhi, N., Michaels, J.E. and Lee, S.J. (2012), Acoustoelastic Lamb wave propagation in biaxially stressed plates, *Journal of the Acoustical Society of America*, 132, 1284-1293, doi: 10.1121/1.4740491.

Gandhi, N., Michaels, J.E. and Lee, S.J. (2012), Acoustoelastic Lamb wave propagation in biaxially stressed plates, *Journal of the Acoustical Society of America*, 132, 1284–1293, doi: 10.1121/1.4740491.

Giurgiutiu, V. (2016), Structural Health Monitoring of Aerospace Composites, Academic Press, London.

Hamilton, M.F., Ilinskii, Y.A. and Zabolotskaya, E.A. (2004), Separation of compressibility and shear deformation in the elastic energy density, *Journal of the Acoustical Society of America*, 116, 41-44, doi: 10.1121/1.1736652.

Hammersley, J.M. and Handscomb, D.C. (1964), Monte Carlo Methods, Monographs on Applied Probability and Statistics, Springer, Netherlands, doi: 10.1007/978-94-009-5819-7.

Hikata, A., Chick, B.B. and Elbaum, C. (1965), Dislocation contribution to the second harmonic generation of ultrasonic waves, *Journal of Applied Physics*, 36, 229–236, doi: /10.1063/1.1713881.

Hiki, Y (1981), Higher order elastic constants of solids, *Annual Review of Materials Science*, 11, 51-73, doi: 10.1146/annurev.ms.11.080181.000411.

Hughes, D.S. and Kelly, J.L. (1953), Second-order elastic deformation of solids, *Physical Review*, 92, 1145–1149, doi: 10.1103/PhysRev.92.1145.

Husson, D. (1985), A perturbation theory for the acoustoelastic effect of surface waves, *Journal of Applied Physics*, 57, 1562–1568, doi: 10.1063/1.334471.

Jhang, K.Y. (2009), Nonlinear ultrasonic techniques for nondestructive assessment of micro damage in material: A review, *International Journal of Precision Engineering and Manufacturing*, 10, 123-135, doi: /10.1007/s12541-009-0019-y.

Kaplunov, J.D., Kossovich, L.Y. and Nolde, E.V. (1998), Dynamics of Thin Walled Elastic Bodies, Academic Press, San Diego.

Kaplunov, J.D., Nolde, E.V. and Rogerson, G.A. (2000), A low-frequency model for dynamic motion in pre-stressed incompressible elastic structures, *Proceedings: Mathematical, Physical and Engineering Sciences*, 456, 2589–2610.

Kaplunov, J.D., Nolde, E.V. and Rogerson, G.A. (2002a), An asymptotically consistent model for long-wave high-frequency motion in a pre-stressed elastic plate, *Mathematics and Mechanics of Solids*, 7, 581–606. doi: 10.1177/108128602029660.

Kaplunov, J.D., Nolde, E.V. and Rogerson, G.A. (2002b), Short wave motion in a pre-stressed incompressible elastic plate, *IMA Journal of Applied Mathematics*, 67, 383–399, doi: 10.1093/imamat/67.4.383.

Kayestha, P., Wijeyewickrema, A. and Kishimoto, K. (2011), Wave propagation along a non-principal direction in a compressible pre-stressed elastic layer, *International Journal of Solids and Structures*, 48, 2141–2153, doi: 10.1016/j.ijsolstr.2011.03.022.

Kim, J.Y., Jacobs, L. and Qu, J. (2019), Nonlinear Ultrasonic Techniques for Material Characterization, in Nonlinear Ultrasonic and Vibro-Acoustical Techniques for Nondestructive Evaluation, edited by T. Kundu, pp. 225-261, Springer, Cham.

Kim, K.Y. and Sachse, W. (2001), Acoustoelasticity of elastic solids, in Handbook of Elastic Properties of Solids, Liquids, and Gases, edited by A. Avery and W. Sachse, Academic Press, San Diego), pp. 441–468.

Konstantinidis, G., Drinkwater, B. and Wilcox, P.D. (2006), The temperature stability of guided wave structural health monitoring systems, *Smart Materials and Structures*, 15, 967–976, doi: 10.1088/0964-1726/15/4/010.

Konstantinidis, G., Drinkwater, B.W. and Wilcox, P.D. (2006), The temperature stability of guided wave structural health monitoring systems, *Smart Materials and Structures*, 15, 967-976, doi: 10.1088/0964-1726/15/4/010.

Lamb, H. (1917), On waves in an elastic plate, *Proceedings of the Royal Society of London. Series A*, 93, 114–128, doi: 10.1098/rspa.1917.0008.

Landau, L.D. and Lifshitz, E.M. (1986), Theory of elasticity, Butterworth-Heinemann, Oxford.

Lanza di Scalea, F. and Salamone, S. (2008), Temperature effects in ultrasonic Lamb wave structural health monitoring systems, *Journal of the Acoustical Society of America*, 124, 161-174, doi: 10.1121/1.2932071.

Lee, S.J., Gandhi, N., Michaels, J.E. and Michaels, T.E. (2011), Comparison of the effects of applied loads and temperature variations on guided wave propagation, *AIP Conference Proceedings*, 1335, 175–182, doi: 10.1063/1.3591854.

Love, A. (1926), Some problems of geodynamics, Cambridge University Press, London.

Loveday, P.W. (2009), Semi-analytical finite element analysis of elastic waveguides subjected to axial loads, *Ultrasonics*, 49, 298–300, doi: 10.1016/j.ultras.2008.10.018.

Lu, Y. and Michaels, J.E. (2005), A methodology for structural health monitoring with diffuse ultrasonic waves in the presence of temperature variations, *Ultrasonics*, 43, 717-731, doi: 10.1016/j.ultras.2005.05.001.

Maalej, M., Karasaridis, A., Pantazopoulou, S. and Hatzinakos, D. (2002), Structural health monitoring of smart structures, *Smart Materials and Structures*, 11, 581-589, doi: 10.1088/0964-1726/11/4/314.

Madras, N. (2002), Lectures on Monte Carlo Methods, American Mathematical Society, Providence, Rhode Island.

Matlack, K.H., Jacobs, J.Y., Jacobs, L.J. and Qu, J. (2015), Review of Second Harmonic Generation Measurement Techniques for Material State Determination in Metals, *Journal of Nondestructive Evaluation*, 34, 1-23, doi: /10.1007/s10921-014-0273-5.

Michaels, J.E., Gandhi, N. and Lee, S.J. (2011), Acoustoelastic Lamb Waves and Implications for Structural Health Monitoring, in From Waves in Complex Systems to Dynamics of Generalized Continua, edited by K. Hutter, T.T. Wu and Y.C. Shu, pp. 91-117, World Scientific, New Jersey.

Mitra, M. and Gopalakrishnan, S. (2016), Guided wave based structural health monitoring: A review, *Smart Materials and Structures*, 25, 053001, doi: /10.1088/0964-1726/25/5/053001.

Murnaghan, F.D. (1937), Finite deformations of an elastic solid, *American Journal of Mathematics*, 59, 235–260, doi: 10.2307/2371405.

Murnaghan, F.D. (1951), Finite deformation of an elastic solid, John Wiley & Sons, New York.

Na, J.K., Cantrell, J.H. and Yost, W.T. (1996), Linear and nonlinear ultrasonic properties of fatigued 410Cb stainless steel, in Review of Progress in Quantitative Nondestructive Evaluation, edited by D.O. Thompson and D.E. Chimenti, pp. 1347–1351, Springer, Boston.

Nolde, E.V., Prikazchikova, L.A. and Rogerson, G.A. (2004), Dispersion of small amplitude waves in a pre-stressed, compressible elastic plate, *Journal of Elasticity*, 75, 1–29, doi: 10.1023/B:ELAS.0000039920.67766.d3.

Norris, A. (2007), Small-on-large theory with applications to granular materials and fluid/solid Systems, in Waves in Nonlinear Pre-Stressed Materials, edited by M. Destrade and G. Saccomandi, pp. 27–62, CISM Courses and Lectures, Springer, Vienna, doi: 10.1007/978-3-211-73572-5_2.

Norris, A.N. (1998), Finite amplitude waves in solids, in Nonlinear Acoustics, edited by M.F. Hamilton and D.T. Blackstock, pp. 263-277, Academic Press, San Diego.

Ogden, R.W. (1984), Non-Linear Elastic Deformations, Ellis Horwood, Chichester.

Ogden, R.W. (2007), Incremental statics and dynamics of pre-stressed elastic materials, in Waves in Nonlinear Pre-Stressed Materials, edited by M. Destrade and G. Saccomandi, pp. 1–26, CISM Courses and Lectures, Springer Vienna, doi: 10.1007/978-3-211-73572-5_1.

Pao, Y.-H. (1987), Theory of Acoustoelasticity and Acoustoplasticity, in Solid mechanics research for quantitative non-destructive evaluation, edited by J.D.

Achenbach and Y. Rajapakse, pp. 257–273, Springer, Dordrecht, doi: 10.1007/978-94-009-3523-5_16.

Pao, Y.-H. and Gamer, U. (1985), Acoustoelastic waves in orthotropic media, *Journal of the Acoustical Society of America*, 77, 806–812, doi: 10.1121/1.392384.

Pao, Y.-H., Sachse, W. and Fukuoka, H. (1984), Acoustoelasticity and ultrasonic measurements of residual stresses, in Physical Acoustics: Principles and Methods, vol. 17, edited by W.P. Mason and R.N. Thurston, pp 61–144, Academic Press, New York.

Peddeti, K. and Santhanam, S. (2018), Dispersion curves for Lamb wave propagation in prestressed plates using a semi-analytical finite element analysis, *Journal of the Acoustical Society of America*, 143, 829-840, doi: 10.1121/1.5023335.

Pei, N. and Bond, L. (2016), Higher order acoustoelastic Lamb wave propagation in stressed plates, *Journal of the Acoustical Society of America*, 140, 3834-3843, doi: https://doi.org/10.1121/1.4967756.

Pei, N. and Bond, L. (2017), Comparison of acoustoelastic Lamb wave propagation in stressed plates for different measurement orientations, *Journal of the Acoustical Society of America*, 142, EL327-EL331, doi: 10.1121/1.5004388.

Pichugin, A.V. and Rogerson, G.A. (2001), A two-dimensional model for extensional motion of a pre-stressed incompressible elastic layer near cut-off frequencies, *IMA Journal of Applied Mathematics*, 66, 357–385, doi: 10.1093/imamat/66.4.357.

Pichugin, A.V. and Rogerson, G.A. (2002a), An asymptotic membrane-like theory for long wave motion in a pre-stressed elastic plate, *Proceedings of the Royal Society of London, Series A: Mathematical, Physical and Engineering Sciences*, 458, 1447–1468, doi: /10.1098/rspa.2001.0932.

Pichugin, A.V. and Rogerson, G.A. (2002b), Anti-symmetric motion of a pre-stressed incompressible elastic layer near shear resonance, *Journal of Engineering Mathematics*, 42, 181–202, doi: 10.1023/A:1015293700959.

Pitts, L.E., Plona, T.J. and Mayer, W.G. (1976), Theoretical similarities of Rayleigh and Lamb modes of vibration, *Journal of the Acoustical Society of America*, 60, 374-377, doi: 10.1121/1.381092.

Raghavan, A. and Cesnik, C.E.S. (2007), Review of guided-wave structural health monitoring, *The Shock and Vibration Digest*, 39, 91–114, doi: 10.1177/0583102406075428.

Raghavan, A. and Cesnik, C.E.S. (2008), Effects of Elevated temperature on Guided-wave Structural Health Monitoring, *Journal of Intelligent Material Systems and Structures*, 19, 1383-1398, doi: 10.1177/1045389X07086691.

Rayleigh, L. (1885), On waves propagated along the plane surface of an elastic solid, *Proceedings of the London Mathematical Society*, s1-17, 4–11, doi: 10.1112/plms/s1-17.1.4.

Rogerson, G.A. and Prikazchikova, L.A. (2009), Generalisations of long wave theories for pre-stressed compressible elastic plates, *International Journal of Non-Linear Mechanics*, 44, 520–529, doi: 10.1016/j.ijnonlinmec.2008.11.002.

Rose, J. (2014), Ultrasonic Guided Waves in Solid Media, Cambridge University Press, Cambridge, doi: 10.1017/CBO9781107273610.

Roxburgh, D.G. and Ogden, R.W. (1994), Stability and vibration of pre-stressed compressible elastic plates, *International Journal of Engineering Science*, 32, 427–454, doi: 10.1016/0020-7225(94)90133-3.

Roy, S., Ladpli, P. and Chang, F.-K. (2015), Load monitoring and compensation strategies for guided-waves based structural health monitoring using piezoelectric transducers, *Journal of Sound and Vibration*, 351, 206-220, doi: 10.1016/j.jsv.2015.04.019.

Saccomandi, G. (2007), Finite Amplitude Waves in Nonlinear Elastodynamics and Related Theories: A Personal Overview, in Waves in Nonlinear Pre-

Stressed Materials, edited by M. Destrade and G. Saccomandi, pp. 129–180, CISM Courses and Lectures, Springer Vienna, doi: 10.1007/978-3-211-73572-5_5.

Schmidt, D., Hillger, W., Szewieczek, A. and Sinapius, M. (2013), Structural Health Monitoring Based on Guided Waves, in Adaptive, tolerant and efficient composite structures, edited by M. Wiedemann and M. Sinapius, Springer, Heidelberg, doi: /10.1007/978-3-642-29190-6_37.

Shams, M., Destrade, M. and Ogden, R.W. (2011), Initial stresses in elastic solids: Constitutive laws and acoustoelasticity, *Wave Motion*, 48, 552-567, doi: 10.1016/j.wavemoti.2011.04.004.

Smith, R.T. (1963), Stress-induced anisotropy in solids—the acoustoelastic effect, *Ultrasonics*, 1, 135–147, doi: 10.1016/0041-624X(63)90003-9.

Smith, R.T., Stern, R. and Stephens, R.W.B. (1966), Third-order elastic moduli of polycrystalline metals from ultrasonic velocity measurements, *Journal of the Acoustical Society of America*, 40, 1002–1008, doi: 10.1121/1.1910179.

Sohn, H. (2007), Effects of environmental and operational variability on structural health monitoring, *Philosophical Transactions of the Royal Society A: Mathematical, Physical and Engineering Sciences*, 365, 539–60, doi: 10.1098/rsta.2006.1935.

Spencer, A.J.M. (2004), Continuum Mechanics, Dover Publications, New York.

Staszewski, W., Boller, C. and Tomlinson, G.R. (2004), Health Monitoring of Aerospace Structures: Smart Sensor Technologies and Signal Processing, John Wiley & Sons, Chichester.

Staszewski, W.J. (2005), Ultrasonic/Guided Waves for Structural Health Monitoring, *Key Engineering Materials*, 293-294, 49-62, doi: 10.4028/www.scientific.net/KEM.293-294.49.

Su, Z. and Ye, L. (2009), Identification of Damage Using Lamb Waves: From Fundamentals to Applications, Springer, Berlin, doi: 10.1007/978-1-84882-784-4.

Tang, S. (1967), Wave propagation in initially stressed elastic solids, *Acta Mechanica*, 4, 92–106, doi: 10.1007/BF01291091.

Toupin, R.A. and Bernstein, B. (1961), Sound waves in deformed perfectly elastic materials. Acoustoelastic Effect, *Journal of the Acoustical Society of America*, 33, 216–225, doi: 10.1121/1.1908623.

Chapter 2

Mathematical Preliminaries

Chapter 2

Mathematical Preliminaries

The present chapter provides a brief overview of the theoretical framework used in the study of guided wave acoustoelasticity. This framework is based on the underlying theory of incremental motions superimposed on a finite deformation, which is described within the theory of nonlinear elasticity. Although this chapter aims to provide the necessary background relevant to the theoretical development in the subsequent chapters of this thesis, it is assumed that the reader is familiar with the subject of nonlinear elasticity. For a comprehensive treatment of this subject, the reader is referred to the books by Truesdell and Noll (1965), Ogden (1984), Green and Zerna (1992), and Holzapfel (2001).

2.1 Finite Static Deformation

In the theory of acoustoelasticity, a small amplitude wave is considered to propagate in a body subjected to a large deformation. While small deformations can be described within the linear theory of elasticity, finite or large deformations require the use of the nonlinear theory of elasticity. In this section, the basic equations of the nonlinear theory of elasticity required to describe the finite static deformation of an elastic body are reviewed. This includes a discussion of the mechanics of the deformation, the equilibrium equations and the constitutive laws.

2.1.1 Mechanics of deformation

Following the work of Ogden (2007), consider a homogeneous elastic body which possesses an unstressed reference configuration β_r. Material points in this configuration are denoted by the position vectors $\mathbf{X}$ relative to an arbitrarily chosen origin O. A finite static deformation is then imposed upon β_r to produce a new configuration β, which is referred to as the deformed configuration. The finite static deformation is defined by the vector function $\boldsymbol{\chi}$, which maps the material points $\mathbf{X}$ in the reference configuration β_r to the positions $\mathbf{x} = \boldsymbol{\chi}(\mathbf{X})$

(relative to some other origin o) in the deformed configuration β, as illustrated in Fig. 1. The function $\boldsymbol{\chi}$ is required to be a bijection and is assumed to satisfy appropriate regularity properties (Destrade and Ogden, 2013).

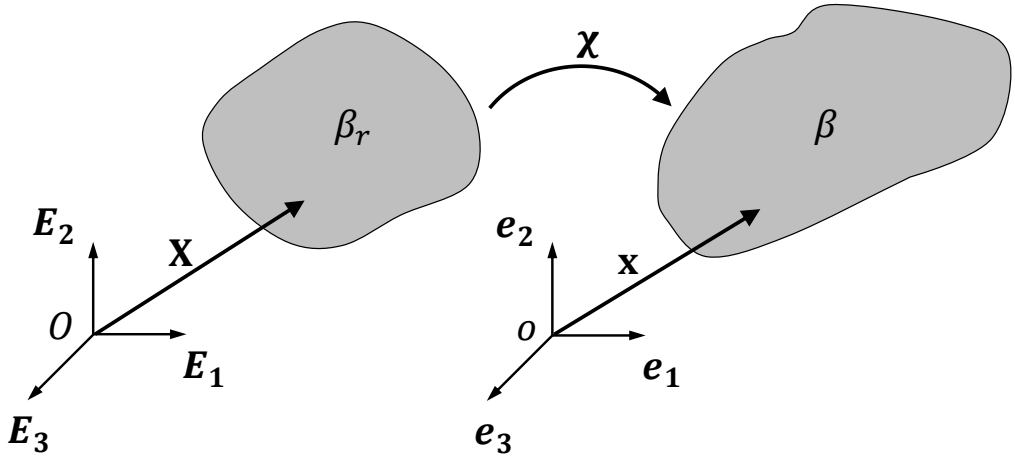

Figure 1. Schematic of the reference configuration $\boldsymbol{\beta_r}$ and the deformed configuration $\boldsymbol{\beta}$. Material points at $\mathbf{X}$ in $\boldsymbol{\beta_r}$ take up the positions $\mathbf{x}$ in $\boldsymbol{\beta}$ due to the deformation $\boldsymbol{\chi}$.

In the present work, vectors and tensors are specified with respect to rectangular Cartesian coordinates and for this purpose, basis vectors $\mathbf{E}_\alpha$ and $\mathbf{e}_i$ are chosen for the reference and deformed configurations respectively. Then, the vectors $\mathbf{X}$ and $\mathbf{x}$ have components

$$\mathbf{X} = X_\alpha \mathbf{E}_{\boldsymbol{\alpha}} , \qquad \mathbf{x} = x_i \mathbf{e}_i , \tag{1}$$

respectively, where $\alpha, i \in \{1,2,3\}$. The Einstein summation convention over repeated indices is adopted in Eq. (1) and is used throughout the remainder of this chapter, unless otherwise stated. It is also emphasised that Greek indices are used to refer to the Lagrangian coordinates in the reference configuration β_r while Roman indices are associated with the Eulerian coordinates in the deformed configuration β.

The deformation gradient tensor associated with the mapping $\boldsymbol{\chi}: \beta_r \rightarrow \beta$ is defined by

$$\mathbf{F} = \text{Grad}\,\mathbf{x} \equiv \text{Grad}\,\boldsymbol{\chi}(\mathbf{X})\,, \tag{2}$$

where Grad is the gradient operator in β_r. The deformation gradient tensor can also be expressed in component form as

$$F_{i\alpha} = \frac{\partial x_i}{\partial X_\alpha}\,. \tag{3}$$

The Jacobian of the deformation is defined by $J = \det \mathbf{F}$ and it is assumed to be positive as $\mathbf{F}$ is required to be non-singular (Ogden, 2001). The Jacobian provides a local measure of the change in the material volume and has important implications for incompressible materials (Dorfmann, 2009). This class of materials, which is considered in Chapter 4 of this thesis, is constrained to undergo isochoric or volume preserving deformations only, given by

$$J = \det \mathbf{F} = 1\,. \tag{4}$$

The constraint imposed by Eq. (4) is typically referred to as the incompressibility constraint.

2.1.2 Equilibrium equations

In the present work, the body is assumed to have been quasi-statically deformed by the application of a certain force, giving rise to a pre-stress. Two different stress measures are commonly utilised to describe the force acting on the body (Hackett, 2016). The first one is the Cauchy stress tensor $\boldsymbol{\sigma}$, which provides a measure of the current force acting per unit surface area in the deformed configuration β. The second one is the nominal stress tensor $\mathbf{S}$, which describes the current force acting per unit surface area in the reference configuration β_r. These two stress tensors are related to each other via the relation

$$\mathbf{S} = J\,\mathbf{F}^{-1}\,\boldsymbol{\sigma}\,. \tag{5}$$

In the absence of couple stresses, the Cauchy stress tensor $\boldsymbol{\sigma}$ is symmetric while the nominal stress tensor $\mathbf{S}$ is, in general, not symmetric (Ogden, 2007). The latter stress tensor satisfies the equation

$$\mathbf{FS} = \mathbf{S}^{\mathrm{T}}\mathbf{F}^{\mathrm{T}}\,, \tag{6}$$

which follows from the balance of moments of the forces acting on the body (Ogden, 2001).

The equilibrium equation may be written in terms of either of the stress tensors as

$$\operatorname{div}\boldsymbol{\sigma} + \rho\mathbf{b} = \mathbf{0}, \qquad \operatorname{Div}\mathbf{S} + \rho_r\mathbf{b} = \mathbf{0}\,, \tag{7}$$

where **b** denotes the body force per unit mass, and div and Div are the divergence operators with respect to β_r and β respectively. Here, ρ and ρ_r are the mass densities in the deformed and reference configurations respectively. The mass densities are related via the connection $\rho_r = J\rho$, which follows from the equation of mass conservation (Ogden, 2001).

In the current work, it is assumed that there are no body forces, in which case the equilibrium equations (7) reduce to the form

$$\operatorname{div}\boldsymbol{\sigma} = \mathbf{0}, \qquad \operatorname{Div}\mathbf{S} = \mathbf{0}\,. \tag{8}$$

Equivalently, these equations may be written in component form as

$$\frac{\partial \sigma_{ij}}{\partial x_j} = 0, \qquad \frac{\partial S_{\alpha i}}{\partial X_\alpha} = 0\,. \tag{9}$$

2.1.3 Constitutive equations

Sections 2.1.1 and 2.1.2 have presented the theoretical framework to describe the finite static deformation of an elastic body, the stress required to maintain the body in that state of deformation and the associated equilibrium equations. In this section, the constitutive equations which describe the relationship between the stress tensors and the deformation gradient are discussed. These constitutive equations are required in order to describe the mechanical response of different types of materials (Beatty, 1987).

In the present work, the elastic body is considered to be composed of a hyperelastic material, which may be described in terms of a strain-energy

function $W = W(\mathbf{F})$, defined per unit volume in β_r. This form of W is completely general and no material symmetry is invoked at this stage. For an unconstrained (compressible) material, the constitutive equations for a finitely deformed body may be written in terms of the nominal stress tensor $\mathbf{S}$ and the strain energy function W as

$$\mathbf{S} = \frac{\partial W}{\partial \mathbf{F}}. \tag{10}$$

Equivalently, the constitutive equations may be expressed in terms of the Cauchy stress tensor $\boldsymbol{\sigma}$ as

$$\boldsymbol{\sigma} = J^{-1}\mathbf{F}\frac{\partial W}{\partial \mathbf{F}}. \tag{11}$$

Using the expression in Eq. (10), the equilibrium equation (9) may be written as

$$\boldsymbol{\mathcal{A}}\frac{\partial^2 \boldsymbol{x}}{\partial \mathbf{X}\partial \mathbf{X}} = 0, \tag{12}$$

where $\boldsymbol{\mathcal{A}}$ is the tensor of first-order elastic moduli (Chadwick and Ogden, 1971), defined by

$$\boldsymbol{\mathcal{A}} = \frac{\partial^2 \boldsymbol{W}}{\partial \mathbf{F}\partial \mathbf{F}}, \tag{13}$$

It is worth noting that $\boldsymbol{\mathcal{A}}$ is a fourth-order tensor and has 81 components but the number of independent components is 45 only due to the major symmetry

$$\mathcal{A}_{\alpha i \beta j} = \mathcal{A}_{\beta j \alpha i}, \tag{14}$$

which follows from Eq. (13) (Ogden, 1984).

For an incompressible material subject to the internal constraint (4), the counterpart of equations (10) and (11) are given by

$$\mathbf{S} = \frac{\partial W}{\partial \mathbf{F}} - p\mathbf{F}^{-1}\,, \tag{15}$$

and

$$\boldsymbol{\sigma} = \mathbf{F}\frac{\partial W}{\partial \mathbf{F}} - p\mathbf{I}\,, \tag{16}$$

respectively, where the scalar p here is an arbitrary hydrostatic pressure which plays the role of a Lagrange multiplier associated with the incompressibility constraint (Ogden, 2001).

Using Eq. (15), the corresponding equilibrium equations for an incompressible material may be written as

$$\boldsymbol{\mathcal{A}}\frac{\partial^2 \boldsymbol{x}}{\partial \mathbf{X}\partial \mathbf{X}} - \frac{\partial p}{\partial \boldsymbol{x}} = 0\,, \tag{17}$$

where the components of the elasticity tensor $\boldsymbol{\mathcal{A}}$ are again given by Eq. (13), except that they are also subject to the incompressibility condition (4).

2.2 Incremental Deformation

In this section, the effect of a small static deformation in addition to the initial finite static deformation is investigated. Due to the 'small' nature of the superimposed deformation as compared to the 'larger' finite deformation, the superimposed deformation is linearized relative to the undeformed configuration. Such a deformation is commonly referred to as an *incremental deformation* (Shams, 2010).

2.2.1 Incremental constitutive equations

The initial finite static deformation $\boldsymbol{\chi}$, with $\mathbf{x} = \boldsymbol{\chi}(\mathbf{X})$, is considered to be followed by a second deformation $\boldsymbol{\chi}'$, with $\mathbf{x}' = \boldsymbol{\chi}'(\mathbf{X})$, which is 'close' to $\boldsymbol{\chi}$. The displacement from $\mathbf{x}$, which is assumed to be a perturbation of $\boldsymbol{\chi}$, can be written as

$$\hat{\mathbf{x}} = \mathbf{x}' - \mathbf{x} = \boldsymbol{\chi}'(\mathbf{X}) - \boldsymbol{\chi}(\mathbf{X}) \equiv \hat{\boldsymbol{\chi}}(\mathbf{X}) \,, \tag{18}$$

where a superposed hat is used to indicate an incremental quantity. The corresponding increment in the deformation gradient is given by

$$\operatorname{Grad} \hat{\boldsymbol{\chi}} = \operatorname{Grad} \boldsymbol{\chi}' - \operatorname{Grad} \boldsymbol{\chi} \equiv \hat{\mathbf{F}} \,. \tag{19}$$

The above expression is exact; however, in order to determine the incremental constitutive equations, linear approximations in terms of the incremental deformation $\hat{\mathbf{x}}$ and its associated deformation gradient $\hat{\mathbf{F}}$ will be required (Ogden, 2001).

For an unconstrained material, the incremental nominal stress tensor, in its exact form, is given by

$$\hat{\mathbf{S}} = \mathbf{S}' - \mathbf{S} = \frac{\partial W}{\partial \mathbf{F}}(\mathbf{F}') - \frac{\partial W}{\partial \mathbf{F}}(\mathbf{F}) \,. \tag{20}$$

and its associated linear approximation may be written as

$$\hat{\mathbf{S}} = \mathcal{A}\hat{\mathbf{F}} \,, \tag{21}$$

where $\mathcal{A}$ is the elasticity tensor defined previously in Eq. (13).

In the case of an incompressible material, the linear approximation of the incremental nominal stress tensor is obtained by taking the increment of Eq. (15) and it is given by

$$\hat{\mathbf{S}} = \mathcal{A}\hat{\mathbf{F}} - \hat{p}\mathbf{F}^{-1} + p\mathbf{F}^{-1}\hat{\mathbf{F}}\mathbf{F}^{-1}, \tag{22}$$

where $\hat{p}$ is the incremental form of p. The linearised incremental form of the associated incompressibility constraint (4) is given by

$$\operatorname{tr}\left(\hat{\mathbf{F}}\mathbf{F}^{-1}\right) = 0 \,. \tag{23}$$

Hence, Eqs. (21) and (22), which is coupled with (23), form the incremental constitutive equations for compressible and incompressible materials respectively.

2.2.2 Incremental equilibrium equations

The incremental form of the equilibrium equation may be obtained by subtracting the equation of motion (8) from its counterpart for $\boldsymbol{\chi}'$

$$\text{Div}\,\hat{\mathbf{S}} = \mathbf{0}\,. \tag{24}$$

The above equation is exact but in the case of an unconstrained material, $\hat{\mathbf{S}}$ can be replaced by its linear approximation (21). The incremental equilibrium equation (24) may then be expanded out in component form as

$$\mathcal{A}_{\alpha i\beta j}\frac{\partial^2 \hat{x}_j}{\partial X_\alpha \partial X_\beta} + \frac{\partial \mathcal{A}_{\alpha i\beta j}}{\partial X_\alpha}\frac{\partial \hat{x}_j}{\partial X_\beta} = 0\,. \tag{25}$$

In the present work, the underlying finite deformation and the material properties are considered to be homogeneous. The deformation gradient **F** and the elasticity tensor $\boldsymbol{\mathcal{A}}$ are then taken to be independent of **X** (Destrade and Ogden., 2013) and equation (25) thus reduces to

$$\mathcal{A}_{\alpha i\beta j}\frac{\partial^2 \hat{x}_j}{\partial X_\alpha \partial X_\beta} = 0\,. \tag{26}$$

In the case of an incompressible material, the counterpart of Eq. (26) is obtained by using the linear approximation (22) along with the internal constraint (23) as

$$\mathcal{A}_{\alpha i\beta j}\frac{\partial^2 \hat{x}_j}{\partial X_\alpha \partial X_\beta} - \frac{\partial \hat{p}}{\partial x_i} = 0\,. \tag{27}$$

2.2.3 Push forward of the incremental equations

In working with incremental deformations, it is sometimes more convenient to use the deformed configuration β as the reference configuration rather than the initial configuration β_r, in which case the Eulerian form of the incremental quantities are considered (Shams et al., 2011). For this purpose, the updated form of the displacement vector, expressed as a function of **x** instead of **X**, is considered

$$\mathbf{u} = \mathbf{u}(\mathbf{x}) = \hat{\boldsymbol{\chi}}\left(\boldsymbol{\chi}^{-1}(\mathbf{x})\right). \tag{28}$$

The corresponding updated incremental deformation tensor may then be written in terms of the above displacement vector as

$$\hat{\mathbf{F}}_0 = \hat{\mathbf{F}}\mathbf{F}^{-1} = \text{grad}\,\mathbf{u}\,, \tag{29}$$

where a subscript 0 is used to denote a quantity referred to the deformed configuration, also known as the 'push forward' form of that quantity.

The push forward of the incremental nominal stress tensor may be obtained by using the connection $\boldsymbol{\sigma} = J^{-1}\mathbf{F}\mathbf{S}$ from Eq. (5) as

$$\hat{\mathbf{S}}_0 = J^{-1}\mathbf{F}\hat{\mathbf{S}}\,. \tag{30}$$

For a compressible material, the push forward of the nominal stress tensor simplifies, on use of Eq. (21), to

$$\hat{\mathbf{S}}_0 = \boldsymbol{\mathcal{A}}_\mathbf{0}\hat{\mathbf{F}}_\mathbf{0}\,, \tag{31}$$

where $\boldsymbol{\mathcal{A}}_\mathbf{0}$ is the updated form of the elasticity tensor. The components of $\boldsymbol{\mathcal{A}}_\mathbf{0}$ are related to those of $\boldsymbol{\mathcal{A}}$ via

$$\mathcal{A}_{0piqj} = J^{-1}F_{p\alpha}F_{q\beta}\mathcal{A}_{\alpha i\beta j}\,. \tag{32}$$

The updated form elasticity tensor possesses the major symmetry $\mathcal{A}_{0piqj} = \mathcal{A}_{0qjpi}$, which follows directly from equations (13) and (32) (Destrade and Ogden., 2013).

In the case of an incompressible material, the counterpart to Eq. (31) is given by

$$\hat{\mathbf{S}}_0 = \boldsymbol{\mathcal{A}}_\mathbf{0}\hat{\mathbf{F}}_\mathbf{0} + p\hat{\mathbf{F}}_\mathbf{0} - \hat{p}\boldsymbol{I}\,, \tag{33}$$

where the components of $\boldsymbol{\mathcal{A}}_\mathbf{0}$ are again defined as in Eq. (32), with the added restriction $J = 1$. The associated incremental incompressibility constraint (23) may also be updated to the deformed configuration by writing it in terms of $\mathbf{u}$ as

$$\mathrm{tr}\left(\hat{\mathbf{F}}_{\mathbf{0}}\right) \equiv \mathrm{div}\,\mathbf{u} = 0\,. \tag{34}$$

Thus, Eqs. (31) and (33), which is coupled with (34), are the updated forms of the incremental constitutive equations for compressible and incompressible materials respectively.

The incremental equilibrium equation (24) may also be pushed forward to the deformed configuration β as

$$\mathrm{div}\,\hat{\mathbf{S}}_{\mathbf{0}} = \mathbf{0}\,, \tag{35}$$

On use of the updated forms of the incremental constitutive equations, the above equation may be expressed, in terms of components, as

$$\mathcal{A}_{0piqj}\frac{\partial^2 u_j}{\partial x_p \partial x_q} = 0\,, \tag{36}$$

for an unconstrained material, and

$$\mathcal{A}_{0piqj}\frac{\partial^2 u_j}{\partial x_p \partial x_q} - \frac{\partial \hat{p}}{\partial x_i} = 0\,, \tag{37}$$

along with

$$\frac{\partial u_i}{\partial x_i} = 0\,, \tag{38}$$

for an incompressible material.

2.3 Incremental Time Dependent Motion

Section 2.2 has considered the effect of a small static deformation superimposed upon a finite static deformation. In this section, the small deformation is now assumed to be a time dependent motion. The resulting dynamic problem is analogous to that of small-amplitude waves propagating in a pre-stressed body.

2.3.1 Incremental equations of motion

The superimposed incremental displacement $\hat{\mathbf{x}}$ is now considered to be dependent on time and is written as

$$\hat{\mathbf{x}} = \hat{\boldsymbol{\chi}}(\mathbf{X}, t)\,, \tag{39}$$

where t is time. The counterpart of the incremental equilibrium equation (24) corresponding to the dynamic motion in the absence of body forces is then given by

$$\text{Div}\,\hat{\mathbf{S}} = \rho_r \frac{\partial^2}{\partial t^2}\hat{\mathbf{x}}\,, \tag{40}$$

where ρ_r is the mass density in the reference configuration β_r and $\partial/\partial t$ is the Lagrangian or material time derivative.

The above equation may be linearised in the incremental quantities and it may be expanded out, on use of Eq. (25), as

$$\mathcal{A}_{\alpha i \beta j}\frac{\partial^2 \hat{x}_j}{\partial X_\alpha \partial X_\beta} + \frac{\partial \mathcal{A}_{\alpha i \beta j}}{\partial X_\alpha}\frac{\partial \hat{x}_j}{\partial X_\beta} = \rho_r \frac{\partial^2 \hat{x}_i}{\partial t^2}\,, \tag{41}$$

for a compressible material. If the finite deformation is homogeneous, the deformation gradient and the elasticity tensor may be taken to be independent of $\mathbf{X}$ and hence, Eq. (41) reduces to

$$\mathcal{A}_{\alpha i \beta j}\frac{\partial^2 \hat{x}_j}{\partial X_\alpha \partial X_\beta} = \rho_r \frac{\partial^2 \hat{x}_i}{\partial t^2}\,. \tag{42}$$

It is noted here that the incremental motion is assumed to be superimposed on a static finite deformation. Then, the components of the elasticity tensor $\mathcal{A}_{\alpha i \beta j}$ are not dependent on time but are instead constants involving material properties as well as the deformation gradient (Ogden, 2007).

In the case of an incompressible material, the counterpart of Eq. (42) may be obtained, on use of Eq (27), as

$$\mathcal{A}_{\alpha i\beta j}\frac{\partial^2 \hat{x}_j}{\partial X_\alpha \partial X_\beta}-\frac{\partial \hat{p}}{\partial x_i}=\rho_r\frac{\partial^2 \hat{x}_i}{\partial t^2}\,, \tag{43}$$

and the coupled incremental incompressibility constraint is given by Eq. (23).

2.3.2 Push-forward of the incremental equations of motion

In the above equations, the independent variables are understood to be **X** and t but the Eulerian description with **x** and t as the independent variables may equivalently be used. In this case, the updated form of the incremental displacement is written as

$$\mathbf{u}=\mathbf{u}(\mathbf{x},t)=\hat{\boldsymbol{\chi}}(\boldsymbol{\chi}^{-1}(\mathbf{x}),t)\,. \tag{44}$$

The incremental equation of motion (42) for an unconstrained material may be updated to the deformed configuration β by expressing it in terms of **u** and $\boldsymbol{\mathcal{A}_0}$ as

$$\mathcal{A}_{0piqj}\frac{\partial^2 u_j}{\partial x_p \partial x_q}=\rho\ddot{u}_i\,, \tag{45}$$

where $\rho=\rho_r J^{-1}$ is the mass density in β and a superposed dot is used to indicate partial differentiation with respect to time.

Similarly, the pushed forward form of the incremental equation of motion (43) for an incompressible material may be written as

$$\mathcal{A}_{0piqj}\frac{\partial^2 u_j}{\partial x_p \partial x_q}-\frac{\partial \hat{p}}{\partial x_i}=\rho\ddot{u}_i\,, \tag{46}$$

where $\rho=\rho_r$, which follows from the incompressibility constraint (4). The associated incremental incompressibility constraint takes the same form as Eq. (38). This concludes the derivation of the theory of incremental motions superimposed on a finite deformation, which forms the basis of the theoretical framework used in the study of the acoustoelastic effect.

2.4 Strain Energy Functions

The framework described in the previous section allows the acoustoelastic effect to be investigated by considering the propagation of small-amplitude homogeneous plane waves in the pre-deformed body (Destrade and Ogden, 2013). The mechanical response is also dependent on the material properties of the body, which are specified by means of the strain energy function.

For a hyperelastic material, the strain energy function W is a function of the deformation gradient $\mathbf{F}$, i.e. $W = W(\mathbf{F})$. By objectivity, W depends on $\mathbf{F}$ only through the right Cauchy-Green strain tensor, defined by $\mathbf{C} = \mathbf{F}^{\mathbf{T}}\mathbf{F}$ (Shams et al., 2011) but this form of W is otherwise completely general and no material symmetry is enforced. If the material is isotropic relative to the reference configuration β_r, then W is also an isotropic function of $\mathbf{C}$. It follows that W can be expressed as a function of three independent invariants of $\mathbf{C}$ (Ogden, 2007). These are usually taken to be the principal invariants of $\mathbf{C}$, which are defined by

$$I_1 = \operatorname{tr}\mathbf{C}, \qquad I_2 = \frac{1}{2}[(\operatorname{tr}\mathbf{C})^2 - \operatorname{tr}(\mathbf{C^2})], \qquad I_3 = \det\mathbf{C}\,. \tag{47}$$

In the case of an unconstrained material, the nominal stress tensor $\mathbf{S}$ may be written in terms of these invariants as

$$\mathbf{S} = 2W_1\mathbf{F}^{\mathrm{T}} + 2W_2(I_1\mathbf{I} - \mathbf{C})\,\mathbf{F}^{\mathrm{T}} + 2\,I_3W_3\mathbf{F}^{-1}\,, \tag{48}$$

where $W_i = \partial W/\partial I_i$, $i \in \{1,2,3\}$. The corresponding Cauchy stress tensor $\boldsymbol{\sigma}$ may be obtained via the connection in Eq. (5) as

$$J\boldsymbol{\sigma} = 2W_1\mathbf{B} + 2W_2(I_1\mathbf{B} - \mathbf{B}^2) + 2\,I_3\,W_3\mathbf{I}\,, \tag{49}$$

where $J = \mathrm{I}_3^{1/2}$ and $\mathbf{B}$ is the left Cauchy-Green deformation tensor, defined by $\mathbf{B} = \mathbf{F}\mathbf{F}^{\mathrm{T}}$.

The elasticity tensor $\boldsymbol{\mathcal{A}_0}$ may also be expressed in terms of the invariants as

$$
\begin{aligned}
J\mathcal{A}_{0piqj} = \; & 2(W_1 + I_1 W_2)\, B_{pq}\delta_{ij} \\
& + \; 2W_2\left[2B_{pi}B_{qj} - B_{iq}B_{jp} - B_{pr}B_{rq}\delta_{ij} - B_{pq}B_{ij}\right] \\
& + 2I_3 W_3\left(2\delta_{ip}\delta_{jq} - \delta_{iq}\delta_{jp}\right) + 4W_{11}B_{ip}B_{jq} \\
& + \; 4W_{22}\left(I_1 B_{ip} - B_{ir}B_{rp}\right)\left(I_1 B_{jq} - B_{js}B_{sq}\right) \\
& + \; 4W_{12}\left(2I_1 B_{ip}B_{jq} - B_{ip}B_{jr}B_{rq} - B_{jq}B_{ir}B_{rp}\right) \\
& + \; 4I_3 W_{13}\left(B_{ip}\delta_{jq} + B_{jq}\delta_{ip}\right) \\
& + \; 4I_3 W_{23}\left[I_1\left(B_{ip}\delta_{jq} + B_{jq}\delta_{ip}\right) - \delta_{ip}B_{jr}B_{rq}\right. \\
& \left. - \delta_{jq}B_{ir}B_{rp}\right] + \; 4I_3^2 W_{33}\delta_{ip}\delta_{jq}\,,
\end{aligned}
\tag{50}
$$

where B_{ij} are the components of $\mathbf{B}$, δ_{ij} is the Kronecker delta and $W_{ij} = \partial^2 W/\partial I_i\, \partial I_j,\ i,j \in \{1,2,3\}$.

For an incompressible material, the internal constraint (4) means that $I_3 = 1$ for all deformations and thus, the strain energy function is only a function of I_1 and I_2, i.e. $W = W(I_1, I_2)$. Hence, the counterpart to Eqs. (48), (49) and (50) may be obtained as

$$
\mathbf{S} = 2W_1\mathbf{F}^{\mathrm{T}} + 2W_2(I_1\mathbf{I} - \mathbf{C})\,\mathbf{F}^{\mathrm{T}} - p\mathbf{F}^{-1}\,, \tag{51}
$$

$$
\boldsymbol{\sigma} = 2W_1\mathbf{B} + 2W_2(I_1\mathbf{B} - \mathbf{B}^2) - p\mathbf{I}\ , \tag{52}
$$

and,

$$
\begin{aligned}
\mathcal{A}_{0piqj} = \; & 2(W_1 + I_1 W_2)\, B_{pq}\delta_{ij} \\
& + \; 2W_2\left[2B_{pi}B_{qj} - B_{iq}B_{jp} - B_{pr}B_{rq}\delta_{ij} - B_{pq}B_{ij}\right] \\
& + 4W_{11}B_{ip}B_{jq} \\
& + \; 4W_{22}\left(I_1 B_{ip} - B_{ir}B_{rp}\right)\left(I_1 B_{jq} - B_{js}B_{sq}\right) \\
& + \; 4W_{12}\left(2I_1 B_{ip}B_{jq} - B_{ip}B_{jr}B_{rq} - B_{jq}B_{ir}B_{rp}\right),
\end{aligned}
\tag{53}
$$

respectively. For details on the derivation of the above equations, the reader is referred to Ogden (2007) and Shams et al. (2011).

The strain energy function W may also be considered to depend on the three principal stretches λ_1, λ_2, λ_3 of the deformation, i.e. $W = \overline{W}(\lambda_1, \lambda_2, \lambda_3)$,

rather than the principal invariants of $\boldsymbol{C}$. The principal stretches are the square roots of the eigenvalues of $\boldsymbol{C}$ and are related to the principal invariants by the relations (Ogden 1984)

$$I_1 = \lambda_1^2 + \lambda_2^2 + \lambda_3^2, \qquad I_2 = \lambda_1^2\lambda_2^2 + \lambda_1^2\lambda_3^2 + \lambda_2^2\lambda_3^2, \qquad I_3 = \lambda_1^2\lambda_2^2\lambda_3^2. \tag{54}$$

For an unconstrained material, the principal Cauchy stresses can be expressed in terms of the stretches as

$$J\sigma_i = \lambda_i \overline{W}_i \,, \tag{55}$$

where $J = \lambda_1\lambda_2\lambda_3$ and $\overline{W}_i = \partial\overline{W}/\partial\lambda_i,\ i \in \{1,2,3\}$. The components of the elasticity tensor can also be obtained in terms of the stretches. When referred to the principal axes of $\boldsymbol{C}$, the non-zero components of $\boldsymbol{\mathcal{A}_0}$ are given by (Ogden 1984)

$$\begin{aligned}
J\mathcal{A}_{0iijj} &= \lambda_i\lambda_j\overline{W}_{ij} \,, \\
J\mathcal{A}_{0ijij} &= (\lambda_i\overline{W}_i - \lambda_j\overline{W}_j)\,\lambda_i^2/(\lambda_i^2 - \lambda_j^2), \qquad i \neq j, \lambda_i \neq \lambda_j \\
J\mathcal{A}_{0ijji} &= (\lambda_j\overline{W}_i - \lambda_i\overline{W}_j)\,\lambda_i\lambda_j\,/(\lambda_i^2 - \lambda_j^2), \qquad i \neq j, \lambda_i \neq \lambda_j \\
J\mathcal{A}_{0ijij} &= (\lambda_i^2\overline{W}_{ii} - \lambda_i\lambda_j\overline{W}_{ij} + \lambda_i\overline{W}_i)/2, \qquad i \neq j, \lambda_i = \lambda_j \\
J\mathcal{A}_{0ijji} &= (\lambda_i^2\overline{W}_{ii} - \lambda_i\lambda_j\overline{W}_{ij} - \lambda_i\overline{W}_i)/2, \qquad i \neq j, \lambda_i = \lambda_j
\end{aligned} \tag{56}$$

where $\overline{W}_{ij} = \partial^2\overline{W}/\partial\lambda_i\partial\lambda_j, i,j \in \{1,2,3\}$ and there is no sum on repeated indices.

In the case of an incompressible material, the strain energy function $W = \overline{W}(\lambda_1,\lambda_2,\lambda_3)$ is also subject to the internal constraint $\lambda_1\lambda_2\lambda_3 = 1$. The counterpart to Eq. (55) for the principal Cauchy stresses is then given by

$$\sigma_i = \lambda_i\overline{W}_i - p \,, \tag{57}$$

while the corresponding expression for the elasticity tensor $\boldsymbol{\mathcal{A}_0}$ is obtained by setting $J = 1$ in Eq. (56).

It is worth noting that the internal constraint $\lambda_1\lambda_2\lambda_3 = 1$ means that only two out of the three principal stretches are independent. The strain energy function can thus be written as a function of λ_1 and λ_2 only, with $\lambda_3 = \lambda_1^{-1}\lambda_2^{-1}$, i.e. $W = \widehat{W}(\lambda_1, \lambda_2)$. This allows the scalar p to be eliminated from Eq. (57), yielding the principal stress differences (Ogden 1984)

$$\sigma_1 - \sigma_3 = \lambda_1 \frac{\partial \widehat{W}}{\partial \lambda_1}, \qquad \sigma_2 - \sigma_3 = \lambda_2 \frac{\partial \widehat{W}}{\partial \lambda_2}. \tag{58}$$

2.5 Concluding Remarks

In this chapter, the fundamentals of the theory of incremental motions superimposed on a finite deformation were reviewed. This theory forms the basis of the theoretical framework used in the study of the acoustoelastic effect. This framework will be employed in the next chapter to analyse the propagation of Lamb waves in a pre-stressed compressible plate along a principal direction. The next chapter and the subsequent chapters consist of a combination of the candidate's publications, which are based on the theoretical framework describe above.

References

Beatty, M.F. (1987), Topics in finite elasticity: hyperelasticity of rubber, elastomers, and biological tissues—with examples, *Applied Mechanics Reviews*, 40, 1699-1734, doi:10.1115/1.3149545.

Chadwick, P. and Ogden, R.W. (1971), On the definition of elastic moduli, *Archive for Rational Mechanics and Analysis*, 44, 41-53, doi: 10.1007/BF00250827

Destrade, M. and Ogden, R.W. (2013), On stress-dependent elastic moduli and wave speeds, *IMA Journal of Applied Mathematics*, 78, 965-997, doi: 10.1093/imamat/hxs003.

Dorfmann, A.L. (2009), Modeling of Rubberlike Materials, in Advances in Constitutive Relations Applied in Computer Codes, edited by J. Klepaczko and T. Łodygowski, pp. 147-202, CISM International Centre for Mechanical Sciences, Springer, Vienna, doi: 10.1007/978-3-211-99709-3_2.

Green, A.E. and Zerna, W. (1992), Theoretical Elasticity, Dover Publications, New York.

Hackett, R.M. (2016), Stress Measures, in Hyperelasticity Primer, Springer, Cham, doi: 10.1007/978-3-319-23273-7_5.

Holzapfel, G.A. (2000), Nonlinear Solid Mechanics. A Continuum Approach for Engineering, John Wiley & Sons, Chichester.

Ogden, R.W. (1984), Non-Linear Elastic Deformations, Ellis Horwood, Chichester.

Ogden, R.W. (2001), Elements of the Theory of Finite Elasticity, in Nonlinear Elasticity: Theory and Applications, edited by Y. Fu and R. Ogden, pp. 1-57, London Mathematical Society Lecture Note Series, Cambridge University Press, Cambridge, doi: 10.1017/CBO9780511526466.002.

Ogden, R.W. (2007), Incremental statics and dynamics of pre-stressed elastic materials, in Waves in Nonlinear Pre-Stressed Materials, edited by M. Destrade

and G. Saccomandi, pp. 1–26, CISM Courses and Lectures, Springer Vienna, doi: 10.1007/978-3-211-73572-5_1.

Shams, M. (2010), Wave propagation in residually-stressed materials, PhD thesis, University of Glasgow.

Shams, M., Destrade, M. and Ogden, R.W. (2011), Initial stresses in elastic solids: Constitutive laws and acoustoelasticity, *Wave Motion*, 48, 552-567, doi: 10.1016/j.wavemoti.2011.04.004.

Truesdell, C. and Noll, W. (1965), The Non-Linear Field Theories of Mechanics, Springer-Verlag, Berlin Heidelberg, doi: 10.1007/978-3-662-10388-3.

Chapter 3

Effect of uniaxial stress on the propagation of higher-order Lamb wave modes

Statement of Authorship

Title of Paper	Effect of uniaxial stress on the propagation of higher-order Lamb wave modes.
Publication Status	☑ Published ☐ Accepted for Publication ☐ Submitted for Publication ☐ Unpublished and Unsubmitted w ork w ritten in manuscript style
Publication Details	M. Mohabuth, A. Kotousov and C.T. Ng (2016), Effect of uniaxial stress on the propagation of higher-order Lamb wave modes, *Int. J. Non-Linear Mech.*, 86, 104-11, doi: 10.1016/j.ijnonlinmec.2016.08.006

Principal Author

Name of Principal Author (Candidate)	Munawwar Mohabuth		
Contribution to the Paper	Developed the analytical model, performed all analyses and wrote manuscript.		
Overall percentage (%)	70		
Certification:	This paper reports on original research I conducted during the period of my Higher Degree by Research candidature and is not subject to any obligations or contractual agreements with a third party that would constrain its inclusion in this thesis. I am the primary author of this paper.		
Signature		Date	22 November 2018

Co-Author Contributions

By signing the Statement of Authorship, each author certifies that:

i. the candidate's stated contribution to the publication is accurate (as detailed above);

ii. permission is granted for the candidate in include the publication in the thesis; and

iii. the sum of all co-author contributions is equal to 100% less the candidate's stated contribution.

Name of Co-Author	Andrei Kotousov		
Contribution to the Paper	Supervised the development of the analytical model, helped in interpretation of the results and assisted in the preparation of the manuscript.		
Signature		Date	22 November 2018

Name of Co-Author	Ching-Tai Ng		
Contribution to the Paper	Supervised the work and assisted with editing of the manuscript.		
Signature		Date	16 November 2018

Effect of Uniaxial Stress on the Propagation of Higher–Order Lamb Wave Modes

Munawwar Mohabuth[1*], Andrei Kotousov[1] and Ching-Tai Ng[2]

[1]School of Mechanical Engineering, The University of Adelaide, Adelaide, SA 5005, Australia.

[2]School of Civil, Environmental and Mining Engineering, The University of Adelaide, Adelaide, SA 5005, Australia.

*Corresponding author. Tel.: +61 8 8313 6385.

E-mail address: munawwar.mohabuth@adelaide.edu.au

Abstract

On the basis of the non-linear theory of elasticity and the invariant based formulation developed by Ogden, we analyse the effect of homogeneous stress on the propagation of Lamb waves. Using the theory of incremental deformations superimposed on large deformations, we derive the equations governing the propagation of small amplitude waves in a pre-stressed plate. By enforcing traction-free boundary conditions at the surfaces of the plate, we further obtain the characteristic equations for symmetric and anti-symmetric Lamb wave modes and investigate the effect of stress on the phase velocity, i.e. the acoustoelastic effect. A comparison with experimental data exhibits a better correlation than previously published results. The outcomes of this study can be utilised in the development of new techniques for the measurement of applied stresses based on the acoustoelastic effect. In particular, a strong sensitivity of the phase velocity to the applied stress near the cut-off frequencies of higher-order Lamb wave modes is a very promising option, which seems to have been overlooked in previous studies.

1. Introduction

The study of wave propagation problems in pre-stressed media has been the subject of much research over the past century. However, early works in this area were restricted to linear elasticity and the effect of small deformations on the propagation of small amplitude waves; see, for example, the pioneering contribution by Biot [1,2]. It was not until the development of the finite deformation theory by Murnaghan [3,4] that the non-linear effects of stresses were taken into account.

Two non-linear phenomena are associated with applied stresses: (1) a weak change of the local elastic behaviour of the material, and, (2) a weak non-linearity of the governing equations. As a result, the presence of initial stresses can have a substantial influence on the propagation of elastic waves in solids. In particular, these stresses affect the velocity, attenuation, dispersion and the non-linear aspects of the propagation of bulk waves. This interplay between the applied stress and the properties of the wave forms a conceptual foundation for the practical measurement of stresses in structural components.

The acoustoelastic effect is a non-linear phenomenon that describes the change in the speed of small amplitude waves in an elastic body due to the presence of a static pre-stress [5]. The theory of acoustoelasticity for bulk waves was initially developed by Hughes & Kelly [6] who derived equations relating the wave velocity to the applied stress for isotropic materials subjected to uniaxial and hydrostatic loading. Their work was subsequently generalised by Toupin & Bernstein [7] and Thurston & Brugger [8] to materials of arbitrary crystal symmetry.

Acoustoelasticity is now a well-established procedure utilised in the non-destructive evaluation of applied and residual stresses. Its underlying principles have been comprehensively described in the reviews by Pao *et al.* [9] and Guz & Makhort [10]. Ultrasonic bulk waves and the acoustoelastic effect have been used over the past sixty years in the measurement and control of residual stresses in welded structures and railroad rails, the tightening of bolts and the assessment of stress levels in bars as well as in multi-wire strands [11].

Acoustoelastic procedures are largely based on the measurements of the time-of-flight of an ultrasonic pulse. However, the relative change in the phase velocity, which is directly proportional to the applied stress, is small and therefore, measurements must be performed with very high accuracy. Nevertheless, the main obstacles in ultrasonic pulse techniques are the influences of the microstructure, composition gradients and plastic deformations on the phase velocity, which can all produce changes in the velocity comparable to those due to applied or residual stresses.

With the current ultrasonic testing procedures, it is virtually impossible to distinguish between applied and residual stresses as the length scales of the measurements are often comparable with the length scales of the residual stresses due to fabrication. The latter is normally related to the characteristic size of the cross-sectional area. The use of guided waves instead of bulk waves is promising because guided waves can propagate over distances much larger than the characteristic size of residual stresses. In particular, guided waves in plate-like structures, also known as Lamb waves, have been found to be sensitive to changes in structural properties, temperature and stress [12,13]. Despite that, there has not been much research on the theory of acoustoelasticity in regards to Lamb waves.

The paper by Gandhi *et al.* [14] provides a fairly comprehensive acoustoelastic formulation to analyse the effect of biaxial loading in initially isotropic plates. However, their work is restricted to small initial strains such that the elasticity tensor is obtained to the first order in the infinitesimal strain tensor. In the current work, we extend the framework developed by Ogden [15] for incremental deformations superimposed on large deformations and utilise an invariant-based formulation of the strain-energy function. The wave propagation is considered as an infinitesimal deformation which is superimposed onto a finite static homogeneous deformation. The dispersion relations derived are similar to those obtained by Roxburgh & Ogden [16] for a pre-stressed compressible elastic plate. However, the latter authors did not investigate the acoustoelastic effect but instead focused on vibration and stability phenomena.

In recent years, there have been several important contributions related to the dispersion of small amplitude waves in pre-stressed layers, albeit in a different context to acoustoelasticity. The main motivation behind these contributions was to derive asymptotic models to describe the wave motion in the long and short wave limits. In particular, Kaplunov *et al.* [17-19] developed asymptotic theories to describe the long-wave low-frequency, long-wave high-frequency and short-wave motion along a principal direction in pre-stressed incompressible layers. These theories were then extended by Pichugin & Rogerson [20-22] to consider wave propagation along a non-principal direction. The dynamic response of pre-stressed compressible layers was also studied and we mention the asymptotic models developed by Nolde *et al.* [23], Rogerson & Prikazchikova [24] and Kayestha *et al.* [25]. The derivation of such models is highly desirable as they readily allow for the qualitative analysis of fundamental as well as higher-order wave modes. A detailed asymptotic analysis is beyond the scope of the current paper but the reader is pointed to the books by Berdichevsky [26] and Kaplunov [27] for a comprehensive discussion on the subject.

The aim of the current paper is to investigate the effect of pre-stress on the speed of propagation of Lamb waves. The work of Nolde *et al.* [23] is the most relevant to the present study. The authors derive dispersion relations for wave propagation along a principal direction for a general strain energy function, expressed in terms of invariants of the left Cauchy-Green strain tensor. Motivated by the industrial application of rubber-like materials, numerical results are then presented for the neo-Hookean, Varga and Blatz-Ko strain energy functions. A similar approach is followed in the current paper but the strain energy function is expressed in terms of a different set of invariants. The paper is organised as follows. In Section 2, we review the equations governing incremental motions superimposed on a finite deformation and the constitutive equation for an isotropic hyperelastic pre-stressed solid. The characteristic equations for symmetric and anti-symmetric Lamb wave modes are then derived in Section 3 by considering the propagation of plane waves along the direction of the applied load and by enforcing traction-free boundary conditions at the

surfaces of the plate. These equations are subsequently specialised in Section 4 to the case of weakly non-linear elasticity by considering the Murnaghan form of strain energy function, which is applicable to a large class of engineering materials. Finally, in Section 5, we solve these equations numerically and compare the dispersion results with previously published results and experimental data.

2. Governing Equations

The governing equations used in the theory of acoustoelasticity are briefly reviewed here based on the work of Destrade & Ogden [28]. First, we recall the equations for incremental motions and the constitutive equation for pre-stressed solid. Then, we consider an invariant based formulation of the strain energy function and provide an expression for the components of the elasticity tensor in terms of the invariants. This general framework will be utilised to derive the dispersion relations for acoustoelastic Lamb wave propagation.

2.1 Incremental motions

Following the development by Ogden [29], we consider an isotropic hyperelastic body of density ρ_r in some stress-free reference configuration, denoted by β_r. Suppose the body is subjected to a finite static pure homogeneous deformation, so that it occupies a new configuration, denoted by β_0, referred to as the deformed configuration. The corresponding deformation gradient relating β_r to β_0 is then given by $\mathbf{F} = \partial \boldsymbol{x}/\partial \boldsymbol{X}$, where $\boldsymbol{x}$ is the position vector in β_0 of a particle located at $\mathbf{X}$ in β_r. For a body without internal constraints, the nominal and Cauchy stress tensors are given by

$$\mathbf{S} = \frac{\partial W}{\partial \mathbf{F}}, \qquad \boldsymbol{\sigma} = J^{-1}\mathbf{F}\frac{\partial W}{\partial \mathbf{F}}, \tag{1}$$

respectively, where $\mathrm{W} = \mathrm{W}(\mathbf{F})$ is the strain energy function per unit reference volume and $J = \det \mathbf{F}$.

Next, we consider the superposition of a small-amplitude time-dependent motion upon the static finite deformation. It is then more convenient to use the deformed configuration β_0 as the reference configuration rather than the initial configuration β_r and for this purpose, we define $\boldsymbol{u}(\boldsymbol{x},\mathrm{t})$ as the displacement vector relative to β_0. The corresponding incremental constitutive relation is given in component form by

$$\hat{\mathrm{S}}_{0_{pi}} = \mathcal{A}_{0_{piqj}}\, u_{j,q}\,, \tag{2}$$

where $\hat{\mathrm{S}}_{0_{pi}}$ are the components of the incremental nominal stress tensor, $\mathcal{A}_{0_{piqj}}$ are the components of the fourth-order elasticity tensor of instantaneous elastic moduli and a comma indicates partial differentiation with respect to the Eulerian coordinates.

The incremental governing equations of motion can be written in terms of the components of the elasticity tensor as

$$\mathcal{A}_{0piqj}\, u_{j,pq} = \rho \ddot{u}_i\,, \tag{3}$$

where $\rho = \rho_r J^{-1}$ is the density of the material in the deformed configuration β_0 and a superposed dot indicates partial differentiation with respect to time. The components of the elasticity tensor $\mathcal{A}_{0_{piqj}}$ can be expressed in terms of the strain energy function W as

$$\mathcal{A}_{0piqj} = J^{-1} F_{p\alpha} F_{q\beta} \frac{\partial^2 W}{\partial F_{i\alpha} \partial F_{j\beta}}\,, \tag{3}$$

and we note the major symmetry $\mathcal{A}_{0piqj} = \mathcal{A}_{0qjpi}$ [28].

For a more comprehensive overview of the theory of incremental deformations superimposed on a finite deformation, we refer to Ogden [15,29].

2.2 Invariant-based formulation

The strain-energy function W is required to be objective, which means that W depends on **F** only through the right Cauchy-Green deformation tensor, defined

by $\mathbf{C} = \mathbf{F}^{\mathrm{T}}\mathbf{F}$. Since the material is also assumed to be isotropic relative to β_r, W can be expressed as a function of the principal invariants of $\mathbf{C}$, given by

$$I_1 = \mathrm{tr}\,\mathbf{C}, \qquad I_2 = \frac{1}{2}[(\mathrm{tr}\,\mathbf{C})^2 - \mathrm{tr}\,(\mathbf{C^2})], \qquad I_3 = \det \mathbf{C}\,. \tag{5}$$

The nominal stress tensor and the elasticity tensor can be expanded out in terms of I_1, I_2 and I_3. These involve the computation of

$$\frac{\partial W}{\partial \mathbf{F}} = \sum_{i=1}^{3} W_i \frac{\partial I_i}{\partial \mathbf{F}}, \tag{6}$$

and

$$\frac{\partial^2 W}{\partial \mathbf{F}\,\partial \mathbf{F}} = \sum_{i=1}^{3} W_i \frac{\partial^2 I_i}{\partial \mathbf{F}\,\partial \mathbf{F}} + \sum_{i=1}^{3}\sum_{j=1}^{3} W_{ij} \frac{\partial I_i}{\partial \mathbf{F}} \otimes \frac{\partial I_j}{\partial \mathbf{F}}\,, \tag{7}$$

where $W_i = \partial W/\partial I_i$ and $W_{ij} = \partial^2 W/\partial I_i\,\partial I_j$. The expressions for the derivatives of the invariants, $\partial I_i/\partial \mathbf{F}$ and $\partial^2 I_i/\partial \mathbf{F}\partial \mathbf{F}$, were derived by Shams *et al.* [30] and are not repeated here for brevity.

These expressions enable the nominal stress tensor, $\mathbf{S}$, to be written out as

$$\mathbf{S} = 2\,W_1\,\mathbf{F}^{\mathrm{T}} + 2\,W_2\,(I_1\mathbf{I} - \mathbf{C})\,\mathbf{F}^{\mathrm{T}} + 2\,I_3\,W_3\,\mathbf{F}^{-1}\,. \tag{8}$$

Similarly, the Cauchy stress tensor, $\boldsymbol{\sigma}$, is given by

$$J\,\boldsymbol{\sigma} = 2\,W_1\,\mathbf{B} + 2\,W_2\,(I_1\mathbf{B} - \mathbf{B}^2) + 2\,I_3\,W_3\,\mathbf{I}\,, \tag{9}$$

where $\mathbf{B} = \mathbf{F}\mathbf{F}^{\mathrm{T}}$ is the left Cauchy-Green deformation tensor. The elasticity tensor can also be expressed in terms of the derivatives of the invariants. In component form, it is given by

$$
\begin{aligned}
J\mathcal{A}_{0piqj} = \; & 2(W_1 + I_1 W_2)\, B_{pq}\delta_{ij} \\
& + \; 2W_2\big[2B_{pi}B_{qj} - B_{iq}B_{jp} - B_{pr}B_{rq}\delta_{ij} \\
& - B_{pq}B_{ij}\big] + 2I_3 W_3\big(2\delta_{ip}\delta_{jq} - \delta_{iq}\delta_{jp}\big) \\
& + 4W_{11}B_{ip}B_{jq} \\
& + \; 4W_{22}\big(I_1 B_{ip} - B_{ir}B_{rp}\big)\big(I_1 B_{jq} - B_{js}B_{sq}\big) \\
& + \; 4W_{12}\big(2I_1 B_{ip}B_{jq} - B_{ip}B_{jr}B_{rq} - B_{jq}B_{ir}B_{rp}\big) \\
& + \; 4I_3 W_{13}\big(B_{ip}\delta_{jq} + B_{jq}\delta_{ip}\big) \\
& + \; 4I_3 W_{23}\big[I_1\big(B_{ip}\delta_{jq} + B_{jq}\delta_{ip}\big) - \delta_{ip}B_{jr}B_{rq} \\
& - \delta_{jq}B_{ir}B_{rp}\big] + \; 4I_3^2 W_{33}\delta_{ip}\delta_{jq}\,,
\end{aligned}
\tag{10}
$$

where B_{ij} are the components of the left Cauchy-Green deformation tensor, **B**. The above expression is the specialised form of the elasticity tensor for a pre-stressed isotropic elastic solid, given in Destrade & Ogden [28]. An equivalent expression can be found in Nolde *et al.* [23] but we note that the latter authors have used a different set of invariants.

3. Acoustoelastic Lamb Wave

The general framework described in Section 2 allows the acoustoelastic effect to be investigated by considering the propagation of plane waves in infinite media [28]. In this section, we shall extend this framework to study the propagation of Lamb waves in a pre-stressed plate, along the loading direction. The equations developed have the same canonical form as those derived by Nayfeh & Chimenti [31] for Lamb waves propagating along the principal axes for materials of orthotropic or higher symmetry.

3.1 Uniform extension with lateral contraction

We consider an infinite isotropic plate of thickness D, with the reference Cartesian coordinate system $\mathbf{X} = (X_1, X_2, X_3)$ aligned as shown in Figure 1. The origin of the coordinate system lies at the mid-plane of the plate and the normal to the surface coincides with the X_2 axis of the coordinate system.

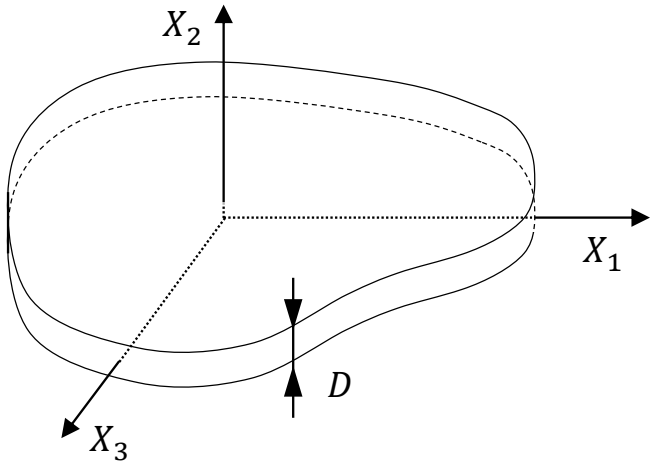

Figure 1. Alignment of the reference Cartesian coordinate system, with its origin lying at the mid-plane of the plate.

Suppose the plate is subjected to a pure homogeneous finite static deformation from the reference configuration. If the Lagrangian and Eulerian Cartesian basis vectors are chosen to coincide with the principal directions of the pre-strain, then the deformation can be expressed as

$$\mathrm{x}_1 = \lambda_1 \mathrm{X}_1, \qquad \mathrm{x}_2 = \lambda_2 \mathrm{X}_2, \qquad \mathrm{x}_3 = \lambda_3 \mathrm{X}_3 , \tag{11}$$

where $\lambda_1, \lambda_2, \lambda_3$ are the principal stretches. As a result, the deformation gradient tensor and the Cauchy-Green deformation tensors are given by $\mathbf{F} = \mathrm{diag}(\lambda_1, \lambda_2, \lambda_3)$ and $\mathbf{B} = \mathbf{C} = \mathrm{diag}\left(\lambda_1{}^2, \lambda_2{}^2, \lambda_3{}^2\right)$ respectively. The principal invariants of $\mathbf{C}$ thus reduce to

$$I_1 = \lambda_1{}^2 + \lambda_2{}^2 + \lambda_3{}^2, \qquad I_2 = \lambda_1{}^2\lambda_2{}^2 + \lambda_2{}^2\lambda_3{}^2 + \lambda_3{}^2\lambda_1{}^2, \qquad I_3 = \lambda_1{}^2 \lambda_2{}^2 \lambda_3{}^2 . \tag{12}$$

We also note that, when referred to axes aligned with the principal axes of pre-strain, the only non-zero components of the elasticity tensor are given by $\mathcal{A}_{0iiii}, \mathcal{A}_{0iijj,}, \mathcal{A}_{0ijij}$ and $\mathcal{A}_{0ijji}, i \neq j$ with $i, j \in \{1,2,3\}$ [15].

We now specialise the deformation to uniaxial tension and assume that the plate has been pre-stressed by the application of a Cauchy stress σ such that the plate is finitely deformed. Without loss of generality, we may take the uniaxial Cauchy stress σ to be along the x_1 axis, such that $\sigma_1 = \sigma$ and the corresponding principal stretch is λ_1. Since there is symmetry perpendicular to the x_1 axis, as the plate was considered to be isotropic in the absence of pre-stress, then λ_2 is equal to λ_3 [15].

For a given uniaxial stress field and strain energy function, the principal stretches can be determined by inverting the connection in equation (9) and using the expression in equation (12). The components of the elasticity tensor, $\mathcal{A}_{0piqj}$, can subsequently be determined using equation (10). In particular, we note that the uniaxial stress field leads to strain induced anisotropy, and as a result, the elastic response of the plate becomes transversely isotropic in nature [28]. However, the elasticity tensor does not possess the same symmetries as the elasticity tensor in the case of classical transversely isotropic linear elasticity.

3.2 Lamb Wave Dispersion Equation

The propagation of acoustoelastic Lamb waves for a homogeneous uniaxial stress field requires the equation governing incremental motions superimposed on a finite deformation as given by equation (3) to be solved, in conjunction with stress-free boundary conditions at the surfaces of the plate.

In this paper, we restrict our attention to the plane strain incremental problem of wave propagation along the direction of the applied uniaxial stress only. The wave motion is modeled as

$$u_j = U_j e^{i\xi(x_1+\alpha x_2-ct)}, \qquad j = 1,2\ , \tag{13}$$

where u_j is the particle displacement, U_j is the amplitude of the displacement, ξ is the wavenumber along the x_1 direction, α is the ratio of the wavenumbers in the x_2 direction to that in the x_1 direction and c is the phase velocity in the x_1 direction. This general form represents plane waves, confined to the $x_1 - x_2$ plane, travelling with a velocity of c in the x_1 direction.

Substituting equation (13) into the equation of motion (3) yields an eigenvalue problem. Using tensor analysis, it is easy to see that $u_{j,pq}$ and $u_{i,tt}$ are given by

$$u_{j,pq} = (-\xi^2)(\beta_{pq})u_j \,, \tag{14}$$

and

$$u_{i,tt} = (-\xi^2)(c^2)\, u_j \delta_{ij} \tag{15}$$

respectively, where $\beta_{pq} = \begin{bmatrix} 1 & \alpha \\ \alpha & \alpha^2 \end{bmatrix}$ and δ_{ij} is the Kronecker delta function.

The eigenvalue problem can be expressed as

$$(\mathcal{A}_{0piqj}\beta_{pq} - \rho c^2 \delta_{ij})u_j = 0 \,, \tag{16}$$

which is a form of the well-known Christoffel equation for anisotropic media [32]. Here, we define a modified form of the Christoffel acoustic tensor as

$$K_{ij} = \mathcal{A}_{0piqj}\beta_{pq} - \rho c^2 \delta_{ij}. \tag{17}$$

Expanding the acoustic tensor, noting that i and j are free indices while p and q are summed over, yields

$$\begin{aligned} K_{11} &= \rho c^2 - \mathcal{A}_{01111} - \mathcal{A}_{02121}\alpha^2 \,, \\ K_{12} &= -\alpha(\mathcal{A}_{01122} + \mathcal{A}_{01221}) \,, \\ K_{21} &= -\alpha(\mathcal{A}_{01221} + \mathcal{A}_{01122}) \,, \\ K_{22} &= \rho c^2 - \mathcal{A}_{01212} - \mathcal{A}_{02222}\alpha^2 \,, \end{aligned} \tag{18}$$

For non-trivial solutions to the eigenvalue problem, the determinant of the acoustic tensor must go to zero. This yields a fourth order equation in α which can be expressed as

$$\mathrm{P}_4\, \alpha^4 + \mathrm{P}_2\, \alpha^2 + \mathrm{P}_0 \, = 0 \,, \tag{19}$$

where the coefficients P_4 , P_2 and P_0 are given by

$$
\begin{aligned}
&\mathrm{P}_4 = \mathcal{A}_{02121}\mathcal{A}_{02222}\,,\\
&\mathrm{P}_2 = -\rho c^2(\mathcal{A}_{02222} + \mathcal{A}_{02121}) + \mathcal{A}_{02222}\mathcal{A}_{01111}\\
&\qquad\qquad + \mathcal{A}_{02121}\mathcal{A}_{01212} - \mathcal{A}_{01122}\mathcal{A}_{01221}\\
&\qquad\qquad - \mathcal{A}_{01122}\mathcal{A}_{01122} - \mathcal{A}_{01221}\mathcal{A}_{01221}\\
&\qquad\qquad - \mathcal{A}_{01221}\mathcal{A}_{01122}\,,\\
&\mathrm{P}_0 = \rho^2 c^4 - \rho c^2(\mathcal{A}_{01212} + \mathcal{A}_{01111}) + \mathcal{A}_{01111}\mathcal{A}_{01212}\,,
\end{aligned}
\tag{20}
$$

The lack of odd power coefficients in equation (19) means that the fourth order equation can be reduced to a quadratic equation in α^2. This simplification results in four solutions for α, which are denoted by α_q, $q \in \{1,2,3,4\}$, with the following properties

$$
\alpha_2 = -\alpha_1, \qquad \alpha_4 = -\alpha_3\,. \tag{21}
$$

These solutions correspond to four partial waves in the $x_1 - x_2$ plane which superpose to form Lamb waves.

In order to satisfy the stress-free boundary conditions, we follow the approach in Nayfeh & Chimenti [31] and define the displacement ratio of U_2 to U_1 for each of the four values of α. Using the relations in equation (21), the displacement ratio for each α_q can be expressed as a function of the wave velocity and the material properties as

$$
W_q = \frac{(\rho c^2 - \mathcal{A}_{01111} - \mathcal{A}_{02121}\alpha_q^2)}{\alpha_q(\mathcal{A}_{01122} + \mathcal{A}_{01221})}, \qquad q \in \{1,2,3,4\}. \tag{22}
$$

The displacement field of the Lamb waves can then be written in terms of the displacement ratio (22) by using the principle of superposition

$$
\begin{aligned}
u_1 &= \sum_{q=1}^{4} U_1(\alpha_q) e^{i\xi(x_1 + \alpha_q x_2 - ct)}\,,\\
u_2 &= \sum_{q=1}^{4} U_1(\alpha_q) W_q e^{i\xi(x_1 + \alpha_q x_2 - ct)}\,.
\end{aligned}
\tag{23}
$$

Similarly, the stress field can be found by substituting the above displacement field into the incremental stress-displacement relations (2). The stress components in the x_2 direction are of interest

$$\hat{\mathrm{S}}_{022} = \sum_{q=1}^{4} i\xi D_{1q} U_1(\alpha_q) e^{i\xi(x_1+\alpha_q x_2-ct)} ,$$
$$\hat{\mathrm{S}}_{021} = \sum_{q=1}^{4} i\xi D_{2q} U_1(\alpha_q) e^{i\xi(x_1+\alpha_q x_2-ct)} , \tag{24}$$

where

$$D_{1q} = \mathcal{A}_{01122} + \alpha_q \mathcal{A}_{02222} W_q ,$$
$$D_{2q} = \mathcal{A}_{02121} \alpha_q + \mathcal{A}_{01221} W_q . \tag{25}$$

Incorporating the relations in (21) in equations (22), (23), (24) and (25) results in the following restrictions

$$W_{j+1} = -W_j ,$$
$$D_{1j+1} = D_{1j} , \tag{26}$$
$$D_{2j+1} = -D_{2j}, \qquad j = 1,3 .$$

In order to satisfy the incremental traction-free boundary conditions at the upper and lower surfaces of the plate, the components of the incremental nominal stress must be set to zero

$$\hat{\mathrm{S}}_{022} = \hat{\mathrm{S}}_{021} = 0 \text{ at } x_2 = \frac{\pm\lambda_2 D}{2} = \frac{\pm d}{2} . \tag{27}$$

This leads to four equations which can be expressed as

$$i\xi \begin{pmatrix} D_{11}E_1 & D_{12}E_2 & D_{13}E_3 & D_{14}E_4 \\ D_{21}E_1 & D_{22}E_2 & D_{23}E_3 & D_{24}E_4 \\ D_{11}\overline{E_1} & D_{12}\overline{E_2} & D_{13}\overline{E_3} & D_{14}\overline{E_4} \\ D_{21}\overline{E_1} & D_{22}\overline{E_2} & D_{23}\overline{E_3} & D_{24}\overline{E_4} \end{pmatrix} \begin{pmatrix} U_{11} \\ U_{12} \\ U_{13} \\ U_{14} \end{pmatrix} e^{i\xi(x_1 - ct)} = \begin{Bmatrix} 0 \\ 0 \\ 0 \\ 0 \end{Bmatrix}, \tag{28}$$

where $U_{1q} = U_1(\alpha_q), E_q = e^{i\xi\alpha_q\frac{d}{2}}$ and $\overline{E_q} = e^{-i\xi\alpha_q\frac{d}{2}}$. For non-trivial solutions, the determinant of the coefficient matrix in (28) must go to zero. Finally, using row and column operations along with the symmetries in (26), the determinant can be reduced to two characteristic equations

$$\begin{aligned} D_{11}D_{23}\cot(\gamma\alpha_1) - D_{13}D_{21}\cot(\gamma\alpha_3) = 0\,, \\ D_{11}D_{23}\tan(\gamma\alpha_1) - D_{13}D_{21}\tan(\gamma\alpha_3) = 0\,, \end{aligned} \tag{29}$$

corresponding to the symmetric and anti-symmetric Lamb wave modes respectively, with $\gamma = \xi d/2 = \omega d/2c$, ω being the angular frequency of the wave.

4. Weakly Non-linear Elasticity

In the theory of incremental deformations superimposed on a finite deformation, the amplitude of the wave motion is assumed to be infinitesimal. However, no restriction is placed on the magnitude of the finite deformation, or on the choice of the strain energy function W. To allow for small but finite effects, the strain energy function is specialised to weakly non-linear elasticity [33], whereby W is expressed as a power series in terms of a particular form of the strain tensor.

In the linear theory of elasticity, the strain energy function is of second order in the strain. However, to study the non-linear behaviour of materials, the strain energy function needs to be expanded to a higher order in the strain. In

this paper, the non-linear effect of interest is the acoustoelastic effect and we aim to determine the second order correction to the wave speed. Thus, the strain energy function is expanded to the third order in the strain tensor and it is typically the Green-Lagrange strain tensor, given by $\mathbf{E} = \frac{1}{2}(\mathbf{C} - \mathbf{I})$, which is employed.

A well-known form of the third-order expanded strain energy function is that due to Murnaghan [3,4]

$$W = \frac{1}{2}(\lambda + 2\mu)i_1^2 - 2\mu i_2 + \frac{1}{3}(l + 2m)i_1^3 - 2m\, i_1 i_2 + n i_3, \tag{30}$$

where i_1, i_2, i_3 are the principal invariants of $\mathbf{E}$, given by $i_1 = \mathrm{tr}\mathbf{E}$, $i_2 = \frac{1}{2}[i_1^2 - \mathrm{tr}(\mathbf{E})^2]$ and $i_3 = \det \mathbf{E}$ respectively. The parameters λ and μ are the classical Lamé elastic constants and l, m, n are the Murnaghan or third-order elastic constants. The Murnaghan model has been widely utilised to describe the behaviour of a large class of engineering materials, particularly in studies of wave propagation [34]. This is because the model takes into account material non-linearity through the presence of the third-order terms. The latter allow various non-linear effects, including acoustoelasticity, to be readily investigated.

In the present work, we shall use a particular form of Murnaghan's expansion, expressed in terms of the principal invariants of $\mathbf{C}$ instead of the principal invariants of $\mathbf{E}$ [30]

$$\begin{aligned} W = {} & \frac{\lambda}{8}(I_1 - 3)^2 + \frac{\mu}{4}\left({I_1}^2 - 2I_1 - 2I_2 + 3\right) + \frac{l}{24}(I_1 - 3)^3 \\ & + \frac{m}{12}(I_1 - 3)\left({I_1}^2 - 3I_2\right) \\ & + \frac{n}{8}(I_1 - I_2 + I_3 - 1), \end{aligned} \tag{31}$$

where $I_1,\ I_2,\ I_3$ are the invariants previously defined in equation (5). For this particular strain energy function, the derivatives W_{13}, W_{22}, W_{23} and W_{33} turn out to be zero and thus, the expression for the elasticity tensor in equation (10) reduces to

$$
\begin{aligned}
J\mathcal{A}_{0piqj} = \; & 2(W_1 + I_1 W_2)\, B_{pq}\delta_{ij} \\
& + \; 2W_2\big[2B_{pi}B_{qj} - B_{iq}B_{jp} - B_{pr}B_{rq}\delta_{ij} \\
& - B_{pq}B_{ij}\big] + \; 2I_3 W_3\big(2\delta_{ip}\delta_{jq} - \delta_{iq}\delta_{jp}\big) \\
& + 4W_{11}B_{ip}B_{jq} \\
& + \; 4W_{12}\big(2I_1 B_{ip}B_{jq} - B_{ip}B_{jr}B_{rq} \\
& - B_{jq}B_{ir}B_{rp}\big)\,.
\end{aligned}
\tag{32}
$$

For a given (Cauchy) uniaxial stress field, the principal stretches can be determined by solving equation (9) along with equations (12) and (31). The components of the elasticity tensor, $\mathcal{A}_{0piqj}$, used in the dispersion relations can then be obtained using equation (32).

5. Selected Results

In this section, we present selected numerical results obtained by solving equation (29) using the algorithm developed by Gandhi [35]. The adopted approach was verified by comparing the numerical results with the asymptotic solutions by Nolde *et al*. [23] for specific ranges of frequencies, namely low, high and near cut-off frequency ranges. The material considered in this study is 6061-T6 Aluminium, which was chosen in order to make contact with previously published analytical predictions and experimental data from Gandhi *et al*. [14]. The material properties of the 6061-T6 Aluminium were sourced from Asay & Guenther [36] and are listed in Table 1.

Figure 2 shows the dispersion curves for an aluminium plate subjected to a uniaxial stress of 100 MPa in tension (continuous line) and in compression (dashed line). The direction of propagation of the waves was chosen to be parallel to the applied load, as it was shown to exhibit the highest sensitivivity of the phase velocity to the applied stress in the case of longitudinal waves [37]. The shear horizontal modes are not shown here as they decouple from the Lamb wave modes. At this scale, the change in the phase velocity is not immediately obvious. However, it can be seen that, in general, the phase velocity seems to be

higher for the compressive load as compared to the tensile load. This finding is consistent with the results of bulk wave acoustoelasticity which predicts that compressive stresses cause an increase in the phase velocity while tensile stresses lead to a decerease in the phase velocity [6].

Table 1. Material Properties of 6061-T6 Aluminium

Elastic properties	Value
λ	54.308 GPa
μ	27.174 GPa
l	−281.5 GPa
m	−339.0 GPa
n	−416.0 GPa
ρ	2704 kg/m^3

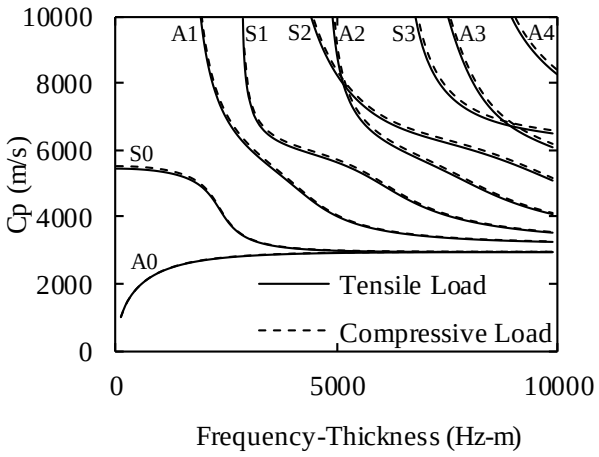

Figure 2. Dispersion curves for waves propagating in an Aluminium plate along the direction of a uniaxial applied stress of 100 MPa

The change in the phase velocity for different symmetric and anti-symmetric Lamb wave modes at varying magnitudes of tensile stress is compared in Figure 3. For reasons of clarity, the results for compressive stresses are not shown here as they only demonstrate an opposite trend to the results obtained for tensile stresses. Figure 3 (a) shows the change in the phase velocity, compared to the unstressed state, of the fundamental symmetric mode (S0) as a function of the magnitude of the applied tensile load. It can be seen that the change in the phase velocity is negative for all the values of applied stress considered, which means that tensile stresses cause a decrease in the phase velocity of the S0 mode. Higher magnitudes of the applied stress result in larger changes in the phase velocity, particularly in the low frequency-thickness region. However, at higher frequency-thickness values, the change in the phase velocity tends to a constant value. This is not surprising since the S0 mode converges to the Rayleigh wave velocity at higher frequencies [32].

The results for the fundamental anti-symmetric mode (A0), shown in Figure 3(b), are very intriguing. At low frequency-thickness values (500–1000 Hz-m), the change in the phase velocity is negative. At higher frequency-thickness values, the change in the phase velocity tends to a constant value as the A0 mode also converges to the Rayleigh wave velocity [32]. However, at very low frequency-thickness values, a different trend is observed; the change in the phase velocity is positive and seems to be inversely proportional to the applied load. The inset plot in Figure 3 (b) shows a particularly interesting behaviour at a frequency-thickness product of approximately 380 Hz-m; it predicts that the change in the phase velocity is zero and, more importantly, is independent of the magnitude of the applied stress. This behaviour seems to be analogous to the isotropic phase velocity observed by Gandhi *et al.* [14] for the A0 mode at varying angles of propagation.

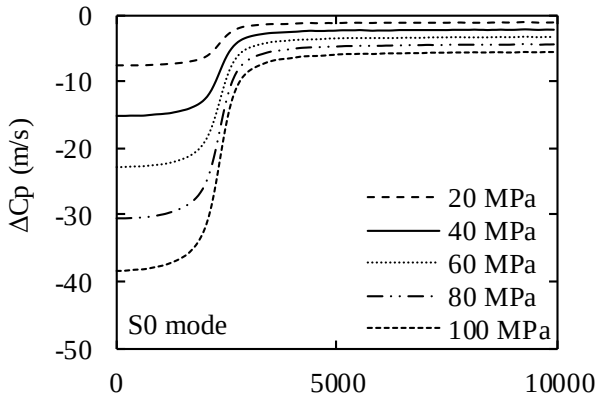
0
-10
-20
-30
-40
-50
ΔCp (m/s)
20 MPa
40 MPa
60 MPa
80 MPa
100 MPa
S0 mode
0
5000
10000
Frequency-Thickness (Hz-m)

(a)

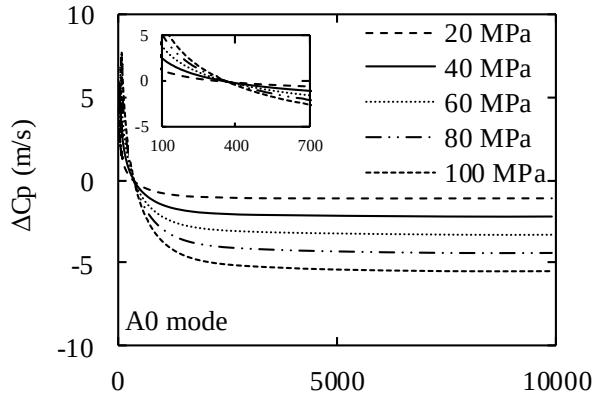
10
5
0
-5
-10
ΔCp (m/s)
5
0
-5
100
400
700
20 MPa
40 MPa
60 MPa
80 MPa
100 MPa
A0 mode
0
5000
10000
Frequency-Thickness (Hz-m)

(b)

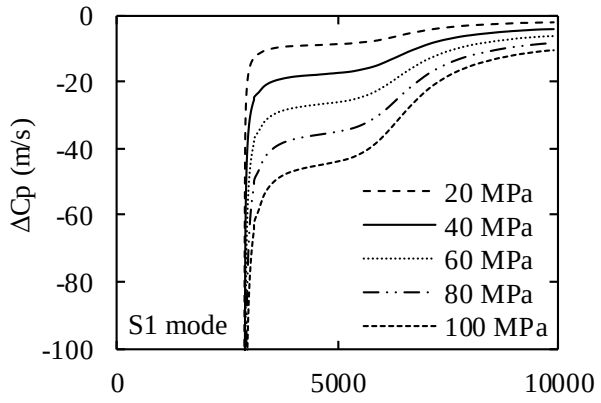
0
-20
-40
-60
-80
-100
ΔCp (m/s)
20 MPa
40 MPa
60 MPa
80 MPa
100 MPa
S1 mode
0
5000
10000
Frequency-Thickness (Hz-m)

(c)

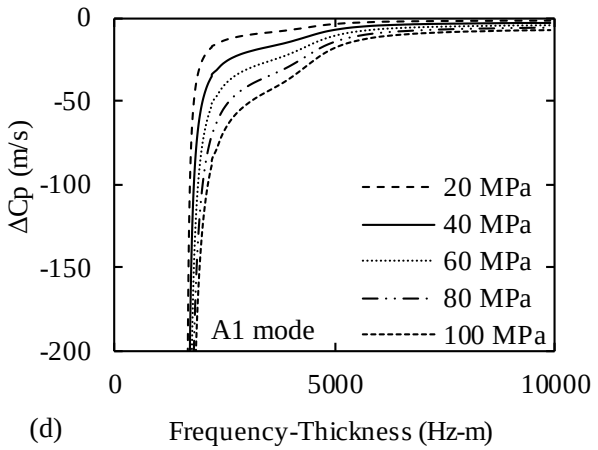

(d)

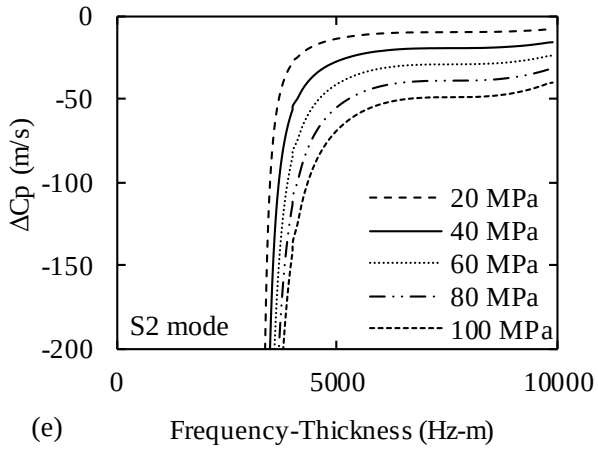

(e)

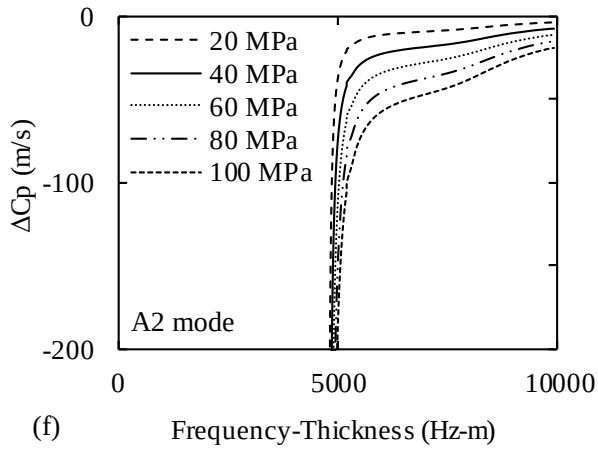

(f)

Figure 3. Change in phase velocity with Frequency-Thickness for modes propagating along the direction of uniaxial applied stress: (a) S0 mode, (b) A0 mode, (c) S1 mode, (d) A1 mode, (e) S2 mode and, (f) A2 mode.

The change in the phase velocity for higher Lamb wave modes is shown in Figures 3(c) S1 mode, 3(d) A1 mode, 3(e) S2 mode and 3(f) A2 mode. At high frequency-thickness values, the higher order modes exhibit a similar behaviour to the fundamental modes as the change in the phase velocity tends to constant value. This is because the higher order modes converge to the transverse wave velocity at high frequencies [32]. However, when the excitation frequency is near the cut-off frequency of the higher order modes, the change in the phase velocity is much higher than for the S0 mode across all frequencies, including the low frequency range. Previous efforts on the utilisation of the acoustoelastic effect for stress monitoring have mainly focused on the fundamental symmetric (S0) mode as well as bulk waves. The findings here suggest that the use of higher order Lamb wave modes with an excitation frequency near the cut-off frequency appears to be more advantageous due to the much higher sensitivity of the phase velocity to the applied stress.

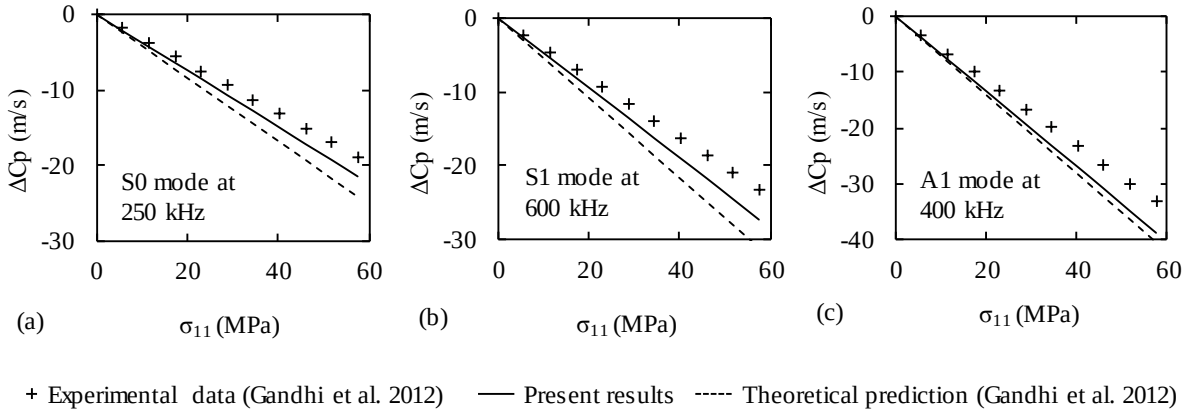

Figure 4. Comparison of the modelling outcomes of the present work with experimental results and theoretical predictions of a previous study. The results are presented for Lamb wave propagation in an Aluminium plate of thickness 6.35 mm along the direction of the uniaxial applied stress.

Next, we compare the change in the phase velocity with both the theoretical and experimental results presented by Gandhi *et al.* [14]. The latter utilised an aluminium plate of thickness 6.35 mm which was subjected to uniaxial loads in the range 0 to 57.5 MPa. The experiments were conducted at three specific values of frequency, corresponding to three different modes, namely the S0 mode at 250 kHz, the S1mode at 600 kHz and and the A1 mode at 400 kHz. Referring to Figure 4, the analytical results from the present study show that a better agreement with the experimental values as compared to the theoretical results predicted by Gandhi *et al.* [14]. For lower values of the applied stress, the analytical results are in excellent agreement with the experimental results, particularly in the case of the symmetric modes shown in Figures 4 (a) and (b). For higher values of the applied stress, the difference in the values is larger but is still within reasonable agreement. Gandhi *et al.* [14] attributed the differences between their theoretical results and the experimental data to the difficulties in evaluating the third order elastic constants accurately. The same argument is also applicable to explain the discrepancy between the present results and the experimental data. Furthermore, we note that the discrepancy is also due to the fact that the experimental phase velocity changes determined by Gandhi *et al.* [14] were calculated in the undeformed coordinate system. However, the phase velocities in the stressed and unstressed configurations are, in general, different due to the stretching of the material when it is subjected to a an applied stress.

6. Concluding Remarks

We have considered the problem of Lamb wave propagation in an initially isotropic plate subjected to a homogeneous uniaxial stress field. The derived governing equations of motion and dispersion equations are based on the non-linear theory of elasticity and utilises an invariant-based formulation of the strain-energy function. New results are presented for the Murnaghan form of the strain energy function, which is applicable to a large class of engineering materials. The results correlate better with the considered experimental data than

previously published numerical results. The theoretical predictions show the same tendencies as the experimental data and demonstrate that the phase velocity decreases with an increase in the magnitude of tensile stress.

The acoustoelastic effect for aluminium plates subjected to a realistic level of applied stresses (below 100 MPa) is quite significant, specifically below approximately 3000 Hz-m for the fundamental symmetric mode. It is, however, much stronger for higher order modes near the cut-off frequencies. Combining the high sensitivity of the phase velocity to applied stresses with the excellent ability of Lamb waves to propagate over large distances without decay, the obtained theoretical equations can form a foundation for practical techniques to measure stresses in plate-like structures. Similar analytical dispersion equations can also be obtained for other simple geometries such as circular rods. In this case, the wave modes are described by the Pochhammer-Chree characteristic equations [11]. However, an analysis of the dispersion equations for more complicated waveguides such as rail-tracks will require the use of numerical tools, including Finite Element Analysis.

One of the promising aspects of experimental techniques based on the theory of acoustoelasticity, specifically for guided wave propagation in slender structures, is a possibility to distinguish between the residual (built-in) stresses and the applied stresses. This is possible because the characteristic length of residual stresses, which is normally related to the characteristic size of the cross-sectional area, is much smaller than the propagation distances of guided waves. Therefore, the influence of residual stresses on wave propagation in slender structures, such as rail-tracks, is likely to decay with distance due to their self-equilibrating nature (no bulk stress).

Acknowledgement

This work was supported by the Australian Research Council through Discovery Project DP160102233 and by the Department of Further Education, Employment, Science & Technology, Government of South Australia, under the Catalyst Research Grant Program. Their support is greatly appreciated.

References

[1] M.A. Biot, The influence of initial stress on elastic waves, J. Appl.Phys. 11 (1940) 522–530.

[2] M.A. Biot, Mechanics of Incremental Deformations, John Wiley, New York, 1965.

[3] F.D. Murnaghan, Finite deformations of an elastic solid, Am. J. Math. 59 (1937) 235–260.

[4] F.D. Murnaghan, Finite Deformation of an Elastic Solid, John Wiley & Sons, New York, 1951.

[5] A.N. Norris, Small-on-Large theory with applications to granular materials and fluid/solid systems, in: M. Destrade, G. Saccomandi (Eds.), Waves in Nonlinear Pre-Stressed Materials, Springer, Wien, 2007, pp. 27–62.

[6] D. Hughes, J. Kelly, Second-order elastic deformation of solids, Phys. Rev. 92 (1953) 1145–1149.

[7] R.A. Toupin, B. Bernstein, Sound waves in deformed perfectly elastic materials. Acoustoelastic effect, J. Acoust. Soc. Am. 33 (1961) 216–225.

[8] R.N. Thurston, K. Brugger, Third-order elastic constants and the velocity of small amplitude elastic waves in homogeneously stressed media, Phys. Rev. 133 (1964) A1604–A1610.

[9] Y.H. Pao, W. Sachse, H. Fukuoka, Acoustoelasticity and ultrasonic measurements of residual stresses, Phys. Acoust. 17 (1983) 61–143.

[10] A.N. Guz, F.G. Makhort, The physical fundamentals of the ultrasonic non-destructive stress analysis of solids, Int. Appl. Mech. 36 (9) (2000) 1119–1149.

[11] S. Chaki, G. Bourse, Guided ultrasonic waves for non-destructive monitoring of the stress levels in prestressed steel strands, Ultrasonics 49 (2009) 162–171.

[12] M. Veidt, C.T. Ng, Influence of stacking sequence on scattering characteristics of the fundamental anti-symmetric Lamb wave at through holes in composite laminates, J. Acoust. Soc. Am. 129 (2011) 1280–1287.

[13] C.T. Ng, M. Veidt, Scattering characteristics of Lamb waves from debondings at structural features in composite laminates, J. Acoust. Soc. Am. 132 (2012) 115–123.

[14] N. Gandhi, J.E. Michaels, S.J. Lee, Acoustoelastic Lamb wave propagation in biaxially stressed plates, J. Acoust. Soc. Am. 132 (2012) 1284–1293.

[15] R.W. Ogden, Non-Linear Elastic Deformations, Ellis Horwood, Chichester, 1984.

[16] D.G. Roxburgh, R.W. Ogden, Stability and vibration of pre-stressed compressible elastic plates, Int. J. Eng. Sci. 32 (1994) 427–454.

[17] J.D. Kaplunov, E.V. Nolde, G.A. Rogerson, A low-frequency model for dynamic motion in pre-stressed incompressible elastic structures, Proc. R. Soc.Lond. A: Math. Phys. Eng. Sci. 456 (2000) 2589–2610.

[18] J.D. Kaplunov, E.V. Nolde, G.A. Rogerson, An asymptotically consistent model for long-wave high-frequency motion in a pre-stressed elastic plate, Math.Mech. Solids 7 (2002) 581–606.

[19] J.D. Kaplunov, E.V. Nolde, G.A. Rogerson, Short wave motion in a pre-stressed incompressible elastic plate, IMA J. Appl. Math. 67 (2002) 383–399.

[20] A.V. Pichugin, G.A. Rogerson, A two-dimensional model for extensional motion of a pre-stressed incompressible elastic layer near cut-off frequencies, IMA J. Appl. Math. 66 (2001) 357–385.

[21] A.V. Pichugin, G.A. Rogerson, An asymptotic membrane-like theory for long wave motion in a pre-stressed elastic plate, Proc. R. Soc. Lond. A: Math. Phys. Eng. Sci. 458 (2002) 1447–1468.

[22] A.V. Pichugin, G.A. Rogerson, Anti-symmetric motion of a pre-stressed incompressible elastic layer near shear resonance, J. Eng. Math. 42 (2002) 181–202.

[23] E.V. Nolde, L.A. Prikazchikova, G.A. Rogerson, Dispersion of small amplitude waves in a pre-stressed, compressible elastic plate, J. Elast. 75 (2004) 1–29.

[24] G.A. Rogerson, L.A. Prikazchikova, Generalisations of long wave theories for pre-stressed compressible elastic plates, Int. J. Non-Linear Mech. 44 (2009) 520–529.

[25] P. Kayestha, A. Wijeyewickrema, K. Kishimoto, Wave propagation along a non-principal direction in a compressible pre-stressed elastic layer, Int. J. Solids Struct. 48 (2011) 2141–2153.

[26] V.L. Berdichevsky, Variational Principles of Continuum Mechanics, in: L. Truskinovsky (Ed.), Interaction of Mechanics and Mathematics, Springer-Verlag, Berlin Heidelberg, 2009.

[27]] J.D. Kaplunov, L.Y. Kossovich, E.V. Nolde, Dynamics of Thin Walled Elastic Bodies, Academic Press, San Diego, 1998.

[28] M. Destrade, R.W. Ogden, On stress-dependent elastic moduli and wave speeds, IMA J. Appl. Math. 78 (2012) 965–997.

[29] R.W. Ogden, Incremental statics and dynamics of pre-stressed elastic materials, in: M. Destrade, G. Saccomandi (Eds.), Waves in Nonlinear Pre-Stressed Materials, Springer, Wien, 2007, pp. 1–26.

[30] M. Shams, M. Destrade, R.W. Ogden, Initial stresses in elastic solids: constitutive laws and acoustoelasticity, Wave Motion 48 (7) (2011) 552–567.

[31] A.H. Nayfeh, D.E. Chimenti, Free wave propagation in plates of general anisotropic media, J. Appl. Mech. 56 (1989) 881–886.

[32] J.L. Rose, Ultrasonic Waves in Solid Media, Cambridge University Press, Cambridge, United Kingdom, 1999.

[33] L.D. Landau, E.M. Lifshitz, Theory of Elasticity, Butterworth-Heinemann, Oxford, 1986.

[34] J.J. Rushchitsky, Nonlinear Elastic Waves in Materials, in: V. Babitsky, J. Wittenburg (Eds.), Foundations of Engineering Mechanics, Springer International Publishing, Heidelberg, 2014.

[35] N. Gandhi, Determination of Dispersion Curves for Acoustoelastic Lamb Wave Propagation (MS thesis), Georgia Institute of Technology, Atlanta, 2010.

[36] J.R. Asay, A.H. Guenther, Ultrasonic studies of 1060 and 6061-T6 aluminum, J.Appl. Phys. 38 (1967) 4086–4088.

[37] D.M. Egle, D.E. Bray, Measurement of acoustoelastic and third-order elastic constants for rail steel, J. Acoust. Soc. Am. 60 (1976) 741–744.

Chapter 4

Large acoustoelastic effect for Lamb waves propagating in an incompressible elastic plate

Statement of Authorship

Title of Paper	Large acoustoelastic effect for Lamb waves propagating in an incompressible elastic plate.
Publication Status	☑ Published ☐ Accepted for Publication ☐ Submitted for Publication ☐ Unpublished and Unsubmitted w ork w ritten in manuscript style
Publication Details	M. Mohabuth, A. Kotousov and C.T. Ng (2018), Large acoustoelastic effect for Lamb waves propagating in an incompressible elastic plate, *J. Acoust. Soc. Am.*, 145, 1221-1229, doi: 10.1121/1.5092604

Principal Author

Name of Principal Author (Candidate)	Munawwar Mohabuth		
Contribution to the Paper	Developed the analytical model, performed all analyses and wrote manuscript.		
Overall percentage (%)	70		
Certification:	This paper reports on original research I conducted during the period of my Higher Degree by Research candidature and is not subject to any obligations or contractual agreements with a third party that would constrain its inclusion in this thesis. I am the primary author of this paper.		
Signature		Date	13/05/2019

Co-Author Contributions

By signing the Statement of Authorship, each author certifies that:

i. the candidate's stated contribution to the publication is accurate (as detailed above);

ii. permission is granted for the candidate in include the publication in the thesis; and

iii. the sum of all co-author contributions is equal to 100% less the candidate's stated contribution.

Name of Co-Author	Andrei Kotousov		
Contribution to the Paper	Supervised the development of the analytical model, helped in interpretation of the results and assisted in the preparation of the manuscript.		
Signature		Date	13/05/2019

Name of Co-Author	Ching-Tai Ng		
Contribution to the Paper	Supervised the work and assisted with editing of the manuscript.		
Signature		Date	13/05/2019

Large acoustoelastic effect for Lamb waves propagating in an incompressible elastic plate

Munawwar Mohabuth[1*], Andrei Kotousov[1] and Ching-Tai Ng[2]

[1]School of Mechanical Engineering, The University of Adelaide, Adelaide, SA 5005, Australia.

[2]School of Civil, Environmental and Mining Engineering, The University of Adelaide, Adelaide, SA 5005, Australia.

*Corresponding author. Tel.: +61 8 8313 6385.

E-mail address: munawwar.mohabuth@adelaide.edu.au

Abstract

In this paper, the effect of a large pre-stress on the propagation of small amplitude Lamb waves in an incompressible elastic plate is investigated. Using the theory of incremental elasticity, the dispersion equations, which give the phase velocity of the symmetric and anti-symmetric wave modes as a function of the wavenumber, plate thickness and pre-stress state, are derived for a general strain energy function. By considering the fourth order strain energy function of incompressible isotropic elasticity, the correction to the phase velocity due to the pre-stress is obtained implicitly to the second order in the pre-strain/stress and depends on the second, third and fourth order elastic constants. Numerical results are presented to show the dependence of the phase velocity of the Lamb wave modes upon the applied stress. These are compared to the first order correction and agree well with the limiting and asymptotic values obtained previously. It is envisaged that the present results may well find important practical applications in various guided wave based ultrasonic techniques utilising gels and rubber-like materials.

1. Introduction

In recent years, there has been an increased interest in the acoustics of rubber-like solids as well as soft biological tissues, with the ultimate objective of mastering all aspects of ultrasonic wave techniques. In particular, much research has been directed towards the investigation of the acoustoelastic effect associated with bulk waves (Destrade and Ogden, 2010; Destrade *et al*., 2010a). Another type of wave motion, which is of great importance in practical applications, is represented by guided waves. Lamb waves, which are guided waves in plate-like structures, are widely utilised in the imaging of defects (Ng, 2015; Aryan *et al*., 2017) and have many advantages as compared to bulk waves, including a longer propagation range, higher sensitivity to damage and a lower energy requirement for excitation and sensing (Su and Ye, 2009; Rose, 2014). These advantages are yet to be utilised for soft materials and rubber-like solids. Such materials often exhibit nearly incompressible behaviour and are constrained to undergo essentially volume preserving deformations. At the same time, the strain conditions may reach up to hundreds of percent (Destrade *et al.*, 2010a). Therefore, it is important to understand the effect of these conditions on the wave propagation characteristics; the latter is the focus of the current paper.

The problem of wave propagation in pre-stressed plates has been an active research topic over the past decades. Two approaches have been established for treating this problem, namely the theory of exact nonlinear elasticity and the theory of weakly nonlinear elasticity. The first approach is amenable to large deformations and has been used to study the behaviour of elastomers and soft solids (Destrade *et al.*, 2010a). In this framework, the strain energy function is written in a general form as a function of the first three principal invariants of the right Cauchy-Green strain tensor (Destrade *et al.*, 2010b). A comprehensive treatment of the foundations of this framework can be found in the pioneering paper by Ogden and Roxburgh (1993). These authors derived dispersion relations for wave propagation in a pre-stressed incompressible finite plate and investigated the vibration and stability phenomena. Since then, there has been a number of contributions on the dynamics of incompressible (Rogerson and Fu, 1995; Rogerson, 1997; Rogerson and Sandiford, 1999; Kaplunov *et al.*, 2000,

2002a, 2002b; Pichugin and Rogerson, 2001, 2002a, 2002b) and compressible (Nolde *et al.*, 2004; Rogerson and Prikazchikova, 2009; Kayestha *et al.*, 2011) pre-stressed plates, focusing on the asymptotic analysis of the dispersion relations.

The second approach, the theory of weakly nonlinear elasticity, is often used in the study of small but not necessarily infinitesimal deformations. In this approach, the strain energy function is generally expanded in terms of the invariants of the Green-Lagrange strain tensor or some other measure of strain (Destrade *et al.*, 2010c). This framework has been employed to describe the acoustoelastic effect, which explains the change in the wave speed with the applied stress. Whilst the theory of acoustoelasticity is well established for bulk waves (Pao *et al.*, 1984; Pao and Gamer, 1985; Guz and Makhort, 2000; Kim and Sachse, 2001), comparatively little attention has been given to Lamb waves. An extensive analytical framework was established by Gandhi *et al.* (2012) to analyse the effect of biaxial loading in an initially isotropic compressible plate. Pau and Lanza di Scalea (2015) also developed a nonlinear model to investigate wave propagation in pre-stressed plates. Their model recovers the results of Gandhi (2012) in the linearised case but in the nonlinear case, it gives the variation of the amplitude of the second harmonic component as a function of the pre-stress. Other related studies within the weakly nonlinear elasticity framework include Kubrusly *et al.* (2016), Mohabuth *et al.* (2016, 2018), Pei and Bond (2016, 2017), Peddeti and Santhanam (2018) and Dubuc *et al.* (2017, 2018).

In all of the above-mentioned research set within the theory of weakly nonlinear elasticity, the strain energy function was expanded to the third order in the strain and higher-order terms were neglected. The tacit assumption was that the pre-deformation is small and the correction to the wave speed was obtained implicitly to the first order in the strain and involves second as well as third order elastic constants. Motivated by the simplicity of the fourth order strain energy function of incompressible isotropic elasticity (Hamilton *et al.*, 2004), Destrade *et al.* (2010a) obtained the secular equations for shear wave and surface wave speeds to the second order in the strain for an incompressible solid

subjected to a uniaxial pre-stress. Subsequently, Abiza *et al.* (2012) determined the second order correction to the longitudinal and shear wave speeds for compressible solids in the case of hydrostatic pre-stress and uniaxial pre-stress. These equations involve a combination of the second, third, and fourth order constants and describe the so-called large acoustoelastic effect which couples the speed of a small amplitude wave to a small-but-finite pre-deformation. These relationships provide a theoretical framework for the experimental determination of third and fourth order constants.

The objective of this work is to investigate the large acoustoelastic effect associated with the propagation of Lamb waves in an isotropic incompressible elastic plate. The paper is organised as follows. In Section 2, the equations governing the propagation of small-amplitude waves in pre-stressed media are briefly reviewed. The dispersion relations for Lamb waves propagating in a pre-stressed plate along a principal direction are then derived in Section 3 for a general form of the strain energy function. The latter is specialised to weakly nonlinear elasticity in Section 4 by considering the fourth order strain energy function of incompressible isotropic elasticity which is applicable to rubber-like materials with large elastic strain limits. It is noted here that the dispersion relations depend on the strain energy function and the pre-stress through the components of the elasticity tensor. In Section 5, the pre-stress is specialised to the case of a small-but-finite uniaxial pre-deformation along the direction of wave propagation and the components of the elasticity tensor are expanded up to the second order in the pre-strain. In Section 6, the dispersion relations are solved numerically to obtain, implicitly, the second order correction to the phase velocity due to the pre-stress, i.e. the large acoustoelastic effect. The results are compared to the classical acoustoelastic effect, with particular attention to the limiting behaviour of the fundamental and higher order modes in the long and short wave regions.

2. Governing Equations

In this section, the equations governing the propagation of small amplitude waves in pre-stressed incompressible media are briefly reviewed. These equations are derived based on the theory of incremental motions superimposed a finite deformation. For a comprehensive discussion of the latter theory, the reader is referred to Ogden (1984, 2007). This framework is used in the derivation of dispersion relations for waves propagating in a pre-stressed incompressible plate.

Consider an isotropic hyperelastic incompressible body in some stress-free reference configuration. Suppose the body is subjected to a pure homogeneous finite static deformation such that a material point $\boldsymbol{X}$ in the reference configuration takes up the position $\boldsymbol{x}$ in the deformed configuration. If $\boldsymbol{X}$ and $\boldsymbol{x}$ are referred to the same fixed rectangular Cartesian system of axes, the deformation can be expressed as

$$x_i = \lambda_i X_i, \qquad i \in \{1,2,3\}, \tag{1}$$

where the constants λ_i are the principal stretches of the deformation and the principal axes of the deformation are taken to coincide with the Cartesian coordinate directions. The principal Cauchy stresses required to maintain the body in the static state of deformation are given by

$$\sigma_i = \lambda_i \frac{\partial W}{\partial \lambda_i} - p, \qquad i \in \{1,2,3\}, \tag{2}$$

where W is the strain energy function per unit volume and p is a Lagrange multiplier associated with the incompressibility constraint, $\lambda_1\lambda_2\lambda_3 = 1$. The usual summation convention does not apply to equations (1) and (2).

A small-amplitude time dependent motion, given by the mechanical displacement $\boldsymbol{u} = \boldsymbol{u}(\boldsymbol{x}, t)$ where t is time, is then superimposed on the static finite deformation. The mechanical response is described by the incremental constitutive equations (Dowaikh and Ogden, 1990)

$$\hat{\mathrm{S}}_{ij} = \mathcal{A}_{ijkl} u_{l,k} + p u_{i,j} - p^* \delta_{ij}, \qquad i,j \in \{1,2,3\}, \tag{3}$$

where $\hat{\mathrm{S}}_{ij}$ is the incremental nominal stress tensor, $\mathcal{A}_{ijkl}$ is the fourth order elasticity tensor of instantaneous elastic moduli, p^* is the incremental form of p and a comma indicates partial differentiation with respect to the current coordinates $\boldsymbol{x} \equiv x_i$. The corresponding incremental equations of motion then read

$$\mathcal{A}_{ijkl}\, u_{l,ik} - p^*_{,j} = \rho \ddot{u}_j, \qquad i,j \in \{1,2,3\}, \tag{4}$$

where ρ is the density of the material and a superposed dot indicates partial differentiation with respect to time. The coupled incremental incompressibility constraint has the form

$$u_{i,i} = 0, \qquad i \in \{1,2,3\}. \tag{5}$$

It is worth noting for later reference that relative to the principal axes of the deformation, the non-zero components of the elasticity tensor are given by

$$\begin{aligned} \mathcal{A}_{iijj} &= \lambda_i \lambda_j W_{ij}\,, \\ \mathcal{A}_{ijij} &= (\lambda_i W_i - \lambda_j W_j)\, \lambda_i^2/(\lambda_i^2 - \lambda_j^2), \qquad i \neq j, \lambda_i \neq \lambda_j \\ \mathcal{A}_{ijij} &= (\mathcal{A}_{iiii} - \mathcal{A}_{iijj} + \lambda_i W_i)\, /2, \qquad i \neq j, \lambda_i = \lambda_j \\ \mathcal{A}_{ijji} &= \mathcal{A}_{jiij} = \mathcal{A}_{ijij} - \lambda_i W_i, \qquad i \neq j, \end{aligned} \tag{6}$$

where $W_{ij} = \partial W/\partial \lambda_i, W_{ij} = \partial^2 W/\partial \lambda_i \partial \lambda_j, i,j \in \{1,2,3\}$ and there is no sum on repeated indices.

3. Dispersion Relations

The framework described in Section 2 allows the acoustoelastic effect to be investigated by considering the propagation of small-amplitude homogeneous plane waves in a deformed body. This framework is here extended to study the propagation of Lamb waves in a pre-stressed incompressible plate.

Consider the unstressed body to correspond to a plate of thickness h_0 and infinite lateral extent. Suppose the plate is subjected to a pure homogeneous strain such that its thickness changes to h in the deformed configuration. The Cartesian coordinate system is chosen to be coaxial with the principal axes of the deformation, with the origin in the mid-plane of the plate and the x_2 axis normal to the plane of the plate.

In this paper, the analysis is restricted to wave propagation along an in-plane principal direction. For simplicity, the principal direction is taken to be along the x_1 axis and the analysis is confined to plane incremental motions in the $x_1 - x_2$ plane, with $u_3 = 0$ and u_1 and u_2 taken as independent of x_3. The incremental equations of motion (4) and the incompressibility constraint (5) then reduce to

$$\begin{aligned} \rho\ddot{u}_1 &= \mathcal{A}_{1111}\, u_{1,11} + (\mathcal{A}_{1122} + \mathcal{A}_{2112})u_{2,12} + \mathcal{A}_{2121}\, u_{1,22} - p^*_{,1}, \\ \rho\ddot{u}_2 &= \mathcal{A}_{1212}\, u_{2,11} + (\mathcal{A}_{1122} + \mathcal{A}_{2112})u_{1,12} + \mathcal{A}_{2222}\, u_{2,22} - p^*_{,2}, \end{aligned} \tag{7}$$

and

$$u_{1,1} + u_{2,2} = 0. \tag{8}$$

The corresponding incremental surface tractions are obtainable from equations (3) and can be written explicitly as

$$\begin{aligned} \hat{\mathrm{S}}_{22} &= \mathcal{A}_{2211}u_{1,1} + (\mathcal{A}_{2222} + p)u_{2,2} - p^*, \\ \hat{\mathrm{S}}_{21} &= (\mathcal{A}_{2112} + p)u_{2,1} + \mathcal{A}_{2121}u_{1,2}. \end{aligned} \tag{9}$$

The propagation of acoustoelastic Lamb waves requires the incremental equations of motion to be solved, in conjunction with the incompressibility constraint and incremental traction free boundary conditions at the surfaces of the plate, i.e $\hat{\mathrm{S}}_{22} = \hat{\mathrm{S}}_{21} = 0$ at $x_2 = \pm\lambda_2 h_0/2 = \pm h/2$. The detailed solution process is rather lengthy and only the final characteristic equations are presented here. These are given by

$$D_{11}D_{23}\cot(\gamma\alpha_1) - D_{13}D_{21}\cot(\gamma\alpha_3) = 0\,,$$
$$D_{11}D_{23}\tan(\gamma\alpha_1) - D_{13}D_{21}\tan(\gamma\alpha_3) = 0\,, \tag{10}$$

corresponding to the symmetric and anti-symmetric Lamb wave modes respectively, with $\gamma = kh/2$. These equations form the secular dispersion relations which provide an implicit relationship between the phase velocity and the wavenumber. The definition of the various terms used in the above equations are provided in the Appendix of this paper.

It is worth noting that similar dispersion relations have been derived by Ogden and Roxburgh (1993), albeit their efforts were focused on the effect of the pre-stress on the modes of vibrations of an incompressible finite plate and the stability of the underlying deformed configuration.

4. Weakly Nonlinear Elasticity

In the theory of incremental elasticity, the amplitude of the wave motion is assumed to be infinitesimal but no restriction is imposed on the magnitude of the pre-deformation. For small pre-deformations, the strain energy function is often prescribed using the theory of weakly nonlinear elasticity. In this theory, the strain energy function is usually expressed as a power series in terms of the invariants of the Green-Lagrange strain tensor, $\boldsymbol{E}$ (Destrade and Ogden, 2010)

$$I_1 = tr\,\boldsymbol{E}, \qquad I_2 = tr\,\boldsymbol{E}^2, \qquad I_3 = tr\,\boldsymbol{E}^3. \tag{11}$$

In classical acoustoelasticity, the aim is to determine the first order corrections to the wave speeds for an infinitesimal pre-strain and thus, the strain energy function is expanded to the third order in the strain. For an incompressible isotropic material, the general weakly nonlinear third order expansion is given by

$$W = \mu I_2 + \frac{A}{3} I_3, \tag{12}$$

where μ and A are the second and third order elasticity constants. In order to study the large acoustoelastic effect for small-but-finite pre-deformations, the strain energy function is truncated at the fourth order term and the corrections to the wave speeds are then obtained to the second order in the strain. The general strain energy function of fourth order incompressible elasticity was recently established by Hamilton *et al.* (2004) and has the form

$$W = \mu I_2 + \frac{A}{3} I_3 + D I_2^2, \tag{13}$$

where D is the so-called fourth order elastic constant.

The implications of the fourth order expansion on the acoustoelasticity of shear waves and surface waves was considered by Destrade *et al.* (2010a). These authors derived explicit expressions for the second order corrections to the wave speeds in the case of a uniaxial pre-stress. Their results show that for "soft" solids it is sufficient to elongate the material by a few percent to perceive the large acoustoelastic effect. In passing, it should be noted that a fourth order expansion of the strain energy can also be obtained for compressible isotropic materials and similar explicit expressions for the corrections to the wave speeds can be derived (see, for example, Abiza *et al.*, 2012). However, fourth order constants are not readily available for metals and other stiff solids due to yielding and plasticity.

In the present work, a particular form of Hamilton's expansion cast in terms of the principal stretches of the deformation shall be employed

$$\begin{aligned} W = \frac{\mu}{4}[(\lambda_1^2-1)^2 + (\lambda_2^2-1)^2 + (\lambda_3^2-1)^2] \\ + \frac{A}{24}[(\lambda_1^2-1)^3 + (\lambda_2^2-1)^3 + (\lambda_3^2-1)^3] \\ + \frac{D}{16}[(\lambda_1^2-1)^2 + (\lambda_2^2-1)^2 + (\lambda_3^2-1)^2]^2, \end{aligned} \tag{14}$$

in which the connection between the eigenvalues E_i of the Green-Lagrange strain tensor and the principal stretches given by $E_i = (\lambda_i^2 - 1)/2$ has been utilised. It should be noted here that the principal stretches are not independent but are related by the incompressibility condition, $\lambda_1\lambda_2\lambda_3 = 1$.

5. Uniaxial Pre-deformation

In this section, the pre-deformation is specialised to a uniaxial tension in the plane of the plate. It is assumed that the plate has been pre-stressed by the application of a Cauchy stress σ_1 along the x_1 direction such that it is finitely deformed. The elongation in this direction is denoted by $e_1 = \lambda_1 - 1$, where λ_1 is the corresponding axial stretch. Because of symmetry, the lateral stretches in the x_2 and x_3 directions are equal to each other, indicating that the deformation is equi-biaxial. It follows from the incompressibility constraint that the stretch ratios are related by

$$\lambda_3 = \lambda_2 = \lambda_1^{-1/2}. \tag{15}$$

For the specified form of the strain energy function in equation (14), the Cauchy stress σ_1 can be computed using equations (2) and (15). The pre-stress can then be expanded in terms of the pre-strain e_1, up to the second order, as (Destrade et al., 2010a)

$$\sigma_1 = 3\mu e_1 + 3\left(\mu + \frac{A}{4}\right)e_1^2. \tag{16}$$

Alternatively, the pre-strain can be expressed in terms of the pre-stress as (Destrade et al., 2010a)

$$e_1 = \frac{1}{3\mu}\sigma_1 - \frac{1}{9\mu^3}\left(\mu + \frac{A}{4}\right)\sigma_1^2. \tag{17}$$

In deriving equations (16) and (17), use has been made of the fact that $p = \lambda_2 W_2$, which is obtained from the condition that the lateral faces are traction free ($\sigma_3 = \sigma_2 = 0$).

The components of the elasticity tensor can similarly be expanded up to the second order in the pre-strain using equations (6), (14) and (15). For brevity, only the non-zero components of the elasticity tensor used in the derivation of the dispersion relations in equation (10) are listed here

$$\mathcal{A}_{1111} = 2\mu + (10\mu + 2A)e_1 + (17\mu + 10A + 14D)e_1^2,$$

$$\mathcal{A}_{2222} = 2\mu - (5\mu + A)e_1 + (8\mu + 13A/4 + 8D)e_1^2,$$

$$\mathcal{A}_{1122} = -4De_1^2,$$

$$\mathcal{A}_{1221} = \mu + (\mu + A/4)e_1 + (3A/4 + 3D)e_1^2, \quad (18)$$

$$\mathcal{A}_{2121} = \mu + (A/4)e_1 + (2\mu + A + 3D)e_1^2,$$

$$\mathcal{A}_{1212} = \mu + (3\mu + A/4)e_1 + (5\mu + 7A/4 + 3D)e_1^2.$$

It is worth noting that the expressions for $\mathcal{A}_{1111}$, $\mathcal{A}_{1212}$, $\mathcal{A}_{2222}$ and $\mathcal{A}_{2121}$were first obtained by Abiza et al. (2012).

For a given uniaxial stress field defined by σ_1 (with $\sigma_3 = \sigma_2 = 0$), the elongation e_1 can be evaluated using equation (17) and the components of the elasticity tensor, $\mathcal{A}_{ijkl}$, can then be determined using equation (18). Using the latter components, the dispersion relations in equation (10) can be solved to obtain, implicitly, the second order correction to the phase velocity due to the pre-stress.

6. Numerical Results

The dispersion relations (10) provide an implicit relationship between the phase velocity, wavenumber, plate thickness and applied stress. These relations can only be solved numerically and the results are typically presented in the form of dispersion curves, showing the variation of the phase velocity of the Lamb wave modes as a function of the wavenumber-thickness product for different magnitudes of the applied stress. The material considered in this study is Silicone Rubber, which was selected due to its large elastic strain limit. The elastic properties of this material were obtained from the experimental data of Abiza *et al.* (2012) and are summarised in Table 1.

Table 1. Elastic Properties for Silicone Rubber

Parameter	Value (kPa)
μ	109.35
A	-454.18
D	109.27

Fig. 1 shows the dispersion curves associated with the first three modes of symmetric and anti-symmetric motion for a plate subjected to a uniaxial tension of $\bar{\sigma}_1 = \sigma_1/\mu = 1.37$. The results are here presented in terms of the non-dimensional squared phase velocity $\bar{v} = \rho v^2/\mu$ as a function of the non-dimensional wavenumber $k \cdot h_0$. It is emphasised that the thickness of the undeformed plate, h_0, is used here rather than the deformed plate thickness, h, in order to take into account the effect of the applied stress on the phase velocity due to the change in the plate thickness. A semi-log scale is used here to clearly show the behaviour of the different modes in the low and high wavenumber limits. In the long wave region as $k \cdot h_0 \rightarrow 0$, it can be seen that the fundamental symmetric (S0) and anti-symmetric (A0) modes have distinct squared phase velocity limits but in the short wave region as $k \cdot h_0 \rightarrow \infty$, they both approach the same squared phase velocity limit. On the other hand, the higher order modes of both the symmetric and anti-symmetric motion have infinite squared phase velocity limits as $k \cdot h_0 \rightarrow 0$ but they all tend to the same squared phase velocity limit (distinct from that of the fundamental modes) as $k \cdot h_0 \rightarrow \infty$. These limiting behaviours have been investigated by several researchers who derived appropriate asymptotic expansions (see, for example, Rogerson, 1997). These expansions were used as a means to verify the current approach and numerical results.

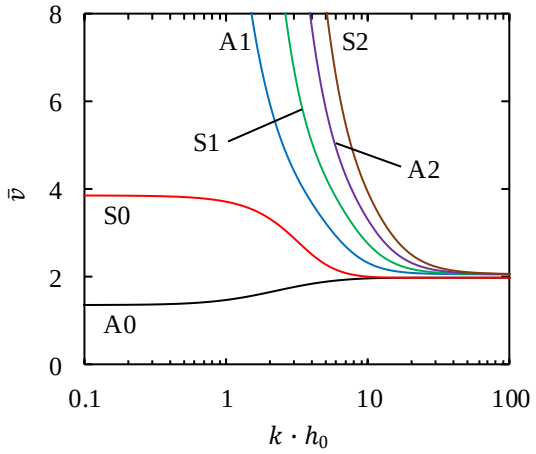

Figure 1. Dispersion curves for the first three symmetric and anti-symmetric modes propagating in an incompressible plate of Silicone Rubber subjected to a uniaxial tension of $\bar{\sigma}_1 = 1.37$.

The effect of applied stress on the propagation of the different Lamb wave modes is analysed in Fig. 2. The left column shows the variation of the squared phase velocity as a function of the wavenumber-thickness product for different magnitudes of the applied stress. The right column shows the variation of the squared phase velocity as a function of the applied stress for selected values of the wavenumber-thickness product. In both cases, the solid and dashed lines correspond to the large and classical acoustoelastic effects respectively. The former is concerned with the second order correction to the squared phase velocity while the latter is concerned with the first order correction. To obtain the first order correction, it suffices to keep the linear terms in the expansions (16)-(18) of the stress-strain relation and the components of the elasticity tensor.

The dependence of the fundamental anti-symmetric (A0) mode on the applied stress is shown in Fig. 2(a). It is evident that the squared phase velocity increases monotonically with the magnitude of the applied stress. It can also be seen that for compressive stresses the A0 mode seems to have specific cut-off values of $k \cdot h_0$ below which the wave no longer propagates but are instead growing standing waves (Rogerson and Fu, 1995). These cut-off values depend on the magnitude of $\bar{\sigma}_1$ and correspond to the points at which the curves intersect

the axis $\bar{v} = 0$. Below these cut-off values, the phase velocity becomes negative and the underlying deformation becomes unstable for the A0 mode (Ogden and Roxburgh, 1993, Rogerson and Fu, 1995). It is also interesting to find that at a pre-stress of $\bar{\sigma}_1 = -1.37$, the classical acoustoelastic formulation predicts that the A0 mode does not propagate whereas the large acoustoelastic formulation predicts otherwise.

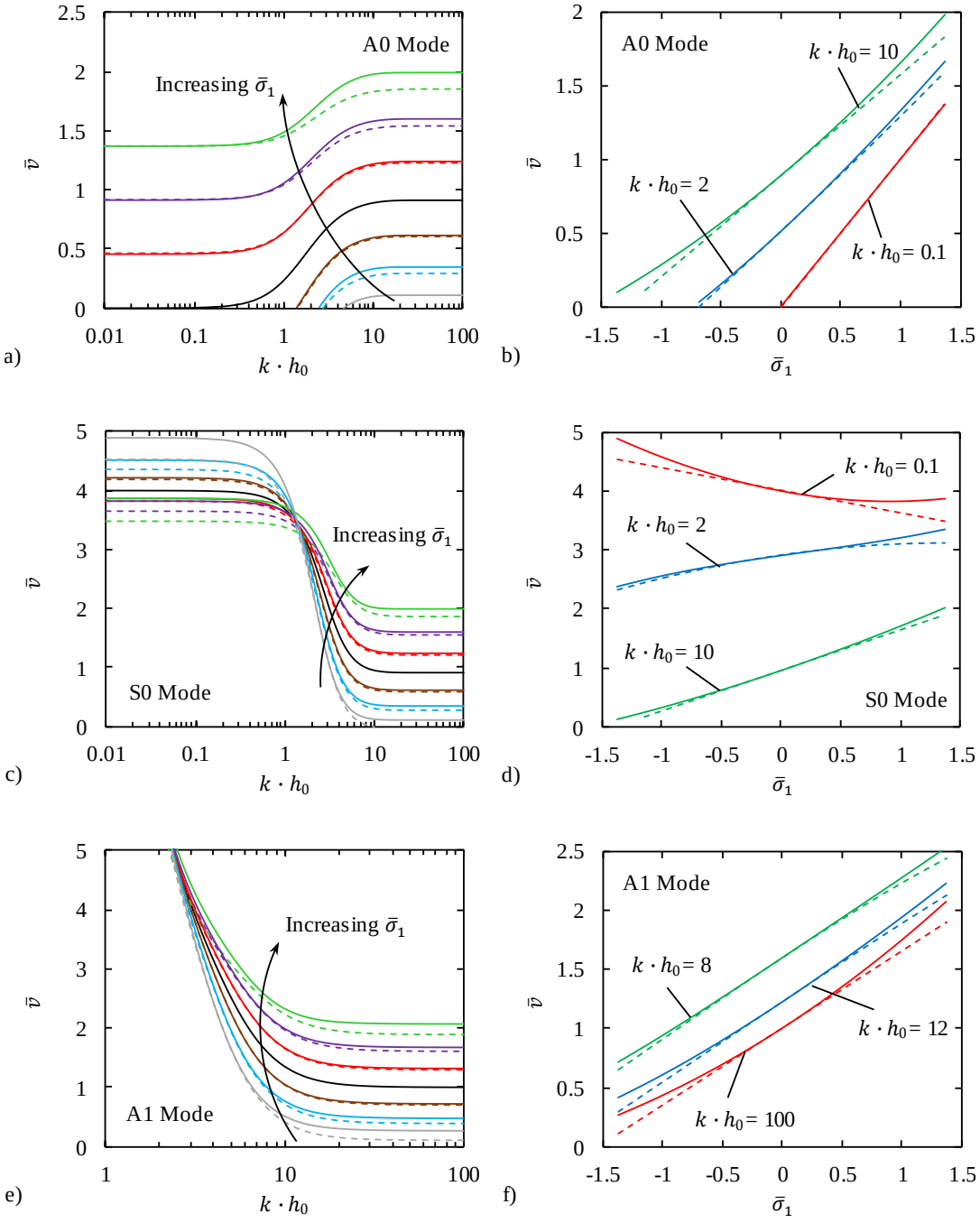

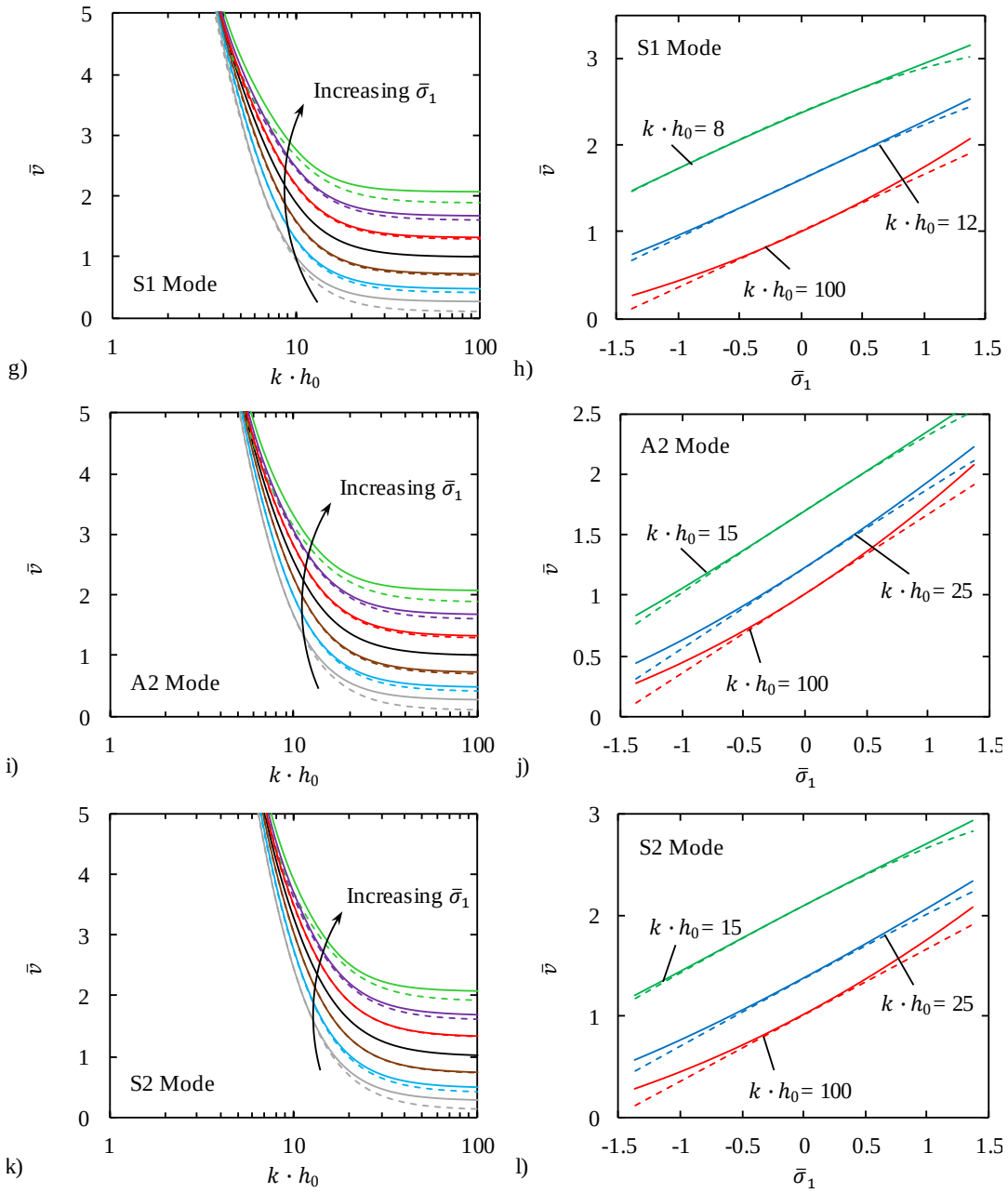

Figure 2. Effect of the applied uniaxial stress on the propagation of Lamb waves in an incompressible layer of Silicone Rubber. Left column: variation of the squared phase velocity as a function of the wavenumber-thickness product for different magnitudes of the applied stress $\bar{\sigma}_1 = \{-1.37, -0.91, -0.46, 0, 0.46, 0.91, 1.37\}$. Right column: variation of the squared phase velocity as a function of the applied stress for selected values of the wavenumber-thickness product. (a-b) A0 mode, (c-d) S0 mode, (e-f) A1 mode, (g-h) S1 mode, (i-j) A2 mode and, (k-l) S2 mode. The solid (dashed) lines correspond to the large (small) acoustoelastic effect.

In Figs. 2(e)-(l), the first two higher order modes of symmetric and anti-symmetric motion are presented. It can be seen that these modes behave in a similar way and have infinite squared phase velocity limits in the long wave region as $k \cdot h_0 \rightarrow 0$. The higher order modes are all highly dispersive in the low and moderate wavenumber regimes and hence, the squared phase velocity is dependent on the applied stress as well as on the wavenumber-thickness product. In the moderate wavenumber regime, the squared phase velocity is found to increase monotonically with the applied stress. The variation of $\bar{v}$ with $\bar{\sigma}_1$ is approximately linear for the large acoustoelastic effect whereas an approximately quadratic variation is observed for the classical acoustoelastic effect. However, the opposite trend is seen in the high wavenumber regime; the large acoustoelastic effect predicts a quadratic dependence of $\bar{v}$ on $\bar{\sigma}_1$ while the classical acoustoelastic effect predicts a linear dependence. This behaviour is expected as in the short wave region as $k \cdot h_0 \rightarrow \infty$, the higher order modes are largely non-dispersive and converge to the same squared phase velocity limit corresponding to that of a shear wave propagating along the x_1 direction (Rogerson, 1997). The squared phase velocity limit is given by $\bar{v} = \mathcal{A}_{1212}/\mu$, where the expression for $\mathcal{A}_{1212}$ is obtained from the expansions in equation (18). At low magnitudes of the applied stress, the curves for the large and classical acoustoelastic effects overlap as the contribution of the second order terms is relatively small. However, at higher magnitudes of the applied stress, the contribution of the second order terms is significant, leading to a quadratic increase in the squared phase velocity.

Overall, the wavenumber-thickness range of $k \cdot h_0 > 20$ and the applied stress range of $\bar{\sigma}_1 > 0.5$ represent a region of practical interest with respect to the experimental determination of the fourth order constants using guided waves. In general, fourth order constants cannot be evaluated using these results for metals and other ordinary elastic solids because of yielding and plasticity. However, for soft solids such as Silicone Rubber, an elongation of about 15% (corresponding to $\bar{\sigma}_1 = 0.5$) seems to be sufficient to reveal the large acoustoelastic effect. This behaviour is in good agreement with the results of

Abiza *et al.* (2012) who showed that an elongation of about 20% is sufficient to evaluate the fourth order constants experimentally using bulk shear waves.

It is also interesting to compare the results presented here for Silicone Rubber to those obtained for metals. Several studies have shown that, in the case of Aluminium, tensile stresses cause a decrease in the phase velocity of the different Lamb wave modes for wave propagation along the direction of the applied load (Pau and Lanza di Scalea, 2015; Pei and Bond, 2017), which is consistent with the results of bulk wave acoustoelasticity (Hughes and Kelly, 1953). In contrast, the results obtained for Silicone Rubber show that tensile stresses lead to an increase in the phase velocity of the different modes, apart from the S0 mode in the long wave region. This opposing behaviour is a consequence of the values of the higher order elastic constants, which are of the same order of magnitude as the second order constants for Silicone Rubber.

7. Conclusion

The classical acoustoelastic theory allows the determination of third order elastic constants and the evaluation of applied stresses in ordinary elastic materials using bulk waves. However, this theory can produce large discrepancies in the case of relatively soft tissues and rubber-like materials which are often subjected to high strains. These discrepancies can become quite pronounced in the case of guided waves as the phase velocities of the different wave modes are dependent on the applied stress as well as the wavenumber-thickness product.

This paper aimed at uncovering the acoustoelastic effect associated with the propagation of small-amplitude Lamb waves in incompressible plate-like structures subjected to a large pre-stress. A new acoustoelastic formulation based on a fourth order strain energy function was developed to study the effect of a large applied uniaxial stress on the squared phase velocity of the different Lamb wave modes. Dispersion results were presented for a Silicone Rubber plate and were compared with the results obtained using the classical acoustoelastic formulation. At lower magnitudes of the applied stress, the deviation between the large and classical acoustoelastic formulations was found to be relatively

small. However, the difference was found to be quite significant at higher magnitudes of the applied stress, showing that the large acoustoelastic formulation should be considered when evaluating the stress in rubber-like materials subjected to high strains.

In general, this paper provides useful analytical benchmarks for experimental studies and the development of guided wave based ultrasonic techniques for soft tissues and rubber-like materials. The presented results can also be easily generalised, for example, to torsional or interfacial waves. Although the framework developed can be extended to compressible materials, the lack of fourth order elastic constants coupled with the low elastic strain limit of ordinary stiff materials makes this option less attractive.

Acknowledgments

This work was supported by the Australian Research Council through Discovery Project DP160102233. The first author also gratefully acknowledges the support of the Australian Government Research Training Program Scholarship.

Appendix

Following the work of Mohabuth *et al.* (2016), the propagation of homogeneous plane waves in the form

$$\{u_j, p^*\} = \{U_j, kP\}e^{ik(x_1+\alpha x_2-ct)}\,, \qquad j \in \{1,2\} \tag{A1}$$

is considered, where U_j is the amplitude of the displacement, P is a scalar, k is the wavenumber along the x_1 direction, α is the ratio of the wavenumbers in the x_2 direction to that in the x_1 direction and c is the phase velocity in the x_1 direction.

Substituting solutions of this form into equations (7) and (8) yields

$$\begin{aligned} \rho U_1 c^2 - \mathcal{A}_{1111}\, U_1 - (\mathcal{A}_{1122} + \mathcal{A}_{2112})U_2\alpha - \mathcal{A}_{2121}\, U_1\alpha^2 - iP = 0, \\ \rho U_2 c^2 - \mathcal{A}_{1212}\, U_2 - (\mathcal{A}_{1122} + \mathcal{A}_{2112})U_1\alpha - \mathcal{A}_{2222}\, U_2\alpha^2 - i\alpha P = 0, \end{aligned} \tag{A2}$$

and

$$U_1 + U_2\alpha = 0. \tag{A3}$$

Using the incompressibility constraint (A3) to eliminate U_2 in favour of U_1 in the equations of motion (A2), two homogeneous equations are obtained

$$\begin{aligned} U_1(\rho c^2 - \mathcal{A}_{1111} + \mathcal{A}_{1122} + \mathcal{A}_{2112} - \mathcal{A}_{2121}\,\alpha^2) - iP = 0, \\ U_1(-\rho c^2 + \mathcal{A}_{1212} + (\mathcal{A}_{2222} - \mathcal{A}_{1122} - \mathcal{A}_{2112})\alpha^2) - i\alpha^2 P = 0. \end{aligned} \tag{A4}$$

These can be shown to have a non-trivial solution provided that

$$\Lambda_4\,\alpha^4 + \Lambda_2\,\alpha^2 + \Lambda_0 \;= 0\,, \tag{A5}$$

where

$$\begin{aligned} \Lambda_4 &= \mathcal{A}_{2121}\,, \\ \Lambda_2 &= \mathcal{A}_{1111} + \mathcal{A}_{2222} - 2\mathcal{A}_{1122} - 2\mathcal{A}_{2112} - \rho c^2\,, \\ \Lambda_0 &= \mathcal{A}_{1212} - \rho c^2\,. \end{aligned} \tag{A6}$$

The lack of odd power coefficients in equation (A5) means that the fourth order equation can be reduced to a quadratic equation in α^2. This simplification yields four solutions for α, which are denoted by α_q, $q \in \{1,2,3,4\}$, with the following properties

$$\alpha_2 = -\alpha_1, \qquad \alpha_4 = -\alpha_3 \,. \tag{A7}$$

The general solution for u_j and p^* may be expressed as a linear combination of the four linearly independent solutions

$$\{u_1, u_2, p^*\} = \sum_{q=1}^{4} \{1, V_q, kW_q\}\, U_{1q}\, e^{ik(x_1+\alpha_q x_2-ct)}, \tag{A8}$$

where $V_q = U_{2q}/U_{1q}$ and $W_q = P_q/U_{1q}$. These ratios are given by

$$\begin{aligned} V_q &= -1/\alpha_q, \\ W_q &= -i\left(\rho c^2 - \mathcal{A}_{1111} + \mathcal{A}_{1122} + \mathcal{A}_{2112} - \mathcal{A}_{2121}\,\alpha_q^2\right), \end{aligned} \tag{A9}$$

which are obtained using the relations in equations (A3) and (A4) respectively.

Explicit expressions for the incremental surface tractions may then be found by substituting equation (A8) into equation (9)

$$\begin{aligned} \hat{\mathrm{S}}_{22} &= \sum_{q=1}^{4} ikD_{1q}U_{1q}\, e^{ik(x_1+\alpha_q x_2-ct)}, \\ \hat{\mathrm{S}}_{21} &= \sum_{q=1}^{4} ikD_{2q}U_{1q}\, e^{ik(x_1+\alpha_q x_2-ct)}, \end{aligned} \tag{A10}$$

where

$$\begin{aligned} D_{1q} = \rho c^2 &- \mathcal{A}_{1111} - \mathcal{A}_{2222} + 2\mathcal{A}_{2112} + 2\mathcal{A}_{1122} - \mathcal{A}_{2121} \\ &- \mathcal{A}_{2121}\alpha_q^2 + \sigma_2, \\ D_{2q} &= \mathcal{A}_{2121}\alpha_q - \mathcal{A}_{2121}/\alpha_q + \sigma_2/\alpha_q. \end{aligned} \tag{A11}$$

It is noted that in deriving the above expressions, use has been made of the fact that $p = \mathcal{A}_{2121} - \mathcal{A}_{2112} - \sigma_2$ (Ogden, 1984).

The dispersion relations are obtained by imposing incremental traction free boundary conditions on the upper and lower free surfaces of the plate, namely $\hat{\mathrm{S}}_{22} = \hat{\mathrm{S}}_{21} = 0$ at $x_2 = \pm\lambda_2 h_0/2 = \pm h/2$. This yields a homogeneous system of four equations which can be expressed as

$$i\xi \begin{pmatrix} D_{11}E_1 & D_{12}E_2 & D_{13}E_3 & D_{14}E_4 \\ D_{21}E_1 & D_{22}E_2 & D_{23}E_3 & D_{24}E_4 \\ D_{11}\overline{E_1} & D_{12}\overline{E_2} & D_{13}\overline{E_3} & D_{14}\overline{E_4} \\ D_{21}\overline{E_1} & D_{22}\overline{E_2} & D_{23}\overline{E_3} & D_{24}\overline{E_4} \end{pmatrix} \begin{pmatrix} U_{11} \\ U_{12} \\ U_{13} \\ U_{14} \end{pmatrix} e^{ik(x_1 - ct)} = \begin{Bmatrix} 0 \\ 0 \\ 0 \\ 0 \end{Bmatrix}, \tag{A12}$$

where $E_q = e^{ik\alpha_q \frac{h}{2}}$ and $\overline{E_q} = e^{-ik\alpha_q \frac{h}{2}}$. For non-trivial solutions, the determinant of the coefficient matrix in equation (A12) is set to zero. After some algebra, the determinant can be reduced to two characteristic equations

$$\begin{aligned} D_{11}D_{23}\cot(\gamma\alpha_1) - D_{13}D_{21}\cot(\gamma\alpha_3) = 0\,, \\ D_{11}D_{23}\tan(\gamma\alpha_1) - D_{13}D_{21}\tan(\gamma\alpha_3) = 0\,, \end{aligned} \tag{A13}$$

corresponding to the symmetric and anti-symmetric Lamb wave modes respectively, with $\gamma = kh/2$.

References

Abiza, Z., Destrade, M., and Ogden, R. W. (**2012**). "Large acoustoelastic effect," Wave Motion **49**, 364–374. https://doi.org/10.1016/j.wavemoti.2011.12.002

Aryan, P., Kotousov, A., Ng, C. T., and Cazzolato, B. S. (**2017**). "A baseline-free and non-contact method for detection and imaging of structural damage using 3D laser vibrometry," Structural Control and Health Monitoring **24**, e1894. https://doi.org/10.1002/stc.1894

Destrade, M., and Ogden, R. W. (**2010**). "On the third- and fourth-order constants of incompressible isotropic elasticity," J. Acoust. Soc. Am. **128**, 3334-3343. https://doi.org/10.1121/1.3505102

Destrade, M., Gilchrist, M. D., and Saccomandi, G. (**2010a**). "Third- and fourth-order constants of incompressible soft solids and the acousto-elastic effect," J. Acoust. Soc. Am. **127**, 2759-2763. https://doi.org/10.1121/1.3372624

Destrade, M., Gilchrist, M. D., and Ogden, R. W. (**2010b**). "Third- and fourth-order elasticities of biological soft tissues," J. Acoust. Soc. Am. **127**, 2103-2106. https://doi.org/10.1121/1.3337232

Destrade, M., Gilchrist, M. D., and Murphy, J. G. (**2010c**). "Onset of nonlinearity in the elastic bending of blocks," J. Appl. Mech. **77**(6), 061015. https://doi.org/10.1115/1.4001282

Dowaikh, M. A., and Ogden, R. W. (**1990**). "On surface waves and deformations in a pre-stressed incompressible elastic solid," IMA J. Appl. Math. **44**, 261–284. https://doi.org/10.1093/imamat/44.3.261

Dubuc, B., Ebrahimkhanlou, A., and Salamone, S. (**2017**). "The effect of applied stress on the phase and group velocity of guided waves in anisotropic plates," J. Acoust. Soc. Am. **142**, 3553-3563. https://doi.org/10.1121/1.5016969

Dubuc, B., Ebrahimkhanlou, A., and Salamone, S. (**2018**). "Computation of propagating and non-propagating guided modes in nonuniformly stressed

plates using spectral methods," J. Acoust. Soc. Am. **143**, 3220-3230. https://doi.org/10.1121/1.5040140

Gandhi, N., Michaels, J. E., and Lee, S. J. (**2012**). "Acoustoelastic Lamb wave propagation in biaxially stressed plates," J. Acoust. Soc. Am. **132**, 1284-1293. https://doi.org/10.1121/1.4740491

Guz, A. N., and Makhort, F. G. (**2000**). "The physical fundamentals of the ultrasonic nondestructive stress analysis of solids," Int. Appl. Mech. **36** (9), 1119-1149. https://doi.org/10.1023/A:100944213206

Hughes, D. S., and Kelly, J. L. (**1953**). "Second-order elastic deformation of solids," Phys. Rev. **92**, 1145-1149. https://doi.org/10.1103/PhysRev.92.1145

Hamilton, M. F., Ilinskii, Y. A., and Zabolotskaya, E. A. (**2004**). "Separation of compressibility and shear deformation in the elastic energy density," J. Acoust. Soc. Am. **116**, 41-44. https://doi.org/10.1121/1.1736652

Kaplunov, J. D., Nolde, E. V., and Rogerson, G. A. (**2000**). "A low-frequency model for dynamic motion in pre-stressed incompressible elastic structures," Proc. R. Soc. Lond. A **456**, 2589–2610. https://doi.org/10.1098/rspa.2000.0627

Kaplunov, J. D., Nolde, E. V., and Rogerson, G. A. (**2002a**). "An asymptotically consistent model for long-wave high-frequency motion in a pre-stressed elastic plate," Math. Mech. Solids **7**(6), 581–606. https://doi.org/10.1177/108128602029660

Kaplunov, J. D., Nolde, E. V., and Rogerson, G. A. (**2002b**). "Short wave motion in a pre-stressed incompressible elastic plate," IMA J. Appl. Math. **67**, 383-399. https://doi.org/10.1093/imamat/67.4.383

Kayestha, P., Wijeyewickrema, A. C., and Kishimoto, K. (**2011**). "Wave propagation along a non-principal direction in a compressible pre-stressed elastic layer," Int. J. Solids Struct. **48**, 2141–2153. https://doi.org/10.1016/j.ijsolstr.2011.03.022

Kim, K. Y., and Sachse, W. (**2001**). "Acoustoelasticity of elastic solids," in *Handbook of Elastic Properties of Solids, Liquids, and Gases*, edited by A. G. Avery and W. Sachse (Academic Press, San Diego), Vol. 1, pp. 441–468.

Kubrusly, A. C., Braga, A. M. B., and Von der Weid, J. P. (**2016**). "Derivation of acoustoelastic Lamb wave dispersion curves in anisotropic plates at the initial and natural frames of reference," J. Acoust. Soc. Am. **140**, 2412-2417. https://doi.org/10.1121/1.4964343

Mohabuth, M., Kotousov, A., and Ng, C.-T. (**2016**). "Effect of uniaxial stress on the propagation of higher-order Lamb wave modes," Int. J. Nonlinear Mech. **86**, 104–111. https://doi.org/10.1016/j.ijnonlinmec.2016.08.006

Mohabuth, M., Kotousov, A., Ng, C.-T., and Rose, L. R. F. (**2018**). "Implication of changing loading conditions on structural health monitoring utilising guided waves," Smart Mater. Struct. **27**, 025003. https://doi.org/10.1088/1361-665X/aa9f89

Ng, C. T. (**2015**). "A two-stage approach for quantitative damage imaging in metallic plates using Lamb waves," Earthquakes and Structures **8**, 821-841. https://doi.org/10.12989/eas.2015.8.4.821

Nolde, E. V., Prikazchikova, L. A., and Rogerson, G. A. (**2004**). "Dispersion of small amplitude waves in a pre-stressed, compressible elastic plate," J. Elasticity **75**, 1–29. https://doi.org/10.1023/B:ELAS.0000039920.67766.d3

Ogden, R. W. (**1984**). *Non-Linear Elastic Deformations* (Ellis Horwood, Chichester).

Ogden, R. W., and Roxburgh, D. G. (**1993**). "The effect of pre-stress on the vibration and stability of elastic plates," Int. J. Eng. Sci. **31**(12), 1611-1639. https://doi.org/10.1016/0020-7225(93)90079-A

Ogden, R. W. (**2007**). "Incremental statics and dynamics of pre-stressed elastic materials," in *Waves in Nonlinear Pre-Stressed Materials*, edited by M. Destrade and G. Saccomandi (Springer, Vienna), Vol. 495, pp. 1–26. https://doi.org/10.1007/978-3-211-73572-5_1

Pao, Y.-H., Sachse, W., and Fukuoka, H. (**1984**). "Acoustoelasticity and Ultrasonic Measurements of Residual Stresses," in *Physical Acoustics*, edited by W. P. Mason and R. N. Thurston (Academic Press, New York), Vol. 17, pp. 61–143.

Pao, Y.-H., and Gamer, U. (**1985**). "Acoustoelastic waves in orthotropic media," J. Acoust. Soc. Am. **77**, 806. https://doi.org/10.1121/1.392384

Pau, A., and Lanza di Scalea, F. (**2015**). "Nonlinear guided wave propagation in prestressed plates," J. Acoust. Soc. Am. **137**, 1529-1540. https://doi.org/10.1121/1.4908237

Peddeti, K., and Santhanam, S. (**2018**). "Dispersion curves for Lamb wave propagation in prestressed plates using a semi-analytical finite element analysis," J. Acoust. Soc. Am. **143**, 829-840. https://doi.org/10.1121/1.5023335

Pei, N., and Bond, L. (**2016**). "Higher order acoustoelastic Lamb wave propagation in stressed plates," J. Acoust. Soc. Am. **140**, 3834-3843. https://doi.org/10.1121/1.4967756

Pei, N., and Bond, L. (**2017**). "Comparison of acoustoelastic Lamb wave propagation in stressed plates for different measurement orientations," J. Acoust. Soc. Am. **142**, EL327-EL331. https://doi.org/10.1121/1.5004388

Pichugin, A. V., and Rogerson, G. A. (**2001**). "A two-dimensional model for extensional motion of a pre-stressed incompressible elastic layer near cut-off frequencies," IMA J. Appl. Math. **66**, 357–385. https://doi.org/10.1093/imamat/66.4.357

Pichugin, A. V., and Rogerson, G. A. (**2002a**). "An asymptotic membrane-like theory for long wave motion in a pre-stressed elastic plate," Proc. R. Soc. Lond. A **458**, 1447–1468. https://doi.org/10.1093/imamat/66.4.357

Pichugin, A. V., and Rogerson, G. A. (**2002b**). "Anti-symmetric motion of a pre-stressed incompressible elastic layer near shear resonance," J. Eng. Math. 42, 181–202. https://doi.org/10.1023/A:1015293700959

Rogerson, G. A., and Fu, Y. B. (**1995**). "An asymptotic analysis of the dispersion relation of a pre-stressed incompressible elastic plate," Acta Mech. **111**, 59–74. https://doi.org/10.1007/BF01187727

Rogerson, G. A. (**1997**). “Some asymptotic expansions of the dispersion relation for an incompressible elastic plate,” Int. J. Solids Struct. **34**(22), 2785-2802. https://doi.org/10.1016/S0020-7683(96)00218-1

Rogerson, G. A., and Sandiford, K. J. (**1999**). “Harmonic wave propagation along a non-principal direction in a pre-stressed elastic plate,” Int. J. Eng. Sci. **37**(13), 1663–1691. https://doi.org/10.1016/S0020-7225(98)00146-3

Rogerson, G. A., and Prikazchikova, L. A. (**2009**). “Generalisations of long wave theories for pre-stressed compressible elastic plates,” Int. J. Non-Linear Mech. **44**, 520–529. https://doi.org/10.1016/j.ijnonlinmec.2008.11.002

Rose, J. **(2014)**. *Ultrasonic Guided Waves in Solid Media* (Cambridge University Press, Cambridge). https://doi.org/10.1017/CBO9781107273610

Su, Z., and Ye, L. (**2009**). “Identification of Damage Using Lamb Waves: From Fundamentals to Applications,” in *Lecture Notes in Applied and Computational Mechanics*, edited by F. Pfeiffer and P. Wriggers (Springer, Berlin). https://doi.org/10.1007/978-1-84882-784-4

Chapter 5

Implication of changing loading conditions on structural health monitoring utilising guided waves

Statement of Authorship

Title of Paper	Implication of changing loading conditions on structural health monitoring utilising guided waves.
Publication Status	☑ Published ☐ Accepted for Publication ☐ Submitted for Publication ☐ Unpublished and Unsubmitted work written in manuscript style
Publication Details	M. Mohabuth, A. Kotousov, C.T. Ng and L.R.F. Rose (2018), Implication of changing loading conditions on structural health monitoring utilising guided waves, *Smart Mater. Struct.*, 27, 1-12, doi: 10.1088/1361-665X/aa9f89.

Principal Author

Name of Principal Author (Candidate)	Munawwar Mohabuth		
Contribution to the Paper	Developed the analytical model, performed all analyses and wrote manuscript.		
Overall percentage (%)	70		
Certification:	This paper reports on original research I conducted during the period of my Higher Degree by Research candidature and is not subject to any obligations or contractual agreements with a third party that would constrain its inclusion in this thesis. I am the primary author of this paper.		
Signature		Date	23 Nov 2018

Co-Author Contributions

By signing the Statement of Authorship, each author certifies that:

i. the candidate's stated contribution to the publication is accurate (as detailed above);

ii. permission is granted for the candidate in include the publication in the thesis; and

iii. the sum of all co-author contributions is equal to 100% less the candidate's stated contribution.

Name of Co-Author	Andrei Kotousov		
Contribution to the Paper	Supervised the development of the analytical model, helped in interpretation of the results and assisted in the preparation of the manuscript.		
Signature		Date	23 Nov 2018

Name of Co-Author	Ching-Tai Ng		
Contribution to the Paper	Supervised the work and assisted with editing of the manuscript.		
Signature		Date	20 Nov 2018

Name of Co-Author	L. R. Francis Rose		
Contribution to the Paper	Provided advice on the modelling approach and interpretation of the results. Assisted with editing of the manuscript.		
Signature		Date	17 Nov 2018

Implication of changing loading conditions on structural health monitoring utilising guided waves

Munawwar Mohabuth[1], Andrei Kotousov[1*], Ching-Tai Ng[2] and L. R. Francis Rose[3]

[1]School of Mechanical Engineering, The University of Adelaide, Adelaide, SA 5005, Australia.

[2]School of Civil, Environmental and Mining Engineering, The University of Adelaide, Adelaide, SA 5005, Australia.

[3]Aerospace Division, Defence Science and Technology Group, Fishermen's Bend, VIC 3207, Australia.

*Corresponding author. Tel.: +61 8 8313 6385.

E-mail address: andrei.kotousov@adelaide.edu.au

Abstract

Structural health monitoring systems based on guided waves typically utilise a network of embedded or permanently attached sensors, allowing for the continuous detection of damage remote from a sensor location. The presence of damage is often diagnosed by analysing the residual signals from the structure after subtracting damage-free reference data. However, variations in environmental and operational conditions such as temperature, humidity, applied or thermally-induced stresses affect the measured residuals. A previously developed acoustoelastic formulation is here extended and employed as the basis for a simplified analytical model to estimate the effect of applied or thermally-induced stresses on the propagation characteristics of the fundamental Lamb wave modes. It is noted that there are special combinations of frequency, biaxial stress ratio and direction of wave propagation for which there is no change in the phase velocity of the fundamental anti-symmetric mode. The implication of these results in devising effective strategies to mitigate the effect of stress induced variations in guided-wave damage diagnostics is briefly discussed.

1. Introduction

Damage diagnostics is often necessary for the safe and efficient operation of civil and mechanical engineering infrastructure. Structural health monitoring (SHM) normally refers to a process for the in-situ monitoring of the integrity of structures using real-time data obtained from a permanently attached or embedded sensor network. Therefore, there is no need for disassembly of the components to be inspected as the sensors are an inherent part of these structures. This approach represents an alternative to traditional time consuming and labour intensive non-destructing evaluation procedures [1-3].

In recent years, significant progress was achieved in the development of SHM techniques utilising guided waves [4-13]. In particular, it was found that Lamb waves, which are guided waves in traction-free plates, can propagate over several metres without significant decay, thereby offering the possibility of interrogating large areas of plate-like structures with a small number of sensors [14-16]. A typical guided wave (GW) based SHM system incorporates a grid of permanently bonded or embedded transducers. One of the transducers (or transmitters) is excited with a tone burst of a few cycles, generating a stress wave that propagates along the structure. The time-domain responses from the transmitter and the receiving transducers are then recorded. This process is repeated using different transducers as transmitters. The signal remaining after subtraction from damage-free reference data which exceeds the background noise is assumed to be linked to a defect or mechanical damage. However, one of the main contributions to the background noise in real-world situations arises from variations in environmental and operational conditions (EOC) such as temperature [17-21] and loading [22-27]. These contributions will be referred to as noise in the sense that they represent unwanted contributions. They are, however, deterministic contributions that can be predicted and compensated for.

Changing EOC is arguably the main reason why SHM systems, which have been developed and successfully demonstrated in the last two decades in laboratory conditions, often fail to prove their efficiency in the real-world environment. The background noise due to changing EOC can interfere with the

operation of SHM systems leading to false alarms or to the prevention of the critical damage from being detected in service. One way to address this problem is to increase the number of sensors, which however can adversely affect the cost, weight and power efficiency of the SHM system. For example, Croxford et al. [28] demonstrated that even in the presence of modest temperature fluctuations, the number of sensors required for damage detection can be prohibitively high. Therefore, some form of compensation for changing EOC is often essential for guided wave based SHM systems to be viable [29,30].

The effect of temperature variations on damage detection has been extensively documented in literature over the past two decades. Subsequently, a large effort has been directed to the development of various temperature compensation techniques [31-38]. The current paper is focused on the noise generation due to variations in applied or thermally induced stresses. It is shown that the effect of these variations on the noise generation is comparable with that of moderate temperature fluctuations. Therefore, both effects need to be considered when developing SHM systems for real-world applications. Another interesting outcome of this work is the identification of certain combinations of frequency, biaxial stress ratio and wave propagation direction, for which the applied stress has a minor effect on the phase velocity of the fundamental anti-symmetric mode (A0). Favourable operating points for the fundamental symmetric mode (S0) are also discussed. These results can provide a basis for developing stress mitigation techniques, which might be necessary to comply with cost, energy or weight constraints of the SHM system.

The current paper is structured as follows. In Section 2, we review the fundamentals of the theory of acoustoelasticity following the work of Ogden [39]. This formulation is then used to derive dispersion equations for Lamb waves propagating along a non-principal direction in a plate subjected to biaxial stresses. In Section 3, we provide numerical results to demonstrate the effect of the applied stress, propagation direction and frequency on the propagation of the fundamental Lamb wave modes. Then, in Section 4, we present an analytical model to quantify the noise due to the applied stress and compare the noise levels due to temperature variations and thermally-induced stresses. Finally, in Section

5, we propose different strategies to minimize the effect of applied stress in Lamb wave based SHM systems.

2. Acoustoelastic Lamb Wave Propagation

The equations governing the propagation of small-amplitude waves in pre-stressed plates are briefly reviewed here, following the work of Mohabuth et al. [40]. These authors used the theory of small deformations superimposed on a large deformation [39] to derive dispersion equations for Lamb wave propagation along a principal direction in a plate subjected to uniaxial stress. This framework is extended to consider the propagation of Lamb waves along a non-principal direction in a plate subjected to biaxial stresses.

Consider an isotropic plate of density ρ_0 and thickness h_0 in a stress-free reference configuration. Suppose biaxial stresses are applied in the plane of the plate such that its density and thickness change to ρ and h respectively. The deformed configuration is shown in figure 1, where the biaxial stresses σ_1 and σ_2 are assumed to be applied along the x_1 and x_2 directions of a Cartesian coordinate system $x_i = (x_1, x_2, x_3)$. The propagation of small-amplitude plane waves at an arbitrary azimuthal angle ϕ to the x_1 direction is then considered.

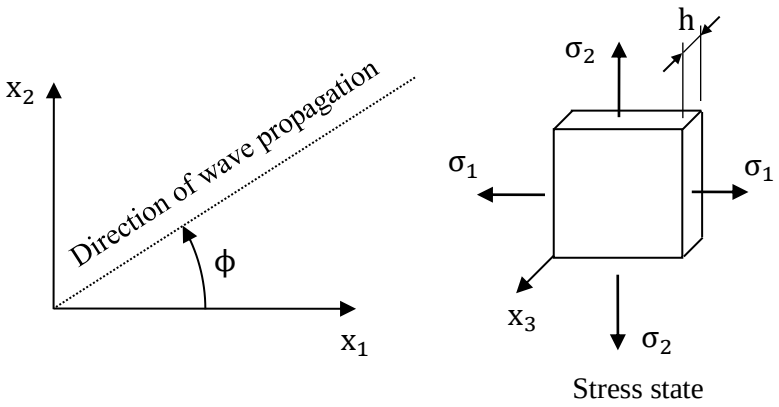

Figure 1. An infinite plate of thickness, h, subjected to biaxial loading.

The equation of motion in the pre-stressed plate and the corresponding constitutive equation are given by

$$\mathcal{A}_{piqj}\,\frac{\partial^2 u_j}{\partial x_p\,\partial x_q}=\rho\frac{\partial^2 u_i}{\partial t^2}, \tag{1}$$

and

$$\hat{S}_{pi}=\mathcal{A}_{piqj}\,\frac{\partial u_j}{\partial x_q}, \tag{2}$$

respectively, where $\boldsymbol{\mathcal{A}_0}$ is the fourth-order tensor of instantaneous elastic moduli, $\mathbf{u}$ is the incremental displacement vector associated with the wave, t is the time and $\hat{\mathbf{S}}$ is the incremental nominal stress tensor. For brevity, the derivation of the above equations is not shown here but we refer to [39] for further details.

In the present work, the elasticity tensor is expressed in terms of a third-order expanded strain energy function due to Murnaghan [41]. This form of the strain energy function is commonly used to evaluate the acoustoelastic effect in engineering materials subjected to a small pre-stress. The elasticity tensor can be obtained to the first-order in the strain as

$$\begin{aligned}J\mathcal{A}_{piqj}=\;&\mu\left(\delta_{ij}\delta_{pq}+\delta_{iq}\delta_{jp}\right)+\lambda\delta_{ip}\delta_{jq}\\&+2\mu\left(2\delta_{ij}E_{pq}+\delta_{pq}E_{ij}+\delta_{iq}E_{jp}+\delta_{jp}E_{iq}\right)\\&+\lambda\left(E\delta_{ij}\delta_{pq}+2\delta_{ip}E_{jq}+2\delta_{jq}E_{ip}\right)+2lE\delta_{ip}\delta_{jq}\\&+m\left[E\left(\delta_{ij}\delta_{pq}+\delta_{iq}\delta_{jp}-2\delta_{ip}\delta_{jq}\right)\right.\\&\left.+2\left(\delta_{ip}E_{jq}+\delta_{jq}E_{ip}\right)\right]\\&+\frac{1}{2}n\left[\delta_{ij}E_{pq}+\delta_{pq}E_{ij}+\delta_{iq}E_{jp}+\delta_{jp}E_{iq}-2\delta_{ip}E_{jq}\right.\\&\left.-2\delta_{jq}E_{ip}-E\left(\delta_{ij}\delta_{pq}+\delta_{iq}\delta_{jp}-2\delta_{ip}\delta_{jq}\right)\right],\end{aligned} \tag{3}$$

where $\mathbf{E}$ is the Green-Lagrange strain tensor, $E=\mathrm{tr}\,\mathbf{E}$, $J=1+E$, λ and μ are the classical Lamé elastic constants and l, m, n are the third-order elastic

constants. For a given biaxial stress field defined by σ_1 and σ_2 (with $\sigma_3 = 0$), the components of **E** can simply be evaluated by means of the linear theory.

Since the wave propagation is assumed to be along a non-principal direction, the analysis is conducted in a transformed coordinate system $x_i' = (x_1', x_2', x_3')$ formed by a rotation of the x_1 and x_2 axes about the x_3 axis through the angle ϕ. The equation of motion (1) and the constitutive equation (2) then transform to

$$\mathcal{A}'_{piqj} \frac{\partial^2 u_j'}{\partial x_p' \partial x_q'} = \rho \frac{\partial^2 u_i'}{\partial t^2}, \tag{4}$$

and

$$\hat{S}'_{pi} = \mathcal{A}'_{piqj} \frac{\partial u_j'}{\partial x_q'}, \tag{5}$$

where all the quantities are now expressed in terms of the rotated coordinate system. We note that the elasticity tensor in the rotated coordinate system is related to the elasticity tensor in the original coordinate system via the tensor transformation

$$\mathcal{A}'_{piqj} = \beta_{pr}\beta_{ik}\beta_{qs}\beta_{jl}\mathcal{A}_{rksl}, \tag{6}$$

where β_{ij} is the cosine of the angle between x_i' and x_j.

The derivation of dispersion equations for Acoustoelastic Lamb wave propagation requires the equation of motion (4) to be solved in conjunction with stress-free boundary conditions at the surfaces of the pre-stressed plate, i.e. $\hat{S}'_{31} = \hat{S}'_{32} = \hat{S}'_{33} = 0$ at $x_3' = \pm h/2$. Following the approach of Nayfeh and Chimenti [42], we consider solutions in the form of plane waves propagating along the x_1' direction

$$u_j' = U_j e^{i\xi(x_1' + \alpha x_3' - ct)}, \tag{7}$$

where U_j is the amplitude of the displacement, ξ is the wavenumber along the x_1' direction, α is the ratio of the wavenumbers in the x_3' direction to that in the x_1' direction and c is the phase velocity in the x_1' direction.

The detailed solution process is rather lengthy and only the final dispersion equations are presented here for reference. These are given by

$$\begin{aligned} &D_{11}G_1\cot(\zeta\alpha_1) - D_{13}G_3\cot(\zeta\alpha_3) + D_{15}G_5\cot(\zeta\alpha_5) = 0\,, \\ &D_{11}G_1\tan(\zeta\alpha_1) - D_{13}G_3\tan(\zeta\alpha_3) + D_{15}G_5\tan(\zeta\alpha_5) = 0\,, \end{aligned} \tag{8}$$

corresponding to the symmetric and anti-symmetric modes respectively. The definition of the various terms used in the above equations are discussed in detail in Appendix A. It is worth noting that Gandhi et al. [43] also derived similar dispersion equations. However, their analysis was performed in the natural (stress-free) coordinate system which yields the so-called natural wave velocity rather than the true wave velocity.

3. Numerical Results

The analytical equations derived can be solved numerically to obtain the phase velocity of the different guided wave modes as a function of the frequency-thickness product, the applied biaxial stress and the angle of wave propagation, i.e. $C_p(f\cdot h, \sigma_1, \sigma_2, \phi)$. The term $f\cdot h$ here refers to the product of the frequency of the wave, f and the thickness of the deformed plate, h, and the other variables are indicated in figure 1. In considering the acoustoelastic effect, it is the change in phase velocity from the unstressed state which is of interest. It is given by

$$\Delta C_p(f\cdot h_0, \sigma_1, \sigma_2, \phi) = C_p(f\cdot h, \sigma_1, \sigma_2, \phi) - C_p(f\cdot h_0, 0, 0, 0)\,, \tag{9}$$

where $C_p(f\cdot h_0, 0, 0, 0)$ refers to the unstressed phase velocity. The latter is evaluated at a frequency-thickness product $f\cdot h_0$, where h_0 corresponds to the thickness of the undeformed plate.

Dispersion results for different loads and directions of wave propagation are not discussed in detail here. These will be the subject of a later paper but we

refer to the article by Gandhi et al. [43] for an overview of typical dispersion results. Although these authors conducted their analysis in the natural or unstressed coordinate system, the results are qualitatively the same as in the case of the deformed coordinate system. In the present paper, we focus on the fundamental symmetric (S0) and anti-symmetric (A0) modes due to their relevance in SHM applications. The material considered is 6061-T6 Aluminium and its elastic properties are summarised in Table 1.

Table 1. Elastic Properties of 6061-T6 Aluminium

Parameter	Value[44]
λ [GPa]	54.308
μ [GPa]	27.174
l [GPa]	-281.5
m [GPa]	-339.0
n [GPa]	-416.0
ρ [kg/m^3]	2704
σ_y [MPa]	300

Note: The yield strength, σ_y , was not mentioned in [44]; thus an average of the typical values for this material is given in Table 1.

Figure 2 shows the change in the phase velocity of the fundamental Lamb wave modes for a plate subjected to a range of uniaxial strains (stresses). The waves are considered to be propagating along the direction of the applied load such that $\phi = 0^o$. It can be seen that at any given frequency-thickness product, the magnitude of the change in the phase velocity is directly proportional to the applied stress (strain) for both the A0 and S0 modes. In the case of the A0 mode, an interesting behaviour can be observed at a frequency-thickness product of approximately 350 Hz-m. As shown in the insert plot in figure 2(a), the change in the phase velocity of the A0 mode is zero at this frequency-thickness product. This particular frequency does not seem to be dependent on the magnitude of the applied strain (stress) as previously reported by Mohabuth et al. [40].

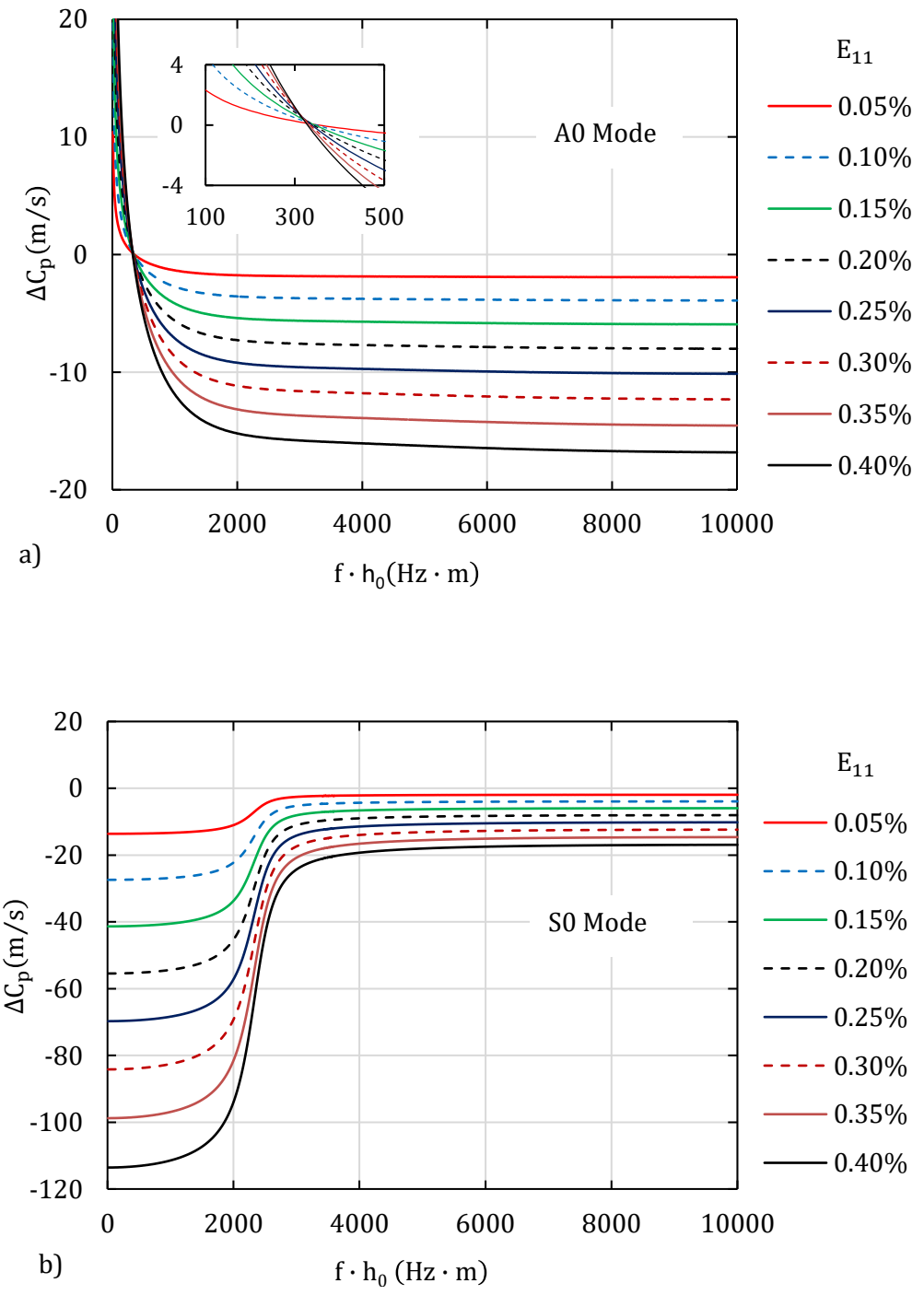

Figure 2. Effect of strain (stress) on the change in phase velocity of the fundamental Lamb wave modes, (a) A0 mode and, (b) S0 mode, propagating along the direction of the applied strain (stress).

Figure 3 shows the change in the phase velocity of the fundamental Lamb wave modes for a plate subjected to a uniaxial stress of 100 MPa at different angles of wave propagation. The load is applied along the x_1 axis such that waves propagating parallel to the applied load are at $\phi = 0^o$. Due to the strain induced anisotropy, the change in the phase velocity is dependent on the direction of wave propagation. However, considering the A0 mode, there is a critical frequency-thickness product (f_{Cr}) of approximately 300 Hz-m at which ΔC_p is invariant of the angle of wave propagation. As shown in the insert plot in figure 3 (a), the magnitude of ΔC_p at this particular frequency is small but non-zero. This phenomenon was also pointed out by Gandhi et al. [43]. At frequencies below f_{Cr}, the magnitude of ΔC_p is lowest when the wave propagation is perpendicular to the applied stress. At higher frequencies, it can be seen that the curves corresponding to $\phi < 60^o$ intersect the horizontal axis ($\Delta C_p = 0$) at different frequencies. These combinations of wave propagation angles and zero-intercept frequencies may be used in the development of stress mitigation strategies. These will be discussed in detail in Section 5.

In the case of the S0 mode, the curves for wave propagation at an oblique angle to the applied stress are not drawn beyond a certain threshold frequency-thickness product (f_{Th}) of 3400 Hz-m. This is because at this frequency, the S0 mode and the fundamental shear-horizontal (SH0) mode interact with each other, split and propagate as two hybridised modes. This behaviour was also reported by Gandhi et al. [43]. For wave propagation at $\phi = 0^0$ or 90^0, this behaviour does not occur as the direction of wave propagation is aligned with the principal axes and therefore, the motion of the S0 and SH0 modes are decoupled.

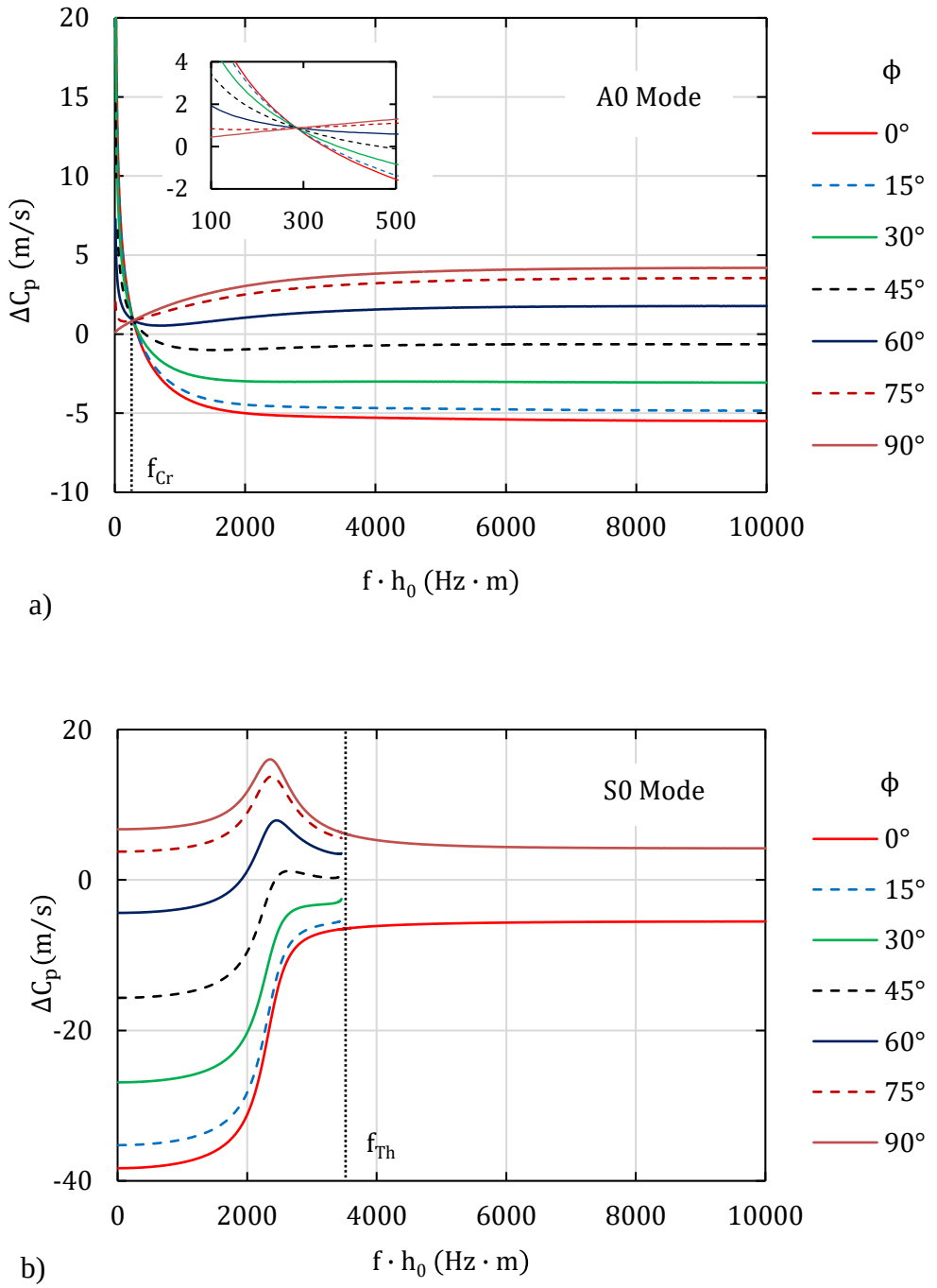

Figure 3. Effect of the direction of wave propagation on the change in phase velocity of the fundamental Lamb wave modes, (a) A0 mode and, (b) S0 mode, in a plate subjected to a uniaxial stress of $\sigma_1 = 100$ MPa (the stress acts along direction $\phi = 0^o$, see Fig.1).

The change in phase velocity for a biaxial stress field can be evaluated from the Taylor series expansion of equation (9) utilising the change in phase velocity due to the two uniaxial contributions. This can be written as

$$\Delta C_p(f \cdot h_0, \sigma_1, \sigma_2, \phi) \approx K_{\sigma_1}\sigma_1 + K_{\sigma_2}\sigma_2 \,, \tag{10}$$

where K_{σ_1} and K_{σ_2} are the coefficients relating changes in the phase velocity due to the uniaxial stresses σ_1 and σ_2 respectively. These are given by

$$K_{\sigma_1} \approx \left.\frac{\partial C_p}{\partial \sigma_1}\right|_{(f\cdot h_0, \sigma_1, 0, \phi)} \approx \frac{C_p(f \cdot h_1, \sigma_1, 0, \phi) - C_p(f \cdot h_0, 0, 0, 0)}{\sigma_1 - 0}, \tag{11}$$

$$K_{\sigma_2} \approx \left.\frac{\partial C_p}{\partial \sigma_2}\right|_{(f\cdot h_0, 0, \sigma_2, \phi)} \approx \frac{C_p(f \cdot h_2, 0, \sigma_2, \phi) - C_p(f \cdot h_0, 0, 0, 0)}{\sigma_2 - 0}, \tag{12}$$

where h_1 and h_2 correspond to the thicknesses of the deformed plate due to the uniaxial stresses σ_1 and σ_2 respectively.

Equation (10) provides a very convenient approximation to estimate the effect of biaxial loading on the phase velocity. It was validated via direct numerical simulations for both the S0 and A0 modes. The validation process was carried out as follows: (i) the change in phase velocity was evaluated for a range of uniaxial stresses and angles of wave propagation; (ii) the coefficients K_{σ_1} and K_{σ_2} were then calculated from the ratio of the change in phase velocity to the uniaxial stress based on equations (11) and (12); (iii) the analytical equations (8) were numerically solved for different biaxial stresses and directions of wave propagation; (iv) the coefficients K_{σ_1} and K_{σ_2} evaluated in (ii) were substituted in equation (10) to approximate the change in the phase velocity predicted by the analytical equations in (iii).

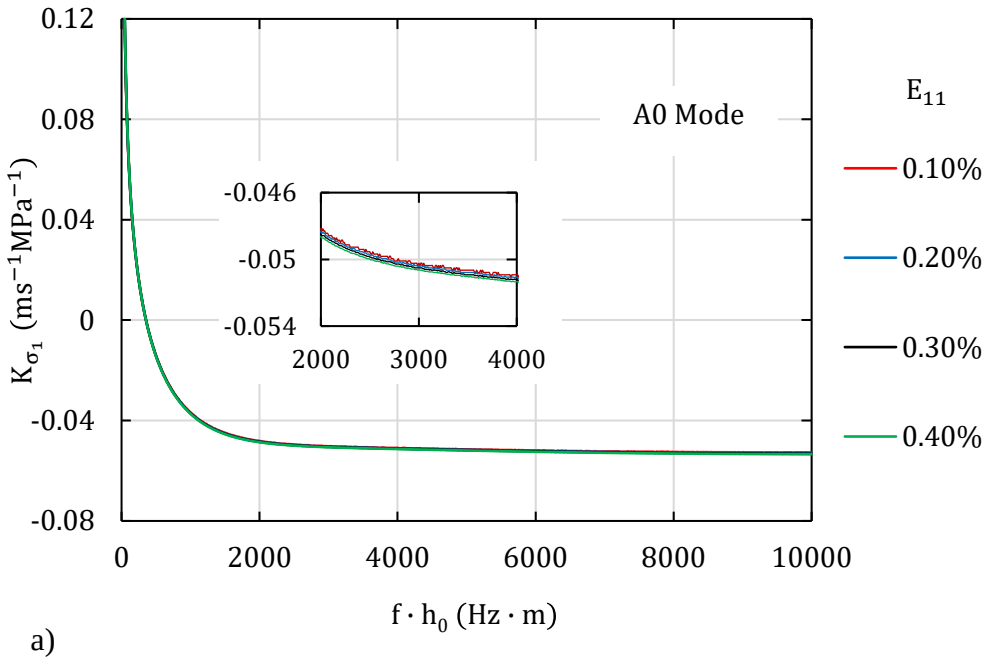

a)

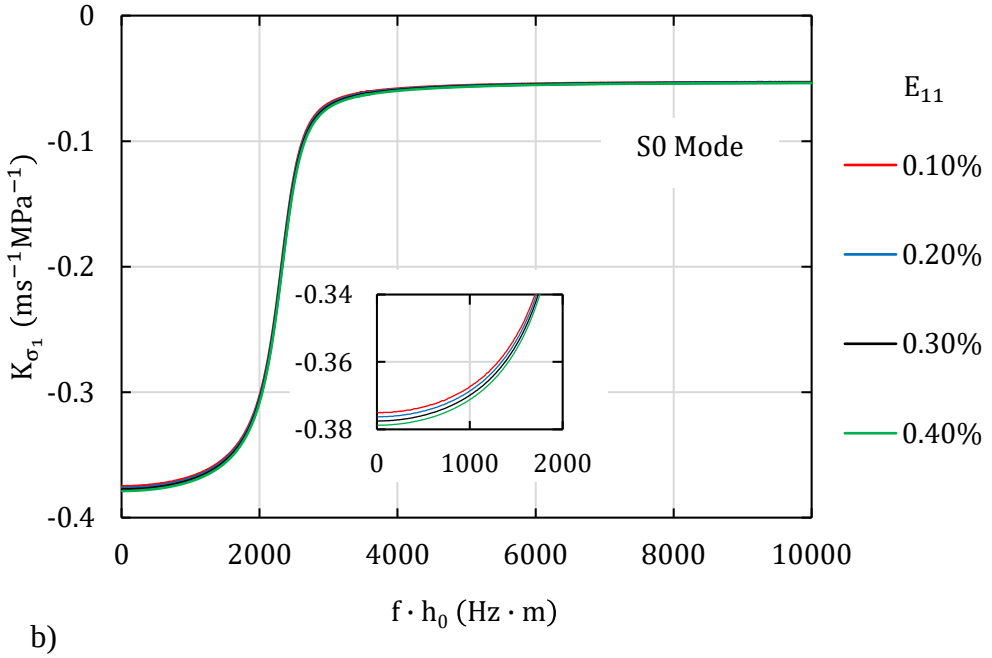

b)

Figure 4. Effect of strain (stress) on the coefficient relating changes in C_p to the applied stress σ_1 for the (a) A0 mode and, (b) S0 mode, propagating along the direction of the applied strain (stress).

Figure 4 shows the variation of the coefficient K_{σ_1} as a function of the frequency-thickness product for the A0 and S0 modes for a range of applied strains (stresses). The waves are considered to be propagating along the direction of the applied strain. The results show that K_{σ_1} does not have any significant dependence on the magnitude of the applied strain. This finding is consistent with the results of Gandhi et al. [43] who demonstrated that the change in the phase velocity is linear with load for a small pre-stress. Thus, in the remainder of the paper, K_{σ_1} will be considered to be only a function of the frequency-thickness product and the angle of wave propagation. For completeness, the variation of K_{σ_1} at different angles of wave propagation is shown in Appendix B. The variation of the coefficient K_{σ_2} is not shown as it may be evaluated from its σ_1 counterpart using the relation $K_{\sigma_2}(f \cdot h_0, \phi) \equiv K_{\sigma_1}(f \cdot h_0, 90^o - \phi)$.

The results obtained using the representation (10), along with the values of K_{σ_1} and K_{σ_2} from figure B1, were found to be in good agreement with the phase velocity changes predicted by the analytical equations (8) for all cases considered. The root mean square (RMS) differences between the two models for a typical case corresponding to $\sigma_1 = 100$ MPa and $\sigma_2 = 50$ MPa are shown in Table 2. The highest RMS difference for the A0 and S0 modes are 0.030 m/s and 0.099 m/s respectively; these relatively small values are representative of all the cases considered. Thus, the approximation in equation (10) may be assumed to be correct. Shi et al. [45] proposed similar equations to estimate the change in phase velocity for various biaxial loads and propagation directions. Although their analysis was conducted in the undeformed (natural) coordinate system, their results also demonstrate the feasibility of estimating the phase velocity changes for a biaxial stress field based on the linear combination of the change in phase velocity due to the uniaxial loads.

Table 2. Root mean square differences between the analytical and approximate models

RMS difference (ms^{-1})		
ϕ	A0 Mode	S0 Mode
0º	0.030	0.078
30º	0.014	0.096
45º	0.030	0.071
60º	0.013	0.099
90º	0.029	0.069

4. Stress Effect on Damage Diagnostic with GWs

In this section, an analytical model is presented to quantify the residual signal (noise) obtained after reference signal subtraction due to the effect of applied (biaxial) stress. Two different methods of signal subtraction are commonly utilised in SHM systems. These are based on either the time shift of the envelope of the wave packet or on the time shift of the individual waves within the wave packet. Although the envelope subtraction method leads to an improved sensitivity to damage, it can result in areas where damage detection is not possible due to the loss of phase information in the enveloping process [28]. Therefore, the focus of this paper will be on the evaluation of the shift of the individual waves in the wave packet due to applied stress, which seems to be a more robust technique for damage diagnostics using GWs.

Following the work of Croxford et al. [28], the reference signal is considered to be a Hanning-windowed toneburst, which is widely utilised in GW based SHM applications. It was demonstrated that in the presence of temperature variations, δT, the algebraic signal subtraction of the time trace affected by temperature from the reference data results in the following expression for the residual signal or noise

$$u_{noise} = 2u_0 \pi f \frac{d}{C_p}\left(\alpha - \frac{K_T}{C_p}\right)\delta T\,, \tag{13}$$

where u_0 is the amplitude of the received signal, f is the centre frequency of the toneburst, d is the propagation distance between the transmitting and receiving transducers, C_p is the phase velocity of the wave, α is the coefficient of thermal expansion of the material and K_T is the coefficient relating changes in C_p to temperature.

Similar to the effect of temperature variations on GW propagation, a change in the stress state of a structure also leads to a translation in time of the received signal. This is because the applied stress not only causes a change in the wave propagation distance due to the induced strain but also leads to a change in the phase velocity due to the strain induced anisotropy. In order to establish a relationship between the change in the arrival time of the received signal, δt, and the change in the stress state of the structure, characterised by $\delta\sigma_1$ and $\delta\sigma_2$, we start from $t = \frac{d}{C_p}$ and take partial derivatives with respect to d and C_p, which gives

$$\delta t = \frac{1}{C_p}\left(\frac{\delta d}{\delta \sigma_1}.\delta\sigma_1 + \frac{\delta d}{\delta \sigma_2}.\delta\sigma_2\right) - \frac{d}{{C_p}^2}\left(\frac{\delta C_p}{\delta \sigma_1}.\delta\sigma_1 + \frac{\delta C_p}{\delta \sigma_2}.\delta\sigma_2\right). \tag{14}$$

If the pre-deformation (from a stress-free reference configuration) is considered to be small, the relationship between the propagation distance and the applied stress can be expressed using Generalised Hooke's law as

$$\begin{aligned} \frac{\delta d}{\delta \sigma_1} &= \frac{d}{2E_Y}[1 - \nu + (1+\nu)\cos(2\phi)] = \beta_1(\phi)d, \\ \frac{\delta d}{\delta \sigma_2} &= \frac{d}{2E_Y}[1 - \nu - (1+\nu)\cos(2\phi)] = \beta_2(\phi)d, \end{aligned} \tag{15}$$

where E_Y is the Young's modulus of the material, ν is the Poisson's ratio and ϕ is the angle of wave propagation (measured relative to the σ_1 axis). The relationship between the wave velocity and the applied stress can be written as

$$\frac{\delta C_p}{\delta \sigma_1} = K_{\sigma_1}(f \cdot h_0, \phi), \qquad \frac{\delta C_p}{\delta \sigma_2} = K_{\sigma_2}(f \cdot h_0, \phi)\,, \tag{16}$$

where K_{σ_1} and K_{σ_2} are the coefficients relating changes in C_p to the uniaxial stresses σ_1 and σ_2 respectively, as defined in equation (10). These coefficients may be evaluated based on the acoustoelastic model described earlier in the paper. They are functions of the frequency-thickness product, $f \cdot h_0$, due to the dispersive nature of guided waves and the angle of wave propagation, ϕ (measured relative to the σ_1 axis). Substituting equations (15) and (16) into equation (14) leads to an expression for δt in terms of $\delta\sigma_1$

$$\delta t = \frac{d}{C_p}\left[(\beta_1 + \beta_2\lambda) - \frac{\left(K_{\sigma_1} + K_{\sigma_2}\lambda\right)}{C_p}\right]\delta\sigma_1\,, \tag{17}$$

where $\lambda = \delta\sigma_2/\delta\sigma_1$ is the biaxial stress ratio.

Assuming that δt is sufficiently small, the noise can be approximated as

$$u_{noise} = 2u_0\pi f\delta t\,. \tag{18}$$

Finally, combining equation (17) with equation (18) gives

$$u_{noise} = 2u_0\pi f\frac{d}{C_p}\left[(\beta_1 + \beta_2\lambda) - \frac{\left(K_{\sigma_1} + K_{\sigma_2}\lambda\right)}{C_p}\right]\delta\sigma_1\,. \tag{19}$$

In general, the magnitudes of K_{σ_1}/C_p and K_{σ_2}/C_p are of the same order as those of β_1 and β_2; so both the change in propagation distance d due to the induced strain and the change in C_p due to the strain induced anisotropy should be considered. However, in the case of thermally induced stress, β_1 and β_2 should be set to zero as the propagation distance remains unchanged.

Both equations (13) and (19) indicate that the noise associated with changing temperature or stress is dependent on the distance between the transmitting and receiving transducers. Thus, if the signal-to-noise ratio is known, the maximum propagation distance or the minimum density of the sensor/transmitter array can be evaluated. These equations also suggest that

faster guided wave modes with higher phase velocities are less affected by changes in temperature or stress as compared to slower modes. However, faster modes typically propagate at relatively high frequencies and, as a result, there is a trade-off between frequency and phase velocity as the noise is directly proportional to f but is inversely proportional to C_p. In general, lower frequencies are preferred for SHM applications as the number of modes propagating in the waveguide is minimized, thus making the signal analysis less complex.

Example

The effect of stress on the residual noise is significant and is in fact comparable to the effect of temperature. To demonstrate this point, consider a $1\ \mathrm{mm}$ thick 6061-T6 Aluminium plate in a stress free state at a reference temperature, T_0. If the in-plane edges of the plate are constrained, a uniform temperature rise of $1\ ^{o}\mathrm{C}$ will induce compressive biaxial stresses of approximately $\sigma_1 = \sigma_2 = -E\alpha/(1-v) \times 1\ ^{o}\mathrm{C} \approx -2.56\ \mathrm{MPa}$. To quantify the effect of temperature and the thermally induced stress, an excitation signal with a centre frequency of $1\ \mathrm{MHz}$ is employed and the direction of wave propagation is chosen to be parallel to the σ_1 direction.

Table 3. Temperature and stress coefficients for a 6061-T6 Aluminium plate at a frequency-thickness product of $1\ \mathrm{MHz-mm}$ and an angle of wave propagation of 0^{o}.

	A0	S0
$K_T\ (\mathrm{ms^{-1}\ ^{o}C^{-1}})$	-0.383	-1.237
$K_{\sigma_1}\ (\mathrm{ms^{-1}MPa^{-1}})$	-0.037	-0.371
$K_{\sigma_2}\ (\mathrm{ms^{-1}MPa^{-1}})$	0.021	0.073

Table 3. summarises the values of the temperature and stress coefficients, K_T, K_{σ_1} and K_{σ_2}, at the corresponding frequency-thickness product for the fundamental Lamb wave modes. The temperature coefficients were extracted using the same approach as in Croxford et al. [28]; the material properties of 6061-T6 Aluminium were used along with $\alpha = 23.6 \times 10^{-6}\ ^{o}C^{-1}$, $k_S = -0.752\ ms^{-1}\ ^{o}C^{-1}$ and $k_L = -1.089\ ms^{-1}\ ^{o}C^{-1}$, where k_S and k_L are the temperature dependence constants for shear and longitudinal wave speeds respectively. The stress coefficients K_{σ_1} and K_{σ_2} were extracted from Appendix B at an angle of propagation of 0^o and 90^o respectively. The effect of temperature on the material properties was not considered while evaluating these stress coefficients.

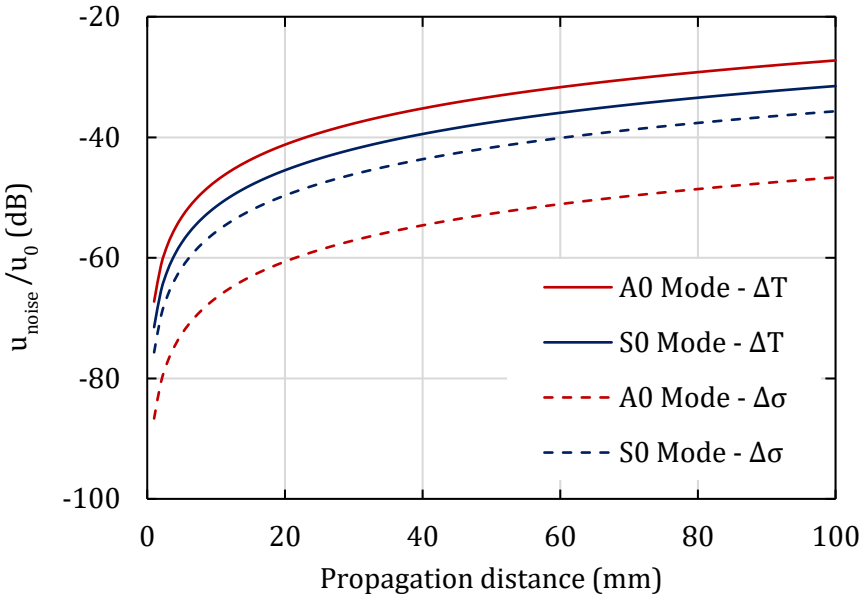

Figure 5. Variation of u_{noise}/u_0 with the propagation distance for the fundamental Lamb wave modes in an Aluminium plate at a frequency-thickness product of $1\ MHz - mm$. The solid lines represent the noise due to a $1\ ^{o}C$ temperature change while the dotted lines represent the noise associated with the induced (biaxial) thermal stress in a plate constrained at its in-plane edges.

The coefficients in Table 3 were then substituted in equations (13) and (19) to predict the noise due to a temperature change of 1 ^{o}C as well as the noise associated with the induced (compressive biaxial) thermal stress. The coefficients α, β_1 and β_2 in the latter equations were set to zero as the propagation distance remains unchanged in the constrained plate. The results are presented in terms of the ratio u_{noise}/u_0 as a function of the propagation distance for the fundamental Lamb wave modes, as shown in figure 5. It can be seen that the noise is more sensitive to the change in temperature as compared to the thermally induced stress. This is not unexpected as the magnitude of K_T is higher than those of K_{σ_1} and K_{σ_2}. It can also be seen that the A0 mode is more affected by the change in temperature than the S0 mode. Croxford et al. [28] attributed this behaviour to the effect of the higher phase velocity of the S0 mode which reduces its sensitivity to temperature. However, in the case of thermally induced stress, this effect is largely mitigated as the stress coefficient K_{σ_1} for the S0 mode is an order of magnitude higher than that of the A0 mode. As a result, the S0 mode exhibits a much larger sensitivity to the thermally induced stress than the A0 mode.

It is interesting to note that in a constrained plate, the thermally induced stress might partially compensate for the effect of temperature on the phase velocity and the associated noise generation. This is because the temperature change and the thermally induced stress usually have an opposite effect on the phase velocity of the fundamental Lamb wave modes. For example, at a frequency-thickness of 1 MHz $-$ mm and an angle of propagation parallel to the σ_1 direction, a positive change in temperature ($\delta T > 0$) leads to a decrease in the phase velocity whereas the induced (compressive) thermal stress ($\delta\sigma_1, \delta\sigma_2 < 0$) causes an increase in the phase velocity. Consequently, the stress effect partially compensates for the effect of temperature on the phase velocity and the associated noise generation. However, this is not always the case as the change in the phase velocity depends on the magnitude and sign of the temperature and stress coefficients. The latter coefficients are both functions of the signal frequency while the stress coefficients also have an additional dependence on the angle of wave propagation.

5. Possible Stress Mitigation Strategies

The behaviour of the A0 mode demonstrates some interesting features, which can potentially be utilised in the development of stress mitigation techniques. In particular, the results presented earlier show the existence of a critical frequency-thickness product, f_{Cr}, at which the phase velocity is invariant of the direction of wave propagation, ϕ. This frequency does not appear to be affected by the magnitude of the applied stress. Although the change in the phase velocity from the unstressed state is non-zero at this critical frequency, its magnitude is relatively small. Therefore, in the case where the Lamb wave toneburst is dominated by the A0 mode and the direction of the applied load is unknown, the influence of the applied stress can be minimized by selecting a frequency close to f_{Cr} at which the values of the stress coefficients, K_{σ_1} and K_{σ_2}, tend to zero.

In practical systems, the excitation signal is typically generated using piezo-ceramic transducers and this causes the signal to have a finite bandwidth. Since the critical frequency f_{Cr} is within the dispersive region of the A0 mode, a large bandwidth may affect the implementation of the above strategy. Windowing techniques such as Hanning window may be used to reduce the bandwidth and ensure that the energy of the signal is concentrated near the central excitation frequency. Although a narrower bandwidth will reduce the problem of dispersion, post processing techniques [46-48] may still be required to compensate for the effect of dispersion.

A more accurate stress mitigation technique may be employed if the direction of the applied load is known. This involves using the frequency at which the change in the phase velocity of the A0 mode from the unstressed state is zero. Figure 6 displays the variation of this zero-intercept frequency, f^*, as a function of the angle of wave propagation for different biaxial stress ratios. The magnitude of the first principal stress, σ_1, is kept constant at 20 MPa. The results indicate that the optimum orientation of transducers is at an angle of 45 degrees to the principal axes. At this angle, the corresponding zero-intercept frequency is independent of the biaxial stress ratio. In addition, the latter frequency only shows a weak dependence on the magnitude of the applied stress σ_1. It can be

hypothesised that a similar behaviour also occurs for other materials. In practice, guided wave based SHM schemes typically utilise an omni-directional transducer array as they rely on multi-directional propagation to achieve full coverage of a structure [49-50]. The transducers in the array are at varying pre-defined angles to each other. In this case, the effect of the applied stress can be effectively negated by selecting an excitation frequency equal to the zero-intercept frequency for the specific angle between two selected transducers.

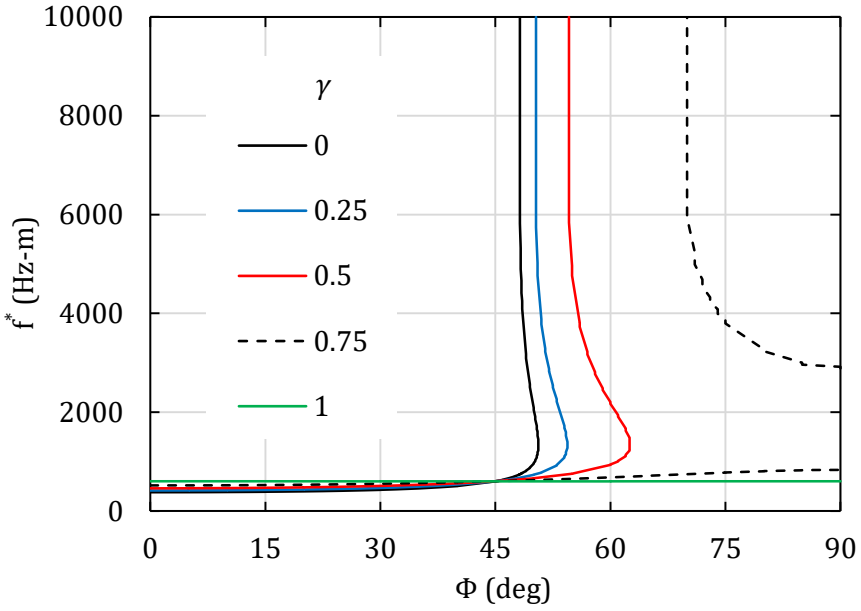

Figure 6. Variation of the zero-intercept frequency, f^*, for the A0 mode as a function of the angle of wave propagation, ϕ, for different biaxial stress ratios, λ, with σ_1= 20 MPa.

For certain guided wave based SHM applications, the S0 mode may be preferred over the A0 mode [51, 52]. In this case, the viable strategy in the reduction of the residual noise due to stress variations would be the utilisation of frequency-thickness products below the threshold frequency shown in figure 3(b). The effect of stress on the change in the phase velocity decreases significantly as we approach this particular frequency. The use of the S0 mode above this threshold frequency-thickness should be avoided due to the complexities associated with mode splitting.

6. Conclusion

In this paper, the effect of stress on the propagation of Lamb waves was analysed using an acoustoelastic formulation to determine the change in the phase velocity as a function of the applied stress, frequency and propagation direction. An analytical model was then developed to assess the residual signal or noise due to applied or thermally-induced stresses. It was demonstrated that the effect of stress can be as strong as the effect of temperature fluctuations, and it has to be considered when implementing guided wave based SHM systems in real-world applications.

It was interesting to find that applied stresses have a very different influence on the phase velocity of the fundamental symmetric and anti-symmetric modes. In particular, for the S0 mode, as we approach a certain threshold frequency, the effect of stress on the change in the phase velocity decreases significantly. In the case of the A0 mode, there is a critical value of frequency at which the influence of stress on the change in the phase velocity is almost negligible. These features can be utilised in the development of effective stress mitigation strategies for on-line SHM systems.

This paper has considered a particular case of a plate made of Aluminium to demonstrate the importance of the stress effect on noise generation after reference signal subtraction. It should be emphasised that any variability in the material properties of the plate, especially in the third-order elastic constants, will lead to a change in the magnitude of the phase velocity dispersion curves. While it is expected that general trends and outcomes of the paper will be qualitatively the same, it would be beneficial to conduct a thorough quantitative analysis in the future.

Acknowledgement

This work was supported by the Australian Government Research Training Program Scholarship, and the Australian Research Council, project DP160102233.

References

[1] Maalej M, Karasaridis A, Pantazopoulou S and Hatzinakos D 2002 Structural health monitoring of smart structures *Smart Mater. Struct.* **11** 581-589

[2] Su Z and Ye L 2009 *Identification of damage using Lamb waves: from fundamentals to applications* ed F Pfeiffer and P Wriggers (Berlin: Springer)

[3] Staszewski W, Boller C and Tomlinson G R 2004 Health Monitoring of Aerospace Structures: Smart Sensor Technologies and Signal Processing (Chichester: John Wiley & Sons)

[4] Staszewski W J 2004 Structural Health Monitoring Using Guided Ultrasonic Waves *Advances in Smart Technologies in Structural Engineering* ed J Holnicki-Szulc and C A Mota Soares (Berlin: Springer) pp 117–162

[5] Su Z, Ye L and Lu Y 2006 Guided Lamb waves for identification of damage in composite structures: a review *J. Sound Vib*. **295** 753–80

[6] Park G, Farrar C R, Lanza di Scalea F and Coccia S 2006 Performance assessment and validation of piezoelectric active-sensors in structural health monitoring *Smart Mater. Struct*. **15** 1673-1683.

[7] Raghavan A and Cesnik C E S 2007 Review of Guided-wave Structural Health Monitoring *The Shock Vib. Dig.* **39** 91-114

[8] Mitra M and Gopalakrishnan S. 2016 Guided wave based structural health monitoring: A review *Smart Mater. Struct*. **25** 053001

[9] Giurgiutiu V 2016 Structural Heal Monitoring of Aerospace Composites (London: Academic Press)

[10] Michaels J E 2008 Detection, localization and characterization of damage in plates with an in situ array of spatially distributed ultrasonic sensors *Smart Mater. Struct*. **17** 1-15

[11] Zak A, Radzienski M, Krawczuk M, Ostachowicz W 2012 Damage detection strategies based on propagation of guided elastic waves *Smart Mater. Struct*. **21** 035024

[12] He S and Ng C T. 2016 A probabilistic approach for quantitative identification of multiple delaminations in laminated composite beams using guided waves *Eng. Struct.* **127** 602-614

[13] He S and Ng C T. 2017 Guided wave-based identification of multiple cracks in beams using a Bayesian approach *Mech. Syst Sig. Process.* **84** 324-345

[14] Staszewski W J 2005 Ultrasonic/Guided Waves for Structural Health Monitoring *Key Eng. Mat.* **293-294** 49-62

[15] Schmidt D, Hillger W, Szewieczek A and Sinapius M 2013 Structural Health Monitoring Based on Guided Waves *Adaptive, tolerant and efficient composite structures* (Heidelberg: Springer) pp 449-462

[16] Diamanti K and Soutis C 2010 Structural health monitoring techniques for aircraft composite structures *Prog. Aerosp. Sci.* **46** 342-352

[17] Konstantinidis G, Drinkwater B W and Wilcox P D 2006 The temperature stability of guided wave structural health monitoring systems. *Smart Mater. Struct*. **15** 967-976

[18] Lanza di Scalea F and Salamone S 2008 Temperature effects in ultrasonic Lamb wave structural health monitoring systems *J. Acoust. Soc. Am.* **124** 161-174

[19] Raghavan A and Cesnik C E S 2008 Effects of Elevated temperature on Guided-wave Structural Health Monitoring *J. Intel. Mat. Sys. Struct*. **19** 1383-1398

[20] Dodson J C and Inman D J 2013 Thermal sensitivity of Lamb waves for structural health monitoring applications *Ultrasonics* **53** 677-685

[21] Dodson J C and Inman D J 2014 Investigating the thermally induced acoustoelastic effect in isotropic media with Lamb waves *J. Acoust. Soc. Am.* **136** 2532-2543

[22] Chen F and Wilcox P D 2007 The effect of load on guided wave propagation *Ultrasonics* **47** 111-122

[23] Sohn H 2007 Effects of environmental and operational variability on structural health monitoring *Phil. Trans. R. Soc. A* **365** 539–60

[24] Michaels J E, Michaels T E and Martin R S 2009 Analysis of global ultrasonic sensor data from a full scale wing panel test *AIP Conference Proceedings* **1096** 950-957

[25] Lee S J, Gandhi N, Michaels J E and Michaels T E 2011 Comparison of the effects of applied loads and temperature variations on guided wave propagation *AIP Conference Proceedings* **1335** 175-182

[26] Michaels J E, Gandhi N and Lee S J 2011 Acoustoelastic Lamb Waves and Implications for Structural Health Monitoring *From Waves in Complex Systems to Dynamics of Generalized Continua* ed K Hutter, T T Wu and Y C Shu (New Jersey: World Scientific) pp 91-117

[27] Roy S, Ladpli P and Chang F-K 2015 Load monitoring and compensation strategies for guided-waves based structural health monitoring using piezoelectric transducers *J. Sound Vib* **351** 206-220

[28] Croxford A J, Wilcox P D, Drinkwater B W and Konstantinidis G 2007 Strategies for guided-wave structural health monitoring *Proc. R. Soc. A* **463** 2961–2981

[29] Aryan P, Kotousov A, Ng C T and Cazzolato B 2017 A model-based method for damage detection with guided waves *Struct. Control Health Monit.* **22** e1884

[30] Aryan P, Kotousov A, Ng C T and Wildy S 2016 Reconstruction of baseline time-trace under changing environmental and operational conditions *Smart Mater. Struct.* **25** 035018

[31] Lu Y and Michaels J E 2005 A methodology for structural health monitoring with diffuse ultrasonic waves in the presence of temperature variations *Ultrasonics* **43** 717-731

[32] Clarke T, Cawley P, Wilcox P D and Croxford A J 2009 Evaluation of the damage detection capability of a sparse-array guided-wave SHM system applied

to a complex structure under varying thermal conditions *IEEE Trans. Ultrason. Ferroelect. Freq. Contr.* **56** 2666-2678

[33] Salamone S, Bartoli I, Lanza di Scalea F and Coccia S 2009 Guided–wave Health Monitoring of Aircraft Composite Panels under Changing Temperature *J. Intel. Mat. Sys. Struct.* **20** 1079-1090

[34] Clarke T, Simonetti F and Cawley P 2010 Guided wave health monitoring of complex structures by sparse-array systems: influence of temperature changes on performance *J. Sound Vib.* **329** 2306-2322

[35] An Y K and Sohn H 2010 Instantaneous crack detection under varying temperature and static loading conditions *Struct. Control Health Monit* **17** 730–741

[36] Croxford A J, Moll J, Wilcox P D and Michaels J E 2010 Efficient temperature compensation strategies for guided wave structural health monitoring *Ultrasonics* **50** 517-528

[37] Dao P B and Staszewski W J 2013 Cointegration approach for temperature effect compensation in Lamb-wave based damage detection *Smart Mater. Struct*. **22** 1-20

[38] Michaels J E 2016 Sparse array imaging with guided waves under variable environmental conditions *Structural Health Monitoring (SHM) in Aerospace Structures* (Cambridge-Woodhead Publishing) pp 255-284

[39] Ogden R W 1984 *Non-Linear Elastic Deformations* (Chichester: Ellis Horwood)

[40] Mohabuth M, Kotousov A and Ng C T 2016 Effect of uniaxial stress on the propagation of higher-order Lamb wave modes *Int. J. Nonlinear Mech.* **86** 104-111

[41] Murnaghan F D 1937 Finite Deformations of an Elastic Solid *Am. J. Math.* **59** 235-260

[42] Nayfeh A H and Chimenti D E 1989 Free Wave Propagation in Plates of General Anisotropic Media *J. Appl. Mech.* **56** 881-886

[43] Gandhi N, Michaels J E and Lee S J 2012 Acoustoelastic Lamb wave propagation in biaxially stressed plates *J. Acoust. Soc. Am*. **132** 1284-1293

[44] Asay J R and Guenther A H 1967 Ultrasonic studies of 1060 and 6061-T6 aluminum *J. Appl. Phys.* **38** 4086–4088

[45] Shi F, Michaels J E and Lee S J 2013 In situ estimation of applied biaxial loads with Lamb waves *J. Acoust. Soc. Am*. **133** 677-687

[46] Wilcox P D 2003 A Rapid Signal Processing Technique to Remove the Effect of Dispersion from Guided Wave Signals *IEEE Trans. Ultrason., Ferroelect., Freq. Contr.* **50** 419-427

[47] Zeng L, Lin J 2014 Chirp-based dispersion pre-compensation for high resolution Lamb wave inspection *NDT & E Int.* **61** 35–44

[48] Liu L and Yuan F G 2009 A linear mapping technique for dispersion removal of Lamb wave *Smart Mater. Struct*. **9** 75-86

[49] Wilcox P D 2003 Omni-Directional Guided Wave Transducer Arrays for the Rapid Inspection of Large Areas of Plate Structures *IEEE Trans. Ultrason., Ferroelect., Freq. Contr.* **50** 699-709

[50] Koduru J P and Rose J L 2012 Transducer arrays for omnidirectional guided wave mode control in plate like structures *Smart Mater. Struct*. **22** 015010

[51] Yang Y, Ng C T, Kotousov A, Sohn H and Lim H J 2018 Second harmonic generation at fatigue cracks by low-frequency Lamb waves: Experimental and numerical studies *Mech. Syst. Sig. Process.* **99** 760-773

[52] He S and Ng C T 2017 Modelling and analysis of Nonlinear guided waves interaction at a breathing crack using time-domain spectral finite element method *Smart Mater. Struct.* **26** 085002

Appendix A

Following the work of Nayfeh and Chimenti [42], the plane waves solution given by equation (7) is substituted into the equation of motion (4). This yields an eigenvalue problem which can be expressed as

$$K_{ij}(\alpha)\, U_j = 0, \qquad i,j = 1,2,3 \tag{A1}$$

where

$$\begin{aligned}
K_{11} &= \rho c^2 - \mathcal{A}'_{1111} - \mathcal{A}'_{3131}\,\alpha^2 - \alpha(\mathcal{A}'_{1131} + \mathcal{A}'_{3111}),\\
K_{12} &= -\mathcal{A}'_{1112} - \mathcal{A}'_{3132}\,\alpha^2 - \alpha(\mathcal{A}'_{1132} + \mathcal{A}'_{3112}),\\
K_{13} &= -\mathcal{A}'_{1113} - \mathcal{A}'_{3133}\,\alpha^2 - \alpha(\mathcal{A}'_{1133} + \mathcal{A}'_{3113}),\\
K_{21} &= -\mathcal{A}'_{1211} - \mathcal{A}'_{3231}\,\alpha^2 - \alpha(\mathcal{A}'_{1231} + \mathcal{A}'_{3211}),\\
K_{22} &= \rho c^2 - \mathcal{A}'_{1212} - \mathcal{A}'_{3232}\,\alpha^2 - \alpha\left(\mathcal{A}'_{1232} + \mathcal{A}'_{0_{3212}}\right),\\
K_{23} &= -\mathcal{A}'_{1213} - \mathcal{A}'_{3233}\,\alpha^2 - \alpha(\mathcal{A}'_{1233} + \mathcal{A}'_{3213}),\\
K_{31} &= -\mathcal{A}'_{1311} - \mathcal{A}'_{3331}\,\alpha^2 - \alpha(\mathcal{A}'_{1331} + \mathcal{A}'_{3311}),\\
K_{32} &= -\mathcal{A}'_{1312} - \mathcal{A}'_{3332}\,\alpha^2 - \alpha(\mathcal{A}'_{1332} + \mathcal{A}'_{3312}),\\
K_{33} &= \rho c^2 - \mathcal{A}'_{1313} - \mathcal{A}'_{3333}\,\alpha^2 - \alpha(\mathcal{A}'_{1333} + \mathcal{A}'_{3313}).
\end{aligned} \tag{A2}$$

The elasticity tensor in the initial coordinate system (x_1, x_2, x_3) exhibits the major symmetry $\mathcal{A}_{piqj} = \mathcal{A}_{qjpi}$. This symmetry persists in the rotated coordinate system (x'_1, x'_2, x'_3) after tensor transformation and as a result, K_{ij} turns out to be symmetric ($K_{ij} = K_{ji}$). Furthermore, for an initially isotropic plate subjected to a biaxial stress field in the $x_1 - x_2$ plane, the latter plane is one of mirror symmetry. This means that the strain induced anisotropy is, at least, of monoclinic symmetry. The latter symmetry is maintained in the $x'_1 - x'_2$ plane after coordinate transformation, leading to further simplification of K_{ij}

$$
\begin{aligned}
K_{11} &= \rho c^2 - \mathcal{A}'_{1111} - \mathcal{A}'_{3131}\,\alpha^2 , \\
K_{12} &= -\mathcal{A}'_{1112} - \mathcal{A}'_{3132}\,\alpha^2 , \\
K_{13} &= -\alpha(\mathcal{A}'_{1133} + \mathcal{A}'_{3113}) , \\
K_{21} &= K_{12} , \\
K_{22} &= \rho c^2 - \mathcal{A}'_{1212} - \mathcal{A}'_{3232}\,\alpha^2 , \\
K_{23} &= -\alpha(\mathcal{A}'_{1233} + \mathcal{A}'_{3213}) , \\
K_{31} &= K_{13} , \\
K_{32} &= K_{23} , \\
K_{33} &= \rho c^2 - \mathcal{A}'_{1313} - \mathcal{A}'_{3333}\,\alpha^2 .
\end{aligned}
\tag{A3}
$$

For non-trivial solutions to the eigenvalue problem, the determinant of K_{ij} is set to zero. This yields a sixth-order equation in α which can be expressed as

$$
P_6\,\alpha^6 + P_4\,\alpha^4 + P_2\,\alpha^2 + P_0 = 0 , \tag{A4}
$$

where the coefficients P_6, P_4, P_2 and P_0 are given by

$$
\begin{aligned}
P_6 &= \mathcal{A}'_{3333}\,\mathcal{A}'^{2}_{3132} - \mathcal{A}'_{3131}\,\mathcal{A}'_{3232}\,\mathcal{A}'_{3333} , \\
P_4 &= \mathcal{A}'^{2}_{1233}\mathcal{A}'_{3131} + \mathcal{A}'^{2}_{1133}\mathcal{A}'_{3232} + \mathcal{A}'^{2}_{3132}\mathcal{A}'_{1313} \\
&\quad + \mathcal{A}'^{2}_{3213}\mathcal{A}'_{3131} + \mathcal{A}'^{2}_{3113}\mathcal{A}'_{3232} \\
&\quad - 2\mathcal{A}'_{1133}\,\mathcal{A}'_{1233}\,\mathcal{A}'_{3132} + 2\mathcal{A}'_{1133}\,\mathcal{A}'_{3113}\,\mathcal{A}'_{3232} \\
&\quad - 2\mathcal{A}'_{1133}\,\mathcal{A}'_{3132}\,\mathcal{A}'_{3213} - 2\mathcal{A}'_{1233}\,\mathcal{A}'_{3113}\,\mathcal{A}'_{3132} \\
&\quad + 2\mathcal{A}'_{1112}\,\mathcal{A}'_{3132}\,\mathcal{A}'_{3333} + 2\mathcal{A}'_{1233}\,\mathcal{A}'_{3131}\,\mathcal{A}'_{3213} \\
&\quad - \mathcal{A}'_{1111}\,\mathcal{A}'_{3232}\,\mathcal{A}'_{3333} - \mathcal{A}'_{1212}\,\mathcal{A}'_{3131}\,\mathcal{A}'_{3333} \\
&\quad - \mathcal{A}'_{1313}\,\mathcal{A}'_{3131}\,\mathcal{A}'_{3232} - 2\mathcal{A}'_{3113}\,\mathcal{A}'_{3132}\,\mathcal{A}'_{3213} \\
&\quad - \mathcal{A}'^{2}_{3132}\rho c^2 + \mathcal{A}'_{3131}\,\mathcal{A}'_{3232}\,\rho c^2 \\
&\quad + \mathcal{A}'_{3131}\,\mathcal{A}'_{3333}\,\rho c^2 + \mathcal{A}'_{3232}\,\mathcal{A}'_{3333}\,\rho c^2 ,
\end{aligned}
\tag{A5}
$$

$$
\begin{aligned}
P_2 = {} & \mathcal{A}'^{2}_{1233}\mathcal{A}'_{1111} + \mathcal{A}'^{2}_{1133}\mathcal{A}'_{1212} + \mathcal{A}'^{2}_{3213}\mathcal{A}'_{1111} \\
& + \mathcal{A}'^{2}_{3113}\mathcal{A}'_{1212} + \mathcal{A}'^{2}_{1112}\mathcal{A}'_{3333} \\
& - 2\mathcal{A}'_{1112}\mathcal{A}'_{1133}\mathcal{A}'_{1233} - 2\mathcal{A}'_{1112}\mathcal{A}'_{1133}\mathcal{A}'_{3213} \\
& - 2\mathcal{A}'_{1112}\mathcal{A}'_{1233}\mathcal{A}'_{3113} + 2\mathcal{A}'_{1133}\mathcal{A}'_{1212}\mathcal{A}'_{3113} \\
& + 2\mathcal{A}'_{1111}\mathcal{A}'_{1233}\mathcal{A}'_{3213} + 2\mathcal{A}'_{1112}\mathcal{A}'_{1313}\mathcal{A}'_{3132} \\
& - \mathcal{A}'_{1111}\mathcal{A}'_{1212}\mathcal{A}'_{3333} - \mathcal{A}'_{1111}\mathcal{A}'_{1313}\mathcal{A}'_{3232} \\
& - \mathcal{A}'_{1212}\mathcal{A}'_{1313}\mathcal{A}'_{3131} - 2\mathcal{A}'_{1112}\mathcal{A}'_{3113}\mathcal{A}'_{3213} \\
& - \mathcal{A}'^{2}_{1133}\rho c^2 - \mathcal{A}'^{2}_{1233}\rho c^2 - \mathcal{A}'^{2}_{3113}\rho c^2 \\
& - \mathcal{A}'_{3131}\rho^2 c^4 - \mathcal{A}'^{2}_{3213}\rho c^2 - \mathcal{A}'_{1111}\mathcal{A}'_{3232}\rho c^2 \\
& + \mathcal{A}'_{1212}\mathcal{A}'_{3131}\rho c^2 + \mathcal{A}'_{1111}\mathcal{A}'_{3333}\rho c^2 \\
& + \mathcal{A}'_{1313}\mathcal{A}'_{3131}\rho c^2 - 2\mathcal{A}'_{1233}\mathcal{A}'_{3213}\rho c^2 \\
& + \mathcal{A}'_{1212}\mathcal{A}'_{3333}\rho c^2 + \mathcal{A}'_{1313}\mathcal{A}'_{3232}\rho c^2,
\end{aligned}
$$

$$
\begin{aligned}
P_0 = {} & \mathcal{A}'^{2}_{1112}\mathcal{A}'_{1313} + \rho^3 c^6 - \mathcal{A}'_{1111}\mathcal{A}'_{1212}\mathcal{A}'_{1313} - \mathcal{A}'^{2}_{1112}\rho c^2 \\
& - \mathcal{A}'_{1111}\rho^2 c^4 - \mathcal{A}'_{1212}\rho^2 c^4 - \mathcal{A}'_{1313}\rho^2 c^4 \\
& + \mathcal{A}'_{1111}\mathcal{A}'_{1212}\rho c^2 + \mathcal{A}'_{1111}\mathcal{A}'_{1313}\rho c^2 \\
& + \mathcal{A}'_{1212}\mathcal{A}'_{1313}\rho c^2,
\end{aligned}
$$

The lack of odd power coefficients in equation (A4) means that the sixth-order equation can be reduced to a cubic equation in α^3. This simplification results in six solutions for α, which are denoted by α_q, $q \in \{1,2,3,4,5,6\}$, with the following properties

$$
\alpha_2 = -\alpha_1, \qquad \alpha_4 = -\alpha_3, \qquad \alpha_6 = -\alpha_5. \tag{A6}
$$

For each α_q, displacement ratios $V_q = {U_{2q}}/{U_{1q}}$ and $W_q = {U_{3q}}/{U_{1q}}$ can be defined using the relations in equation (A1) as

$$
V_q = \frac{K_{11}(\alpha_q)K_{23}(\alpha_q) - K_{13}(\alpha_q)K_{21}(\alpha_q)}{K_{13}(\alpha_q)K_{22}(\alpha_q) - K_{12}(\alpha_q)K_{23}(\alpha_q)}, \tag{A7}
$$

$$
W_q = \frac{K_{11}(\alpha_q)K_{32}(\alpha_q) - K_{31}(\alpha_q)K_{12}(\alpha_q)}{K_{12}(\alpha_q)K_{33}(\alpha_q) - K_{13}(\alpha_q)K_{32}(\alpha_q)}, \qquad q \in \{1,2,3,4,5,6\}. \tag{A8}
$$

The displacement field of the Lamb waves can then be written in terms of the above displacement ratios using the principle of superposition

$$(u_1', u_2', u_3') = \sum_{q=1}^{6} (1, V_q, W_q)\, U_1 e^{i\xi(x_1' + \alpha_q x_3' - ct)} \quad , \tag{A9}$$

Similarly, the stress field can be found by substituting the above displacement field into the incremental constitutive equation (2)

$$(\hat{S}'_{33}, \hat{S}'_{31}, \hat{S}'_{32}) = \sum_{q=1}^{6} i\xi (D_{1q}, D_{2q}, D_{3q})\, U_1 e^{i\xi(x_1' + \alpha_q x_3' - ct)} \, , \tag{A10}$$

where

$$\begin{aligned} D_{1q} &= \mathcal{A}'_{3311} + V_q \mathcal{A}'_{3312} + W_q \mathcal{A}'_{3333}\, \alpha_q \, , \\ D_{2q} &= \mathcal{A}'_{3131}\, \alpha_q + V_q \mathcal{A}'_{3132}\, \alpha_q + W_q \mathcal{A}'_{3113} \, , \\ D_{3q} &= \mathcal{A}'_{3231}\, \alpha_q + V_q \mathcal{A}'_{3232}\, \alpha_q + W_q \mathcal{A}'_{3213} \, . \end{aligned} \tag{A11}$$

Incorporating the relations in (A6) in equations (A7), (A8) and (A11) results in the following restrictions

$$\begin{aligned} V_{j+1} &= V_j \, , \\ W_{j+1} &= -W_j \, , \\ D_{1j+1} &= D_{1j} \, , \\ D_{2j+1} &= -D_{2j}, \\ D_{3j+1} &= -D_{3j}, \qquad j = 1,3,5 \, . \end{aligned} \tag{A12}$$

In order to satisfy the incremental traction-free boundary conditions at the upper and lower surfaces of the plate, the components of the incremental nominal stress must be set to zero

$$\hat{S}'_{31} = \hat{S}'_{32} = \hat{S}'_{33} = 0 \;\; \text{at } x_3' = \pm h/2 \, . \tag{A13}$$

This leads to a system of equations which can be expressed as

$$i\xi\begin{pmatrix} D_{11}E_1 & D_{12}E_2 & D_{13}E_3 & D_{14}E_4 & D_{15}E_5 & D_{16}E_6 \\ D_{21}E_1 & D_{22}E_2 & D_{23}E_3 & D_{24}E_4 & D_{25}E_5 & D_{26}E_6 \\ D_{31}E_1 & D_{32}E_2 & D_{33}E_3 & D_{34}E_4 & D_{35}E_5 & D_{36}E_6 \\ D_{11}\overline{E_1} & D_{12}\overline{E_2} & D_{13}\overline{E_3} & D_{14}\overline{E_4} & D_{15}\overline{E_5} & D_{16}\overline{E_6} \\ D_{21}\overline{E_1} & D_{22}\overline{E_2} & D_{23}\overline{E_3} & D_{24}\overline{E_4} & D_{25}\overline{E_5} & D_{26}\overline{E_6} \\ D_{31}\overline{E_1} & D_{32}\overline{E_2} & D_{33}\overline{E_3} & D_{34}\overline{E_4} & D_{35}\overline{E_5} & D_{36}\overline{E_6} \end{pmatrix} \times \begin{pmatrix} U_{11} \\ U_{12} \\ U_{13} \\ U_{14} \\ U_{15} \\ U_{16} \end{pmatrix} e^{i\xi(x_1'-ct)} = \begin{Bmatrix} 0 \\ 0 \\ 0 \\ 0 \\ 0 \\ 0 \end{Bmatrix}, \tag{A14}$$

where $U_{1q} = U_1(\alpha_q), E_q = e^{i\xi\alpha_q\frac{h}{2}}$ and $\overline{E_q} = e^{-i\xi\alpha_q\frac{h}{2}}$.

For non-trivial solutions, the determinant of the coefficient matrix in (A14) must go to zero. Using row and column operations along with the symmetries in (A12), the determinant can be reduced to two characteristic equations

$$\begin{aligned} D_{11}G_1\cot(\zeta\alpha_1) - D_{13}G_3\cot(\zeta\alpha_3) + D_{15}G_5\cot(\zeta\alpha_5) &= 0 \\ D_{11}G_1\tan(\zeta\alpha_1) - D_{13}G_3\tan(\zeta\alpha_3) + D_{15}G_5\tan(\zeta\alpha_5) &= 0\,, \end{aligned} \tag{A15}$$

corresponding to symmetric and anti-symmetric modes respectively, with

$$\begin{aligned} G_1 &= D_{23}D_{35} - D_{25}D_{33}\,, \qquad G_3 = D_{21}D_{35} - D_{25}D_{31}\,, \\ G_5 &= D_{21}D_{33} - D_{23}D_{31}\,, \qquad \zeta = \frac{\xi h}{2} = \frac{\omega h}{2c}\,. \end{aligned} \tag{A16}$$

Appendix B

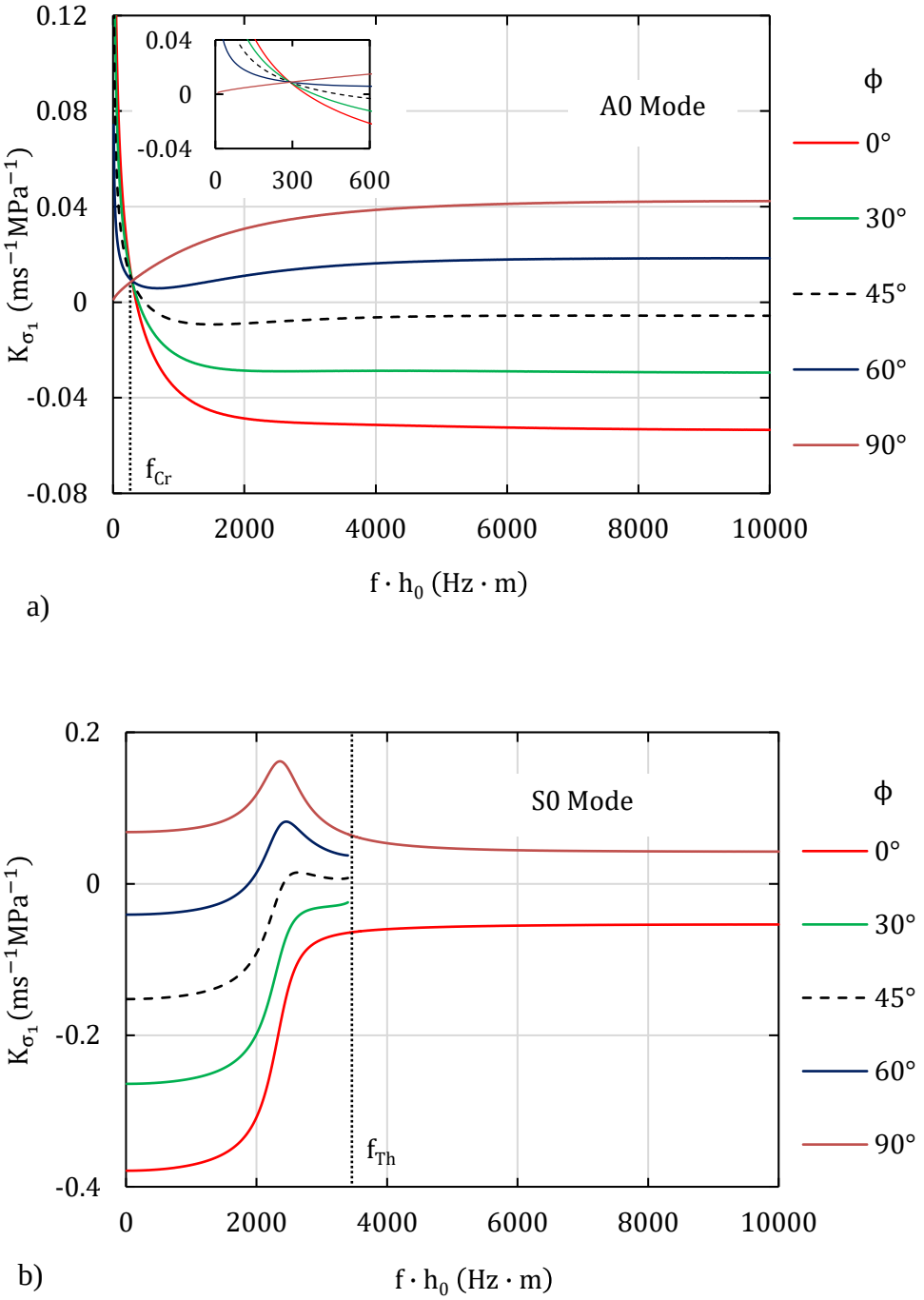

Figure B1. Variation of the coefficient relating changes in C_p to the applied stress σ_1 for the (a) A0 mode and, (b) S0 mode, at different angles of wave propagation, ϕ (measured relative to the σ_1 direction).

Chapter 6

On the determination of the third-order elastic constants of homogeneous isotropic materials utilising Rayleigh waves

Statement of Authorship

Title of Paper	On the determination of the third-order elastic constants of homogeneous isotropic materials utilising Rayleigh waves
Publication Status	☐ Published ☑ Accepted for Publication ☐ Submitted for Publication ☐ Unpublished and Unsubmitted w ork w ritten in manuscript style
Publication Details	M. Mohabuth, A. Khanna, J. Hughes, J. Vidler, A. Kotousov and C.T. Ng (2018), On the determination of the third-order elastic constants of homogeneous isotropic materials utilising Rayleigh waves, *Ultrasonics*, article in press, doi: 10.1016/j.ultras.2019.02.006

Principal Author

Name of Principal Author (Candidate)	Munawwar Mohabuth		
Contribution to the Paper	Derived the analytical equations, performed all analyses and wrote manuscript.		
Overall percentage (%)	60		
Certification:	This paper reports on original research I conducted during the period of my Higher Degree by Research candidature and is not subject to any obligations or contractual agreements with a third party that would constrain its inclusion in this thesis. I am the primary author of this paper.		
Signature		Date	13/05/2019

Co-Author Contributions

By signing the Statement of Authorship, each author certifies that:

i. the candidate's stated contribution to the publication is accurate (as detailed above);

ii. permission is granted for the candidate in include the publication in the thesis; and

iii. the sum of all co-author contributions is equal to 100% less the candidate's stated contribution.

Name of Co-Author	Aditya Khanna		
Contribution to the Paper	Checked the derivation of the equations, helped in interpretation of the results and assisted in the preparation of the manuscript.		
Signature		Date	13/05/2019

Name of Co-Author	James Hughes		
Contribution to the Paper	Assisted in experimental data collection and analysis.		
Signature		Date	13/05/2019

Name of Co-Author	James Vidler		
Contribution to the Paper	Assisted in experimental data collection and analysis.		
Signature		Date	13/05/2019

Name of Co-Author	Andrei Kotousov		
Contribution to the Paper	Supervised the work and assisted with editing of the manuscript.		
Signature		Date	13/05/2019

Name of Co-Author	Ching-Tai Ng		
Contribution to the Paper	Supervised the work and assisted with editing of the manuscript.		
Signature		Date	13/05/2019

On the determination of the third-order elastic constants of homogeneous isotropic materials utilising Rayleigh waves

Munawwar Mohabuth[a,*], Aditya Khanna[a], James Hughes[a], James Vidler[a], Andrei Kotousov[a], Ching-Tai Ng[b]

[a]School of Mechanical Engineering, The University of Adelaide, Adelaide, SA 5005, Australia

[b]School of Civil, Environmental and Mining Engineering, The University of Adelaide, Adelaide, SA 5005, Australia

*Corresponding author. Tel.: +61 8 8313 6385.

E-mail address: munawwar.mohabuth@adelaide.edu.au

Abstract

This paper presents a new method for determining the third-order elastic constants (TOECs) of a homogeneous isotropic material utilising the acoustoelastic effect associated with Rayleigh waves. It is demonstrated that the accuracy of the evaluation of TOECs can be substantially improved by supplementing the classical equations of acoustoelasticity, which describe the effect of applied stress on bulk wave speeds, with the nonlinear characteristic equation for the propagation of Rayleigh waves in pre-stressed media. The developed method can be readily implemented for Structural Health Monitoring applications; for example, the measurement of applied stresses based on the acoustoelastic effect, or the monitoring of near-surface microstructural damage based on the change in magnitude of the TOECs.

1. Introduction

In classical linear elasticity, the stress-strain response of an isotropic material is fully described by two conventional (or second-order) elastic constants. However, several experimentally observed phenomena, such as the variation of wave speeds with applied loading [1-4] or changes in compressibility with hydrostatic pressure [5-9], need consideration of the so-called third order elastic constants (TOECs). These constants arise in the expansion of the elastic strain energy density function and account for the contribution of the third-order products of the strain components. For an isotropic material, it can be shown that, in addition to the two second-order elastic constants, there are three independent third-order elastic constants corresponding to the third-order terms in the power series expansion of the strain energy density [10]. Various definitions of these constants were suggested by Brillouin [11], Biot [12,13], Landau & Lifshitz [14] and others [15-18].

TOECs play an important role in various engineering applications; for example, in the evaluation of applied or residual stresses based on the acoustoelastic theory. This theory describes the propagation of small-amplitude waves in a material subjected to finite deformations [19,20]. Another important recent development exploits the much greater sensitivity of TOECs as compared with second-order elastic constants to dislocation driven damage (fatigue, creep, etc) [21-23]. This effect motivated the development of experimental techniques, such as second and higher harmonic generation to evaluate the so-called early damage [24-27], i.e. microstructural damage accumulated prior to the formation of a propagating dominant crack(s). However, these experimental techniques often require highly accurate measurements of the TOECs to allow for quantitative damage monitoring.

TOECs are typically evaluated by measuring the change in bulk wave speeds with applied stress and fitting the measured values into the analytical equations of the acoustoelastic theory [28-30]. However, these measurements are still very challenging, and a large scatter is normally reported in experimental studies. A high frequency signal (toneburst) in the MHz range is usually

employed in conjunction with a high sampling frequency of the data acquisition system to achieve a good temporal resolution in the wave speed measurements. However, the excitation frequency is restricted by certain natural limitations; for example, the wavelength (or the central frequency of the toneburst) is limited by the size of the surface asperities or the material texture, which can affect the wave propagation and speed measurements. However, it seems that spatial resolution has a greater effect on the accuracy of the evaluation of TOECs with bulk waves, specifically for small specimens and slender structures for which the maximum measurement gauge lengths is relatively small. A significant improvement in the accuracy has been achieved with non-contact laser measurement techniques, such as laser interferometry. However, the reported values still have a large scatter; this might not be satisfactory, specifically, for microstructural damage monitoring, especially in the case of fatigue damage, where the changes in magnitude of the TOECs are expected to be small over the whole fatigue life.

An improvement in the evaluation of TOECs can be achieved using guided waves, which can propagate over large distances without significant attenuation. The advantage of using guided waves includes the possibility of an increased gauge length and hence, an expected improvement in the spatial resolution [31]. Another advantage is the possibility of utilising different types or modes of guided waves, which are known to be more sensitive to applied stresses as compared to bulk waves, specifically near the cut-off frequencies [32]. On the other hand, the main disadvantage of using guided waves is that it requires complex signal processing techniques due to the dependence of the guided wave speeds on the frequency (dispersion) and the excitation of multiple modes, which is inevitable in all guided wave excitation methods.

The present paper investigates the use of Rayleigh waves in conjunction with bulk waves for the evaluation of TOECs. Rayleigh waves are a type of non-dispersive guided waves that propagate near the surface of thick plates. The penetration depth of these surface waves depends on the excitation frequency; this phenomenon can potentially be utilised for tomography of damage or stress state, but this is beyond the scope of the current study. The structure of this paper

is as follows. In the next section, the acoustoelastic theory and the governing equations for bulk waves and Rayleigh waves are reviewed. This set of analytical equations forms the theoretical foundation for different methods of evaluating the TOECs. The accuracy of these methods is investigated using Monte-Carlo simulations, taking into account various types of probabilistic distributions of the wave speed measurements. The main outcomes of this paper are briefly summarised in the conclusion.

2. Review of governing equations of acoustoelasticity

The governing equations of acoustoelasticity are briefly recapped here, following Ogden et al. [33]. The equations for incremental motions due to the propagation of small-amplitude elastic waves as well as the incremental constitutive equation for a homogeneously deformed medium, can be written as:

$$\mathcal{A}_{piqj}\,\frac{\partial^2 u_j}{\partial x_p \partial x_q} = \rho\,\frac{\partial^2 u_i}{\partial t^2}\,, \tag{1}$$

and

$$\hat{S}_{pi} = \mathcal{A}_{piqj}\,\frac{\partial u_j}{\partial x_q}\,, \tag{2}$$

respectively, where $\boldsymbol{\mathcal{A}}$ is the fourth-order tensor of instantaneous elastic moduli, ρ is the density of the material in the deformed configuration, $\boldsymbol{u}$ is the incremental displacement vector associated with the wave, $\boldsymbol{x}$ is the position vector in the deformed configuration, t is the time and $\widehat{\boldsymbol{S}}$ is the incremental nominal stress tensor. The reader is referred to [34] for the derivation of the above equations.

The strain energy function commonly used to evaluate the acoustoelastic effect in engineering materials subjected to a small pre-stress is due to Murnaghan [15] and is given by

$$W = \frac{1}{2}(\lambda + 2\mu)i_1^2 - 2\mu i_2 + \frac{1}{3}(l + 2m)i_1^3 - 2m\, i_1 i_2 + n i_3, \tag{3}$$

where i_1, i_2, i_3 are the principal invariants of the Green-Lagrange strain tensor $\boldsymbol{E}$, given by $i_1 = \mathrm{tr}\boldsymbol{E}$, $i_2 = \frac{1}{2}[i_1^2 - \mathrm{tr}(\boldsymbol{E})^2]$ and $i_3 = \det \boldsymbol{E}$, respectively. The parameters λ and μ are the classical Lamé elastic constants and l, m, n are the Murnaghan or third-order elastic constants. Using the above strain energy function, the elasticity tensor can be obtained to the first order in the strain as [35]

$$\begin{aligned} J\mathcal{A}_{piqj} = {} & \mu\left(\delta_{ij}\delta_{pq} + \delta_{iq}\delta_{jp}\right) + \lambda\delta_{ip}\delta_{jq} \\ & + 2\mu\left(2\delta_{ij}E_{pq} + \delta_{pq}E_{ij} + \delta_{iq}E_{jp} + \delta_{jp}E_{iq}\right) \\ & + \lambda\left(E\delta_{ij}\delta_{pq} + 2\delta_{ip}E_{jq} + 2\delta_{jq}E_{ip}\right) + 2lE\delta_{ip}\delta_{jq} \\ & + m\left[E\left(\delta_{ij}\delta_{pq} + \delta_{iq}\delta_{jp} - 2\delta_{ip}\delta_{jq}\right)\right. \\ & \left. + 2\left(\delta_{ip}E_{jq} + \delta_{jq}E_{ip}\right)\right] \\ & + \frac{1}{2}n\left[\delta_{ij}E_{pq} + \delta_{pq}E_{ij} + \delta_{iq}E_{jp} + \delta_{jp}E_{iq} - 2\delta_{ip}E_{jq}\right. \\ & \left. - 2\delta_{jq}E_{ip} - E\left(\delta_{ij}\delta_{pq} + \delta_{iq}\delta_{jp} - 2\delta_{ip}\delta_{jq}\right)\right], \end{aligned} \tag{4}$$

where $E = \mathrm{tr}\boldsymbol{E}$ and $J = 1 + E$.

For the experimental determination of TOECs, the test specimen is generally subjected to a static uniaxial stress state due to the simplicity of the loading apparatus. For a small applied uniaxial stress σ_{11} in the $\boldsymbol{e_1}$ direction, the components of the strain tensor $\boldsymbol{E}$ can be evaluated using the linear elasticity theory as follows:

$$E_{11} = \frac{\lambda + \mu}{3K\mu}\sigma_{11}, \quad E_{22} = E_{33} = -\frac{\lambda E_{11}}{2(\lambda + \mu)}, \tag{5}$$

where $K = \lambda + 2\mu/3$ is the bulk modulus. The expression for the Jacobian of the deformation then reduces to

$$J = 1 + \frac{\mu E_{11}}{\lambda + \mu} = 1 + \frac{\sigma_{11}}{3K}. \tag{6}$$

2.1. Bulk waves

Hughes and Kelly [1] first obtained the expressions for the stress-dependent speeds of bulk waves propagating along the principal directions, i.e. along the direction $\boldsymbol{e_1}$ of the uniaxial stress, and along the mutually perpendicular directions, $\boldsymbol{e_2}$ and $\boldsymbol{e_3}$, which are equivalent by symmetry. Following Abiza et al. [36] and Hughes and Kelly [1], the expressions for the speed of these principal waves can be written in terms of the components of the elasticity tensor $\boldsymbol{\mathcal{A}}$ as follows:

$$\rho_0 v_{11}^2 = J\mathcal{A}_{1111} = \lambda + 2\mu + \frac{\sigma_{11}}{3K}\left[2l + \lambda + \frac{\lambda+\mu}{\mu}(4m + 4\lambda + 10\mu)\right], \tag{7}$$

$$\rho_0 v_{12}^2 = J\mathcal{A}_{1212} = \mu + \frac{\sigma_{11}}{3K}\left[m + \frac{\lambda}{4\mu}n + 4\lambda + 4\mu\right], \tag{8}$$

$$\rho_0 v_{22}^2 = J\mathcal{A}_{2222} = \lambda + 2\mu + \frac{\sigma_{11}}{3K}\left[2l - \frac{2\lambda}{\mu}(m + \lambda + 2\mu)\right], \tag{9}$$

$$\rho_0 v_{21}^2 = J\mathcal{A}_{2121} = \mu + \frac{\sigma_{11}}{3K}\left[m + \frac{\lambda}{4\mu}n + \lambda + 2\mu\right], \tag{10}$$

$$\rho_0 v_{23}^2 = J\mathcal{A}_{2323} = \mu + \frac{\sigma_{11}}{3K}\left[m - \frac{\lambda+\mu}{2\mu}n - 2\lambda\right]. \tag{11}$$

where $\rho_0 = \rho J$ is the density of the material in the undeformed or unstressed configuration, and the applied uniaxial stress σ_{11} is positive in tension. The elastic moduli $\mathcal{A}_{piqj}$ can be evaluated by substituting Eq. (5) into Eq. (4). The speeds v_{11} and v_{12} in Eqs. (7) and (8) correspond to longitudinal and transverse waves respectively, propagating along the direction $\boldsymbol{e_1}$ of the applied uniaxial stress. In Eq. (9), v_{22} is the speed of the longitudinal wave propagating along the direction $\boldsymbol{e_2}$, which is perpendicular to the applied uniaxial stress. In Eqs. (10) and (11), v_{21} and v_{23} correspond to the speeds of transverse waves propagating along the direction $\boldsymbol{e_2}$ and polarised in the directions $\boldsymbol{e_1}$ and $\boldsymbol{e_3}$, respectively.

2.2. Rayleigh-Lamb waves

Mohabuth et al. [32] presented the general characteristic equations describing the acoustoelastic effect for plane Lamb wave propagation in pre-stressed plates along the principal direction of the applied uniaxial stress. The main steps in the derivation of these characteristic equations are provided in Appendix A. By considering the limit of the plate-thickness tending to infinity, the characteristic equations for Lamb wave propagation can be reduced to the equation governing the acoustoelastic effect for Rayleigh waves. This special case was first investigated by Dowaikh and Ogden [37] and the form of their original equation can be recovered by substituting Eqs. (A8) and (A10) into Eq. (A9), replacing c by c_R and recalling that $\rho = \rho_0 J^{-1}$, as follows:

$$\begin{aligned}&(J\mathcal{A}_{1111} - \rho_0 c_R^2)(J\mathcal{A}_{1212} - \rho_0 c_R^2 - J\mathcal{A}_{2121}) \\ &+ \left(\frac{(J\mathcal{A}_{1111} - \rho_0 c_R^2)(J\mathcal{A}_{1212} - \rho_0 c_R^2)}{(J\mathcal{A}_{2222})(J\mathcal{A}_{2121})}\right)^{\frac{1}{2}} \{J\mathcal{A}_{2222}(J\mathcal{A}_{1111} - \rho_0 c_R^2) \\ &- (J\mathcal{A}_{1122})^2\} = 0.\end{aligned} \tag{12}$$

The stress-dependent elastic moduli $J\mathcal{A}_{1111}, J\mathcal{A}_{1212}, J\mathcal{A}_{2222}$ and $J\mathcal{A}_{2121}$ in the above equation have been defined previously in Eqs. (7)-(10). The remaining elastic modulus $J\mathcal{A}_{1122}$ can be obtained from Eq. (4) as

$$J\mathcal{A}_{1122} = \lambda + \frac{\sigma_{11}}{6K\mu}[4\mu l + 2\lambda m - \lambda n + 2\lambda(\lambda + 2\mu)]. \tag{13}$$

The characteristic Eq. (12) governing the acoustoelastic effect for Rayleigh waves differs from Eqs. (7)-(11) for bulk waves in two important respects. Firstly, the governing equation for Rayleigh waves contains all three TOECs, whereas the equations for bulk waves contain only two out of the three constants. Secondly, the characteristic Eq. (12) for Rayleigh waves contains the TOECs raised to exponents as well as terms involving products of the three TOECs. In principle, this implies that by substituting the measured values of the Rayleigh wave speed at three known stress levels into Eq. (12), a system of three nonlinear equations can be obtained, from which all three TOECs can be determined.

In recent years, similar characteristic equations have also been derived for Rayleigh wave propagation in pre-stressed anisotropic materials [38-44]. However, these equations are much more complex as compared to their isotropic counterpart. For example, in the case of a transversely isotropic material, the characteristic equation involves 5 second-order elastic constants and 9 third-order elastic constants [45]. Determining such a large number of elastic constants is not a trivial task and it is not surprising that practical applications using the acoustoelastic effect has been largely restricted to isotropic materials.

3. Comparison of different methods for the determination of TOECs

Eqs. (7)-(11) provide an overdetermined system of five linear equations in three unknown variables, l, m, and n for known values of the density ρ_0, Lamé constants, λ and μ, as well as the experimentally determined values of the bulk wave speeds at a known stress level, σ_{11}. The unknown TOECs can be determined by solving a system of any three out of five linear equations given by Eqs. (7)-(11). The system of Eqs. (9)-(11) is preferred over other combinations since the experimental setup for the measurement of bulk wave speeds perpendicular the direction of the applied stress is relatively straightforward. As shown in Figure 1, ultrasonic transducers can be placed directly on the lateral surfaces of the specimen and the time of propagation of the bulk wave across the specimen thickness can be measured by either using the pulse-echo or pitch-catch arrangement of the transducers.

Experimental studies utilising this traditional method have reported a large scatter in the obtained values of the constant l, relative to the constants m and n, despite careful measurements of the bulk wave speeds [45]. Some of these reported values for Aluminium alloys are summarised in Table 1. The possibility of reducing the standard deviation in the values of the TOECs is investigated by considering an alternative system of equations comprising the characteristic Eq. (12) for Rayleigh waves and any two out of the three Eqs. (9)-(11). Rayleigh waves can be generated along the direction of the applied uniaxial stress by utilising a wedge-transducer, as shown in Figure 1.

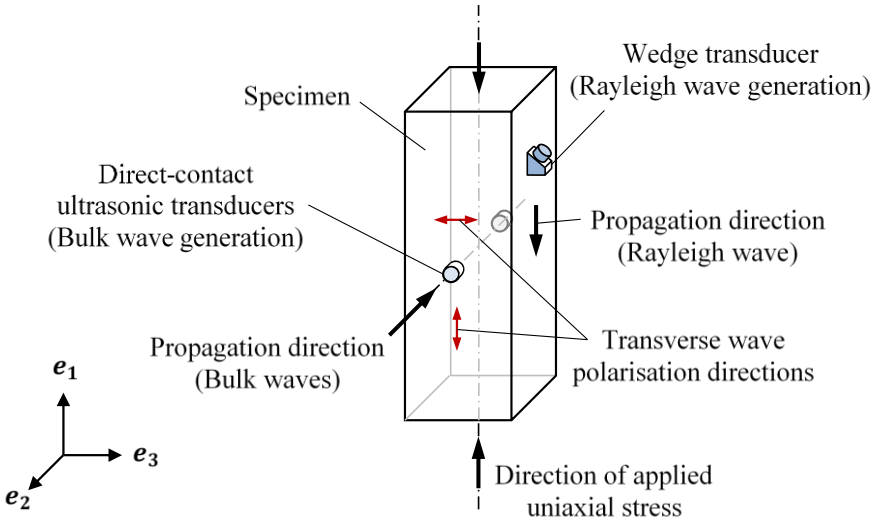

Figure 1. Schematic diagram showing the propagation directions of the elastic waves and the direction of applied stress.

Table 1. Experimentally determined TOECs for Aluminium alloys

Aluminium alloys	Third order elastic constants (GPa)		
	l	m	n
2S [29]	-311 ± 131	-401 ± 78	-408 ± 34
B53S M [29]	-223 ± 61	-237 ± 12	-276 ± 5
B53S P [29]	-201 ± 22	-305 ± 17	-300 ± 6
D54S [29]	-387 ± 10	-358 ± 10	-320 ± 3
JH77S [29]	-337 ± 32	-395 ± 13	-436 ± 7
6061-T6 [45]	-440 ± 31	-383 ± 35	-229 ± 12

The TOECs can be evaluated from the measurements of three wave speeds using any three out of four Eqs. (9)-(12). In this section, a comparative evaluation of the four possible combinations of these equations is conducted to identify the best combination which yields the smallest overall standard deviation in the obtained values of the TOECs. A numerical sensitivity study is conducted based on the various input parameters listed in Table 2. Based on the theoretical values of the Lamé constants, density and TOECs, the theoretical speeds of the three bulk waves, v_{22}, v_{21} and v_{23} and the Rayleigh wave, c_R, are evaluated at the stress level, σ_{11} using Eqs. (9)-(12). Following that, four datasets of 500 random speed measurements are generated with the following statistical distributions: (1) normal distribution with a standard deviation of 1 m/s (Figure 2); (2) normal distribution with a standard deviation of 10 m/s; (3) uniform distribution over the interval defined by the theoretical speed ± 1 m/s; and (4) uniform distribution over the interval defined by the theoretical speed ± 10 m/s. For all four distributions, the mean values are set equal to the theoretical speeds obtained from Eqs. (9)-(12). For each of the four statistical distributions, the TOECs are evaluated for 500^3 = 125 million combinations of three wave speeds.

Table 2. Input parameters for the sensitivity study

Parameter	Value
λ (GPa)	54.308
μ (GPa)	27.174
l (GPa)	-281.5
m (GPa)	-339.0
n (GPa)	-416.0
ρ_0 (kg/m^3)	2704
σ_{11} (MPa)	100

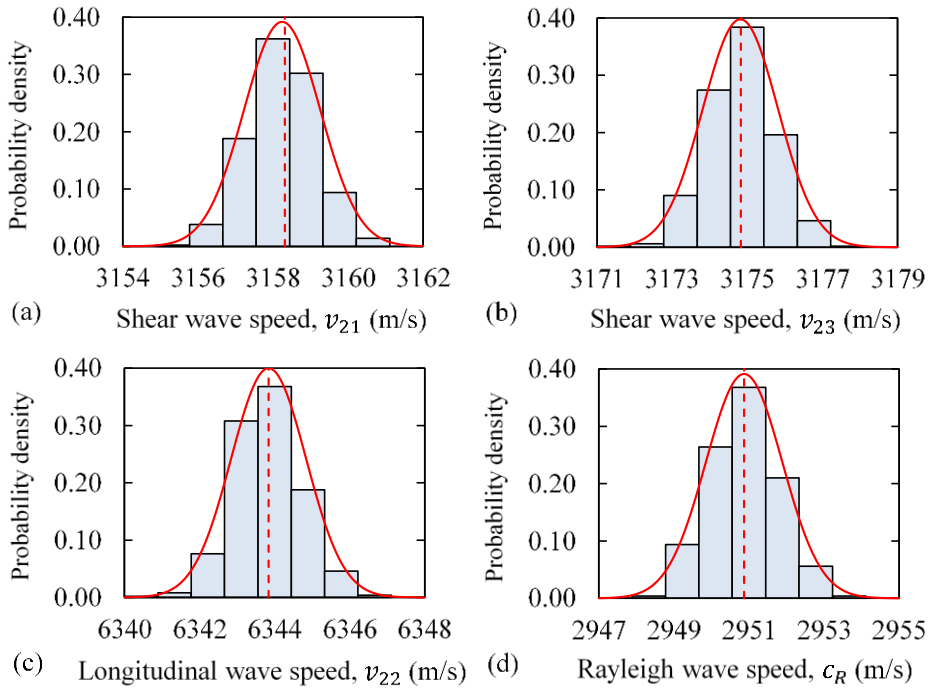

Figure 2. Normal distribution of bulk and Rayleigh wave speeds with a standard deviation of 1 m/s. The sample means are equal to the theoretical wave speeds calculated using the input parameters listed in Table 2.

The results of the sensitivity study are summarised in Tables 3-5. In these tables, the numerical values of the TOECs obtained using the four combinations of Eqs. (9)-(12) are presented for the various statistical distributions of wave speeds described previously. It can be observed that the mean values of the TOECs presented in Tables 3-5 are within a few percent of the exact values listed in Table 2, regardless of the choice of the statistical distribution or the system of equations used. This is in accordance with the law of large numbers, which states that the sample mean converges to the expected value as the number of repeat measurements tends to infinity. However, the standard deviation in the numerical values of all three constants is strongly linked to the scatter in the randomly generated wave speed distributions.

The best combination of three out of four Eqs. (9)-(12) can be identified by comparing the standard deviations in the numerically-evaluated values of the TOECs, presented in Tables 3-5. It is evident from the observation of Table 3 as well as Figure 3 that the standard deviation in the numerical values of the constant l can be reduced substantially by utilising the characteristic Eq. (12) for Rayleigh waves in conjunction with any two out of three Eqs. (9)-(11), i.e. by utilising one of the proposed methods 2-4 rather than the traditionally utilised method 1. The standard deviation in the numerical values of the remaining constants, m and n is relatively insensitive to the choice of the method of solution, i.e. the combination of Eqs. (9)-(12) used. Overall, method 2 appears to be most suitable for the evaluation of the TOECs since it minimises the standard deviation for the constants l and n, while providing marginally greater standard deviation for the constant m, when compared to other methods.

Table 3. Comparison of the exact value of l = -281.5 GPa against numerical values obtained using the four combinations of wave speed measurements.

Wave speed distribution about theoretical value	Numerical value of l (mean ± std. dev.) in GPa			
	Method 1 v_{22}, v_{21}, v_{23}	Method 2 v_{22}, v_{21}, c_R	Method 3 v_{22}, v_{23}, c_R	Method 4 v_{21}, v_{23}, c_R
Normal distribution (std. dev. = 1 m/s)	-278.9 ± 67.8	-281.3 ± 17.5	-281.0 ± 26.8	-281.0 ± 26.0
Normal distribution (std. dev. = 10 m/s)	-282 ± 280	-282.0 ± 23	-282 ± 37	-282 ± 30
Uniform distribution (Resolution = 1 m/s)	-284.5 ± 39.3	-280.6 ± 16.2	-281.0 ± 21.8	-281.0 ± 24.8
Uniform distribution (Resolution = 10 m/s)	-282 ± 280	-282 ± 23	-282 ± 30	-282 ± 30

Table 4. Comparison of the exact value of m = -339 GPa against numerical values obtained using the four combinations of wave speed measurements.

Wave speed distribution about theoretical value	Numerical value of m (mean ± std. dev.) in GPa			
	Method 1 v_{22}, v_{21}, v_{23}	Method 2 v_{22}, v_{21}, c_R	Method 3 v_{22}, v_{23}, c_R	Method 4 v_{21}, v_{23}, c_R
Normal distribution (std. dev. = 1 m/s)	-338.1 ± 28.5	-338.4 ± 34.2	-337.3 ± 36.2	-338.8 ± 29.6
Normal distribution (std. dev. = 10 m/s)	-341 ± 164	-340 ± 269	-333 ± 275	-331 ± 274
Uniform distribution (Resolution = 1 m/s)	-340.3 ± 16.5	-337.7 ± 21.9	-338.7 ± 16.4	-339.0 ± 16.9
Uniform distribution (Resolution = 10 m/s)	-340 ± 164	-340 ± 269	-333 ± 275	-331 ± 274

Table 5. Comparison of the exact value of n = -416 GPa against numerical values obtained using the four combinations of wave speed measurements.

Wave speed distribution about theoretical value	Numerical value of n (mean ± std. dev.) in GPa			
	Method 1 v_{22}, v_{21}, v_{23}	Method 2 v_{22}, v_{21}, c_R	Method 3 v_{22}, v_{23}, c_R	Method 4 v_{21}, v_{23}, c_R
Normal distribution (std. dev. = 1 m/s)	-414.7 ± 25.9	-416.4 ± 14.3	-414.7 ± 32.0	-416.0 ± 12.6
Normal distribution (std. dev. = 10 m/s)	-417 ± 210	-415 ± 105	-412 ± 117	-412 ± 113
Uniform distribution (Resolution = 1 m/s)	-416 ± 15.1	-416.1 ± 12.9	-415.7 ± 12.6	-416.1 ± 7.5
Uniform distribution (Resolution = 10 m/s)	-409 ± 147	-416 ± 64.3	-409 ± 77	-419 ± 71

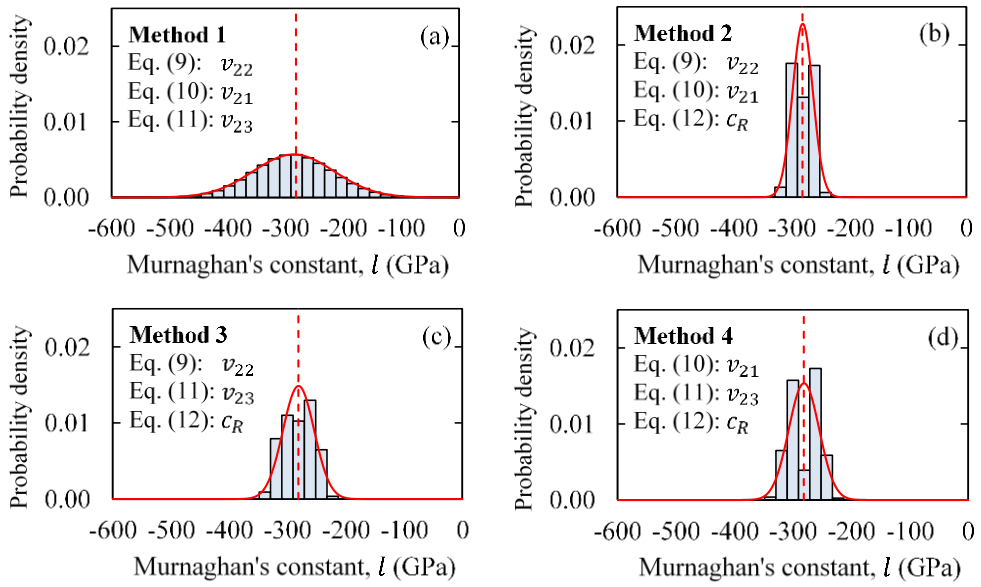

Figure 3. The distribution of numerical values of the constant l obtained for the wave speed distributions shown in Fig. 2.

4. Linearisation of the governing equations of acoustoelasticity

One of the inherent shortcomings in the evaluation of TOECs based on wave speed measurements is the propagation of errors during the calculations. As demonstrated in the previous section, one way to improve the robustness of the calculations is to perform a large number of repeat measurements at a single stress level. Alternatively, one can take advantage of the approximately linear dependence of the wave speed on the applied stress within the elastic region of the stress-strain curve, i.e. for $\sigma_{11} \ll \lambda, \mu$. Rather than making several repeat measurements at a single stress level, the wave speed can also be measured at several increments of the applied stress. The slope of the wave speed vs. applied stress plot can then be evaluated using the method of least squares and the TOECs can be obtained from the linearised form of Eqs. (9)-(11). The linearised equations can be expressed in terms of the experimentally determined slope,

$\partial v_{2k}/\partial\sigma_{11}$, $k \in \{1,2,3\}$, and the known material constants, λ, μ and ρ_0, as follows:

$$2\rho_0 v_{22,0}\frac{\partial v_{22}}{\partial \sigma_{11}} = \frac{1}{3K}\left[2l - \frac{2\lambda}{\mu}(m+\lambda+2\mu)\right], \tag{14}$$

$$2\rho_0 v_{21,0}\frac{\partial v_{21}}{\partial \sigma_{11}} = \frac{1}{3K}\left[m + \frac{\lambda}{4\mu}n + \lambda + 2\mu\right], \tag{15}$$

$$2\rho_0 v_{23,0}\frac{\partial v_{23}}{\partial \sigma_{11}} = \frac{1}{3K}\left[m - \frac{\lambda+\mu}{2\mu}n - 2\lambda\right]. \tag{16}$$

In the above equations, the bulk wave speeds in the unstressed configuration are $v_{22,0} = \sqrt{(\lambda+2\mu)/\rho_0}$ and $v_{21,0} = v_{23,0} = \sqrt{\mu/\rho_0}$. The nonlinear governing equation (12) for Rayleigh waves can also be linearised and written in terms of the experimentally determined slope $\partial c_R/\partial\sigma_{11}$. The resulting equation is quite lengthy and is presented in Appendix B. The correctness of the linearised Eqs. (14)-(16), (B1) can be verified by attempting to recalculate the known values of TOECs listed in Table 2 based on theoretical obtained slopes $\partial v_{2k}/\partial\sigma_{11}$, $k \in \{1,2,3\}$ and $\partial c_R/\partial\sigma_{11}$.

Table 6. Comparison of known and calculated values of TOECs obtained from linearised equations

TOEC	Exact value	Method 1 v_{22}, v_{21}, v_{23}	Method 2 v_{22}, v_{21}, c_R	Method 3 v_{22}, v_{23}, c_R	Method 4 v_{21}, v_{23}, c_R
l (GPa)	-281.5	-281.5	-274.2	-286.3	-204.3
m (GPa)	-339.0	-339.0	-335.4	-341.4	-339.0
n (GPa)	-416.0	- 416.0	-423.3	-417.6	-416.0

The obtained values of the TOECs using various combinations of linearised equations are presented in Table 6. As expected, the system of linear equations (14)-(16) exactly recovers the known values of the TOECs. Methods 2 and 3, which utilise Eq. (14) and Eq. (B1) along with either Eq. (15) or Eq. (16) provide approximate values for the TOECs within 2.5%. This indicates a small error associated with the linearisation of the nonlinear Eq. (12). Method 4, which utilises Eqs. (15),(16) and (B1) must be avoided for the experimental evaluation of the TOECs since it yields a large error of roughly 27% in the value of the constant l.

5. Conclusion

In this paper, a new method for the evaluation of TOECs is presented. This method utilises measurements of the change in Rayleigh and bulk wave speeds with an applied stress. This method is applicable to homogeneous isotropic materials only as the theoretical equations are based on the same underlying assumptions. It was demonstrated via numerical simulations that the incorporation of Rayleigh wave speed measurements allows for a significant improvement in the accuracy of the evaluation of TOECs. While it is also theoretically possible to determine the TOECs solely from measurements of the Rayleigh wave speed due to the inherent non-linearity of the characteristic equation, such an evaluation requires highly accurate measurements due to the relatively-small nonlinear effect.

In practical situations, the near surface material properties of the tested samples or structures are often different to the bulk. The inhomogeneity, anisotropy, accumulation of plastic deformation and damage associated with fabrication processes can affect the measurements of the elastic wave speed. In this case, the evaluation of the TOECs using these measurements may not be appropriate, as the constants obtained would not represent the bulk material properties. However, the actual changes in the wave speed can still be utilised for stress measurement purposes or for the characterisation of near surface mechanical damage. In addition, the near surface propagation nature of Rayleigh

waves can be utilised for measurements of the change in stress, material properties and damage with depth. However, it would be very difficult to separate all these effects from one another in practical situations.

Acknowledgements

This work was supported by the Australian Government Research Training Program Scholarship, and the Australian Research Council, project DP160102233.

References

[1] D. S. Hughes, J. L. Kelly, Second-order elastic deformation of solids, Phys. Rev. 92 (1953) 1145–1149, doi: 10.1103/PhysRev.92.1145

[2] T. Bateman, W. P. Mason, H. J. McSkimin, Third-order elastic moduli of Germanium, J. Appl. Phys. 32 (1961) 928-936, doi: 10.1063/1.1736135

[3] E. H. Bogardus, Third-order elastic constants of Ge, MgO, and fused SiO2, J. Appl. Phys. 26 (1965) 2504-2513, doi: 10.1063/1.1714520

[4] Y. Hiki, A. V. Granato, Anharmonicity in noble metals; Higher order elastic constants, Phys. Rev. 144 (1966) 411-419, doi: 10.1103/PhysRev.144.411

[5] P. W. Bridgman, The effect of pressure on the rigidity of steel and several varieties of glass, Proc. Am. Acad. Arts Sci. 63 (1929) 401-420, doi: 10.2307/20026225

[6] P. W. Bridgman, The effect of pressure on the rigidity of several metals, Proc. Am. Acad. Arts Sci. 64 (1929) 39-49, doi: 10.2307/20026251

[7] F. Birch, The effect of pressure on the modulus of rigidity of several metals and glasses, J. Appl. Phys. 8 (1937) 129-133, doi: 10.1063/1.1710264

[8] F. Birch, The effect of pressure upon the elastic parameters of isotropic solids, according to Murnaghan's theory of finite strain, J. Appl. Phys. 9 (1938) 279-288, doi: 10.1063/1.1710417

[9] F. Birch, Finite elastic strain of cubic crystals, Phys. Rev. 71 (1947) 809-824, doi: 10.1103/PhysRev.71.809

[10] F.D. Murnaghan, Finite deformations of an elastic solid, Am. J. Math. 59 (1937) 235–260, doi: 10.2307/2371405

[11] L. Brillouin, Sur les tensions de radiation, Ann. Phys. Ser. 10 (1925) 528–586, doi: 10.1051/anphys/192510040528

[12] M.A. Biot, The influence of initial stress on elastic waves, J. Appl. Phys. 11 (1940) 522–530, doi: 10.1063/1.1712807

[13] M.A. Biot, Mechanics of Incremental Deformations, John Wiley, New York, 1965.

[14] L.D. Landau, E.M. Lifshitz, Theory of Elasticity, Butterworth-Heinemann, Oxford, 1986.

[15] F.D. Murnaghan, Finite Deformation of an Elastic Solid, John Wiley & Sons, New York, 1951.

[16] R.A. Toupin, B. Bernstein, Sound waves in deformed perfectly elastic materials. Acoustoelastic effect, J. Acoust. Soc. Am. 33 (1961) 216–225, doi: 10.1121/1.1908623

[17] M. Hayes, R.S. Rivlin, Propagation of a plane wave in an isotropic elastic material subjected to pure homogeneous deformation, Arch. Ration. Mech. Anal. 8 (1961) 15–22, doi: 10.1007/BF00277427

[18] D.R. Bland, Nonlinear Dynamic Elasticity, Blaisdell, Waltham, MA, 1969.

[19] Y.H. Pao, W. Sachse, H. Fukuoka, Acoustoelasticity and ultrasonic measurements of residual stresses, in W.P. Mason, R. N. Thurston (Eds.), Physical Acoustics, Academic Press, New York, 1984, pp. 61–143.

[20] A.N. Guz, F.G. Makhort, The physical fundamentals of the ultrasonic non-destructive stress analysis of solids, Int. Appl. Mech. 36 (2000) 1119–1149, doi: 10.1023/A:1009442132064

[21] A. Hikata, B. B. Chick, C. Elbaum, Dislocation contribution to the second harmonic generation of ultrasonic waves, J. Appl. Phys. 36 (1965) 229–236, doi: 10.1063/1.1713881.

[22] J. K. Na, J. H. Cantrell, W. T. Yost, Linear and nonlinear ultrasonic properties of fatigued 410Cb stainless steel, in D. O. Thompson, D. E. Chimenti (Eds.), Review of Progress in Quantitative Nondestructive Evaluation. Springer, Boston, 1996, pp. 1347–1351

[23] J. H. Cantrell, W. T. Yost, Acoustic harmonic generation from fatigue-induced dislocation dipoles, Philos. Mag. A, 69 (1994) 315-326, doi: 10.1080/01418619408244346

[24] K. Y. Jhang, Nonlinear ultrasonic techniques for nondestructive assessment of micro damage in material: A review, Int. J. Precis. Eng. Manuf. 10 (2009) 123-135, doi: 10.1007/s12541-009-0019-y

[25] K. H. Matlack, J. Y. Jacobs, L.J. Jacobs, J. Qu, Review of Second Harmonic Generation Measurement Techniques for Material State Determination in Metals, J Nondestruct Eval 34 (2015) 1-23, doi: 10.1007/s10921-014-0273-5

[26] J. Y. Kim, L. Jacobs, J. Qu, Nonlinear Ultrasonic Techniques for Material Characterization, in T. Kundu (Eds.), Nonlinear Ultrasonic and Vibro-Acoustical Techniques for Nondestructive Evaluation. Springer, Cham, 2019, pp. 225-261

[27] V. Marcantonio, D. Monarca, A. Colantoni, M. Cecchini, Ultrasonic waves for materials evaluation in fatigue, thermal and corrosion damage: A review, Mech. Syst. Signal. Process. 120 (2019) 32-42, doi: 10.1016/j.ymssp.2018.10.012

[28] D. M. Egle, D. E. Bray, Measurement of acoustoelastic and third-order elastic constants for rail steel, J. Acoust. Soc. Am. 60 (1976) 741-744, doi: 10.1121/1.381146

[29] R. T. Smith, R. Stern, R. W. B. Stephens, Third- Order Elastic Moduli of Polycrystalline Metals from Ultrasonic Velocity Measurements, J. Acoust. Soc. Am. 40 (1966) 1002–1008, doi: 10.1121/1.1910179

[30] S. Takahashi, Measurement of third-order elastic constants and stress dependent coefficients for steels, Mech Adv Mater Mod Process 4 (2018) 1-7, doi: 10.1186/s40759-018-0035-7

[31] J. Rose, Ultrasonic Guided Waves in Solid Media, Cambridge University Press, Cambridge, 2014, doi: 10.1017/CBO9781107273610

[32] M. Mohabuth, A. Kotousov, C. T. Ng, Effect of uniaxial stress on the propagation of higher-order Lamb wave modes, Int. J. Nonlinear Mech. 86 (2016) 104-111, doi: 10.1016/j.ijnonlinmec.2016.08.006

[33] R.W. Ogden, Incremental statics and dynamics of pre-stressed elastic materials, in M. Destrade, G. Saccomandi (Eds.), Waves in Nonlinear Pre-Stressed Materials, Springer, Wien, 2007, pp. 1–26.

[34] R.W. Ogden, Non-Linear Elastic Deformations, Ellis Horwood, Chichester, 1984.

[35] M. Destrade, R.W. Ogden, On stress-dependent elastic moduli and wave speeds, IMA J. Appl. Math. 78 (2012) 965–997.

[36] Z. Abiza, M. Destrade, R. W. Ogden, Large acoustoelastic effect, Wave Motion 49 (2012) 364-374, doi: 10.1016/j.wavemoti.2011.12.002

[37] M. A. Dowaikh, R. W. Ogden, On surface waves and deformations in a compressible elastic half-space, Stability Appl. Cont. Mech, 1 (1991) 27-45

[38] G. T. Mase, G. C. Johnson, An acoustoelastic theory for surface waves in anisotropic media, J. Appl. Mech. 54 (1987) 127–135, doi: 10.1115/1.3172946

[39] P. P. Delsanto, A. V. Clark Jr., Rayleigh wave propagation in deformed orthotropic materials, J. Acoust. Soc. Am. 81 (1987) 952–960, doi: /10.1121/1.394575

[40] K. Tanuma, C. S. Man, Perturbation formula for phase velocity of Rayleigh waves in prestressed anisotropic media, J. Elasticity 85 (2006) 21-37, doi: /10.1007/s10659-006-9067-z

[41] K. Tanuma, C. S. Man, Perturbation formulas for polarization ratio and phase shift of Rayleigh waves in prestressed anisotropic media, J. Elasticity 92 (2008) 1-33, doi: /10.1007/s10659-007-9147-8

[42] P. C. Vinh, J. Merodio, Wave velocity formulas to evaluate elastic constants of soft biological tissues, J. Mech. Mater. Struct. 8 (2013) 51-64, doi: /10.2140/jomms.2013.8.51

[43] R. W. Ogden, B. Singh, Propagation of waves in an incompressible transversely isotropic elastic solid with initial stress: Biot revisited, J. Mech. Mater. Struct. 6 (2011) 453-477, doi: 10.2140/jomms.2011.6.453

[44] M. Destrade, M. D. Gilchrist, R. W. Ogden, Third- and fourth-order elasticities of biological soft tissues, J. Acoust. Soc. Am. 127 (2010) 2103-2106, doi: 10.1121/1.3337232

[45] C. L. Nogueira, Ultrasonic evaluation of acoustoelastic parameters in Aluminum, J. Mater. Civ. Eng. 29 (2017) 04017158, doi: 10.1061/(ASCE)MT.1943-5533.0002009

[46] E. V. Nolde, L. A. Prikazchikova, G. A. Rogerson, Dispersion of small amplitude waves in a pre-stressed, compressible elastic plate, J. Elast. 75 (2004) 1–29, doi: 10.1023/B:ELAS.0000039920.67766.d3

Appendix A: Lamb wave dispersion equations

In this section, the derivation of the dispersion equations governing the acoustoelastic effect for Lamb waves is briefly recapped. The results presented in this Appendix were obtained previously in [32,46] and are included here for the sake of completeness. Consider an infinite, isotropic plate of thickness D, with the reference Cartesian coordinates X_1 and X_3 aligned with the mid-plane of the plate and the coordinate X_2 aligned with the outward normal from the mid-plane. The plate is subjected to a uniaxial stress state, with Cauchy stress σ_{11} along the X_1 axis. The finite deformation can be expressed as

$$x_i = \lambda_i X_i, \quad i \in \{1, 2, 3\}, \tag{A1}$$

where the principal stretches $\lambda_i = 1 + E_{ii}$ can be written in terms of the applied stress σ_{11} using Eq. (5). Now, consider the propagation of a small-amplitude plane wave confined to the $x_1 - x_2$ plane, travelling with phase velocity c in the x_1 direction. The general solution to the governing equation for incremental motions, Eq. (1), is of the form:

$$u_j = U_j e^{\xi \alpha x_2} e^{i\xi(x_1 - ct)}, \quad j = 1, 2, \tag{A2}$$

where u_j is the particle displacement and U_j is the amplitude along the x_j coordinate, ξ is the wavenumber along the x_1 direction, t is time and α is the unknown ratio of the wavenumbers in the x_2 and x_1 directions. The solution must satisfy the incremental traction-free boundary conditions at the upper and lower surfaces of the plate, i.e. the corresponding incremental nominal stresses must be zero at the free surfaces:

$$\hat{S}_{22} = \hat{S}_{21} = 0, \quad x_2 = \pm\frac{\lambda_2 D}{2} = \pm\frac{d}{2}. \tag{A3}$$

After substituting Eq. (A2) into Eq. (1), a system of linear homogeneous equations is obtained. Following the procedure outlined in Mohabuth et al. [32], the requirement for obtaining a non-trivial solution to this system of equations can be expressed as:

$$\begin{aligned}&\mathcal{A}_{2121}\mathcal{A}_{2222}\alpha^4\\&\quad+\{\rho c^2(\mathcal{A}_{2121}+\mathcal{A}_{2222})-\mathcal{A}_{1111}\mathcal{A}_{2222}\\&\quad-\mathcal{A}_{1212}\mathcal{A}_{2121}+(\mathcal{A}_{1122}+\mathcal{A}_{2121})^2\}\alpha^2+\rho^2c^4\\&\quad-\rho c^2(\mathcal{A}_{1111}+\mathcal{A}_{1212})+\mathcal{A}_{1111}\mathcal{A}_{1212}=0,\end{aligned}\tag{A4}$$

The lack of odd powers in the fourth-order Eq. (A4) implies that the four roots for α, denoted by $\alpha_q, q \in \{1,2,3,4\}$ are related according to $\alpha_2 = -\alpha_1$ and $\alpha_4 = -\alpha_3$. Using this relation and the identity $e^z = \cosh(z) + \sinh(z)$, the solutions for u_1 and u_2 in Eq. (A2) can be rewritten as a linear combination of the four independent solutions associated with the roots of Eq. (A4) as follows [46]:

$$\begin{aligned}u_1 &= \{A_1\cosh(\xi\alpha_1x_2)+A_2\sinh(\xi\alpha_1x_2)+A_3\cosh(\xi\alpha_3x_2)\\&\quad+A_4\sinh(\xi\alpha_3x_2)\}e^{i\xi(x_1-ct)},\\u_2 &= \left\{\left(\frac{\mathcal{A}_{1111}-\rho c^2-\mathcal{A}_{2121}\alpha_1^2}{i\alpha_1(\mathcal{A}_{1122}+\mathcal{A}_{2121})}\right)[A_1\cosh(\xi\alpha_1x_2)\right.\\&\quad+A_2\sinh(\xi\alpha_1x_2)]\\&\quad+\left(\frac{\mathcal{A}_{1111}-\rho c^2-\mathcal{A}_{2121}\alpha_3^2}{i\alpha_3(\mathcal{A}_{1122}+\mathcal{A}_{2121})}\right)[A_3\cosh(\xi\alpha_3x_2)\\&\quad\left.+A_4\sinh(\xi\alpha_3x_2)]\right\}e^{i\xi(x_1-ct)},\end{aligned}\tag{A5}$$

where the constants $A_q, q \in \{1,2,3,4\}$ are functions of the displacement amplitudes $U_1(\alpha_q)$ in Eq. (A2).

The incremental stress components corresponding to (A5) can be obtained from the incremental stress-displacement relations given by Eq. (2). Satisfying the boundary conditions (A3) with the obtained incremental stress components yields a homogenous system of four equations in four unknowns, A_q. Using the method presented in Mohabuth et al. [32], two characteristic equations which ensure non-trivial solutions to this system of equations are obtained as:

$$\alpha_1(\eta - \zeta\alpha_3^2)\tanh(\gamma\alpha_1) - \alpha_3(\eta - \zeta\alpha_1^2)\tanh(\gamma\alpha_3) = 0, \tag{A6}$$

$$\alpha_1(\eta - \zeta\alpha_3^2)\tanh(\gamma\alpha_3) - \alpha_3(\eta - \zeta\alpha_1^2)\tanh(\gamma\alpha_1) = 0, \tag{A7}$$

which correspond to the anti-symmetric and symmetric Lamb wave modes, respectively, with $\gamma = \xi d/2 = \omega d/2c$. The constants η and ζ are defined as [46]

$$\begin{aligned} \eta &= (\mathcal{A}_{1111} - \rho c^2)(\mathcal{A}_{1212} - \mathcal{A}_{2121} - \rho c^2), \\ \zeta &= \mathcal{A}_{2222}\left(\mathcal{A}_{1111} - \frac{\mathcal{A}_{1122}^2}{\mathcal{A}_{2222}} - \rho c^2\right). \end{aligned} \tag{A8}$$

The characteristic equation governing the acoustoelastic effect for Rayleigh waves propagating in an infinite half-space can be obtained by setting $\gamma = \xi d/2 \to \infty$ in equation (A6) or (A7) and recalling that $\lim_{\gamma\to\infty} \tanh(\gamma) = 1$, as follows

$$\eta + \zeta\alpha_1\alpha_3 = 0. \tag{A9}$$

Since Eq. (A4) is quadratic in α^2, the product $\alpha_1\alpha_3$ can be readily expressed as

$$\alpha_1\alpha_3 = \left(\frac{(\mathcal{A}_{1111} - \rho c^2)(\mathcal{A}_{1212} - \rho c^2)}{\mathcal{A}_{2222}\mathcal{A}_{2121}}\right)^{\frac{1}{2}}. \tag{A10}$$

Appendix B: Linearised Rayleigh wave characteristic equation

The characteristic Eq. (12) governing the propagation of Rayleigh waves along the direction of the applied uniaxial stress can be linearised for $\sigma_{11} \to 0$ as follows:

$$\mathcal{L}_1 + \mathcal{L}_2\mathcal{L}_3 + \mathcal{L}_4(\mathcal{L}_5 + \mathcal{L}_6) = 0, \tag{B1}$$

where the terms

$$\begin{aligned}\mathcal{L}_1 = &-\left(C_{1111} - 2\rho_0 c_{R,0}\frac{\partial c_R}{\partial \sigma}\right)\rho_0 c_{R,0}^2 \\ &+ \left(C_{1212} - C_{2121} - 2\rho_0 c_{R,0}\frac{\partial c_R}{\partial \sigma}\right)\left(\lambda + 2\mu - \rho_0 c_{R,0}^2\right),\end{aligned} \tag{B2}$$

$$\mathcal{L}_2 = \left(\frac{\left(\lambda + 2\mu - \rho_0 c_{R,0}^2\right)\left(\mu - \rho_0 c_{R,0}^2\right)}{\mu(\lambda + 2\mu)}\right)^{\frac{1}{2}}, \tag{B3}$$

$$\mathcal{L}_3 = C_{2222}\left(\lambda + 2\mu - \rho_0 c_{R,0}^2\right) + \left(C_{1111} - 2\rho_0 c_{R,0}\frac{\partial c_R}{\partial \sigma}\right)(\lambda + 2\mu), \tag{B4}$$

$$\mathcal{L}_4 = (\lambda + 2\mu)\left(\lambda + 2\mu - \rho_0 c_{R,0}^2\right) - \lambda^2, \tag{B5}$$

$$\begin{aligned}\mathcal{L}_5 = &\frac{\left(C_{1111} - 2\rho_0 c_{R,0}\frac{\partial c_R}{\partial \sigma}\right)\left(\mu - \rho_0 c_{R,0}^2\right)}{2\left(\lambda + 2\mu - \rho_0 c_{R,0}^2\right)\left(\mu - \rho_0 c_{R,0}^2\right)} \\ &+ \frac{\left(C_{1212} - 2\rho_0 c_{R,0}\frac{\partial c_R}{\partial \sigma}\right)\left(\lambda + 2\mu - \rho_0 c_{R,0}^2\right)}{2\left(\lambda + 2\mu - \rho_0 c_{R,0}^2\right)\left(\mu - \rho_0 c_{R,0}^2\right)},\end{aligned} \tag{B6}$$

$$\mathcal{L}_6 = -\left(\frac{C_{2222}\mu + C_{2121}(\lambda + 2\mu)}{2\mu(\lambda + 2\mu)}\right). \tag{B7}$$

In Eqs. (B2)-(B6), $c_{R,0}$ is the Rayleigh wave speed in the unstressed configuration, which can be determined in terms of the known material constants, λ, μ and ρ_0, by setting $J\mathcal{A}_{1111} = J\mathcal{A}_{2222} = (\lambda + 2\mu)$, $J\mathcal{A}_{1122} = \lambda$, and $J\mathcal{A}_{1212} = J\mathcal{A}_{2121} = \mu$ in Eq. (12). The dimensionless constants C_{ijkl} are

closely related to the stress-dependent elastic moduli $\mathcal{A}_{ijkl}$, and are defined as follows:

$$C_{1111} = \frac{1}{3K}\left[2l + \lambda + \frac{\lambda+\mu}{\mu}(4m + 4\lambda + 10\mu)\right], \tag{B8}$$

$$C_{1212} = \frac{1}{3K}\left[m + \frac{\lambda}{4\mu}n + 4\lambda + 4\mu\right], \tag{B9}$$

$$C_{2222} = \frac{1}{3K}\left[2l - \frac{2\lambda}{\mu}(m + \lambda + 2\mu)\right], \tag{B10}$$

$$C_{2121} = \frac{1}{3K}\left[m + \frac{\lambda}{4\mu}n + \lambda + 2\mu\right], \tag{B11}$$

$$C_{1122} = \frac{1}{6K\mu}[4\mu l + 2\lambda m - \lambda n + 2\lambda(\lambda + 2\mu)]. \tag{B12}$$

Chapter 7

Summary and Recommendations

Chapter 7

Summary and Recommendations

This chapter summarises the main outcomes of the thesis, chapter by chapter, and discusses the possible future research directions arising from the current study.

7.1 Summary of the main outcomes

The main outcomes of the present thesis represent essential advances in four research fields/problems:

i. Analytical modelling of Lamb waves in pre-stressed compressible plates;

ii. Analysis of a large pre-deformation on the propagation of Lamb waves in incompressible plates;

iii. Evaluation of the effect of stress induced variations on damage detection using Lamb waves; and

iv. Assessment of the third-order elastic constants using Rayleigh surface waves.

A detailed explanation of each of these research advances is provided below along with other developments, which were necessary in order to present this work in a cohesive and seamless way.

Chapter 1

This chapter provided the background and motivation behind the current study; these are not included as part of the research articles which form the main body of this thesis, but are important in order to understand the context of the research undertaken. In particular, the current study is of interest in a number of research areas, including material characterisation, bio-mechanics, acoustoelasticity and SHM.

A broad review of literature was also presented as part of this chapter, focusing on the theory of acoustoelasticity, guided waves and an overview of the developments in the area of SHM. This literature review has helped to formulate the specific objectives of the study, which, to the author's knowledge, has not been addressed previously. This introductory chapter also discussed the organisation and outline of the thesis to facilitate the reading and evaluation of the current work.

Chapter 2

This chapter provided a systematic description of the fundamentals of the theory of acoustoelasticity, which is based on the theory of incremental motions superimposed on a finite deformation. Although some of the equations presented can be found in the papers published by the author or in other articles, this systematic description was thought to be necessary for the sake of completeness of this thesis. The presented governing equations describing the mechanical response of the finitely deformed body to small disturbances form the basis of the mathematical framework adopted in this thesis. These governing equations and other theoretical developments were utilised to produce the main outcomes of this thesis, which will be detailed next.

Chapter 3

In this chapter, the problem of Lamb wave propagation in an initially isotropic compressible plate subjected to a uniform uniaxial stress field was considered. Based on the nonlinear theory of elasticity and an invariant-based formulation of the strain energy function, new dispersion equations were derived for wave propagation along the direction of the applied stress for a general form of the strain energy function. These equations were subsequently specialised to the case of weakly nonlinear elasticity, whereby the Murnaghan form of the strain energy function, which is applicable to a large class of engineering materials, was considered. The theoretical predictions obtained demonstrated the same tendencies as previously published experimental data and provided a better

correlation with the experimental data than previously published results obtained by other researchers.

In particular, for aluminium plates subjected to realistic magnitudes of applied stress (below 100 MPa) it was found that the acoustoelastic effect is quite significant below 3000 Hz-m for the fundamental symmetric Lamb wave mode (S_0), and it is even stronger for higher-order wave modes near the cut-off frequencies. These findings can potentially be utilised in the development of new experimental techniques for the evaluation and monitoring of the stress conditions in plate- and shell-like engineering components.

Chapter 4

As mentioned previously, the classical acoustoelastic theory describes the effect of applied stress on the change in the wave speeds of bulk waves, which is essentially a linear effect. However, this theory leads to large discrepancies in experimental observations for rubber-like materials and other elastomers subjected to high levels of deformation. In this case, the non-linear (or large acoustoelastic) effects can become significant. However, there were no studies on the large acoustoelastic effect for guided waves; the present chapter addressed this shortcoming.

The acoustoelastic effect associated with the propagation of small-amplitude Lamb waves in incompressible plate-like structures subjected to a large pre-stress was investigated in this chapter. The study utilised a new acoustoelastic formulation based on a fourth-order strain energy function to examine the effect of a large applied uniaxial deformation on the wave speeds of the symmetric and antisymmetric Lamb wave modes. Particular results were presented for a Silicone Rubber plate, whose higher-order elastic constants are known. The results of the large acoustoelastic formulation were compared with those obtained using the classical acoustoelastic formulation. It was found that at low magnitudes of the applied deformations, the discrepancies between the large and classical acoustoelastic formulations are relatively small. However, the discrepancies were found to be quite significant at high magnitudes of the

applied deformation. The outcomes of this study allows for some guidance in identifying the situations when the large acoustoelastic formulation should be considered and when it can be neglected.

Chapter 5

There have been many studies demonstrating that temperature variations can undermine the damage detecting capabilities of Lamb-wave based SHM systems outside the lab environment, in which these systems are often tested. The main objective of the study undertaken in the current chapter was to evaluate the background noise associated with changing loading conditions. The study focused on SHM systems utilising the reference signal subtraction approach for damage detection, which is a common approach used to monitor the structural integrity in many engineering applications.

For this purpose, an analytical model was developed to assess the residual signal or noise caused by changing stress conditions. It was demonstrated that the effect of changing stress on the noise generation can be as strong as the effect of ambient temperature fluctuations, which is widely acknowledged in SHM research. Therefore, in real-world applications where the loading conditions cannot be controlled or monitored, for example due to environmental or operational conditions, the effect of possible stress fluctuations on the detection of structural damage with Lamb waves has to be considered and incorporated into the operation or development of SHM systems.

Chapter 6

In this chapter, a new method for the determination of the third-order elastic constants of an isotropic material was developed and demonstrated for a particular specimen made of Aluminium. The method is based on the simultaneous measurements of the changes in the wave speeds of Rayleigh and bulk waves propagating in a pre-stressed sample. The main advantage of the proposed method is a radical improvement in the accuracy of the evaluation of

the third-order elastic constants. Specifically, the new method leads to a significant increase in the accuracy of the determination of one of the Murnaghan's constants, *l*, in comparison with the standard techniques, which normally rely solely on the measurements of the change in the bulk wave speeds. As mentioned in chapter 1, the evaluation of third-order elastic constants has recently received a great deal of attention in the context of the monitoring of early damage, specifically fatigue damage. The developed method can be readily implemented to measure the change in the magnitude of the third-order elastic constants, which is related to the state of fatigue damage.

7.2 Future Work

Based on the high sensitivity of the wave speed to applied stress, along with the excellent ability of Lamb waves to propagate over large distances without decay, the theoretical equations obtained in the current work can form a foundation for the development of practical techniques to measure the stress conditions in plate- or shell-like structures. Similar analytical equations can also be derived for other simple geometries such as pipes and circular rods. In the latter case, the guided wave modes are described by the Pochhammer-Chree equations. However, for more complex waveguides such as rail-tracks or I-beams, the use of numerical tools, including Finite Element modelling, will be required. In this case, the theoretical equations developed can serve as a benchmark for the validation of numerical schemes and computational studies.

One of the promising aspects of potential stress monitoring techniques based on the theory of acoustoelasticity, specifically in the case of guided waves, is a possibility to distinguish between residual (built-in) and applied stresses. This is possible because the characteristic length of the residual stress, which is normally related to the characteristic size of the cross-sectional area, is much smaller than the propagation distances of guided waves. Therefore, the influence of the residual stress on the wave propagation is likely to decay with distance due to the self-equilibrating nature (no bulk stress) of the residual stress.

On the other hand, one of the main challenges associated with acoustoelastic based stress measurement techniques is that the correlation between wave velocity and applied stress needs to be established experimentally first before the level of stress in a structure can be evaluated. This means that prior access to a sample of the same material as that of the structure is required, but this may not always be possible in practical situations. Thus, the development of measurement techniques which can provide an estimation of the absolute stress without the need for calibration would be advantageous.

Another challenge associated with acoustoelastic based stress measurement techniques is that real-world structures are often subjected to changes in environmental conditions such as temperature. Both applied loading and temperature fluctuations lead to changes in the wave velocity and therefore, acoustoelastic based techniques will require different strategies to be devised in order to separate the two effects and compensate for the temperature induced variation in the wave velocity. The development of such strategies will be crucial in the future implementation of acoustoelastic based stress measurement techniques.

The theoretical framework and outcomes obtained in the current work can also be applied to improve the operation of existing and future damage detection systems, as illustrated in chapter 5 of this thesis. However, a much bigger challenge will be the incorporation of stress and damage monitoring capabilities within the same network of sensors. This could lead to the development of a new generation of SHM technologies and more accurate structural life forecasting methods. These methods are very attractive for many engineering applications; however, the development of such methods will require significant research effort in the future.

The large acoustoelastic effect investigated in chapter 4 has potential applications in the ultrasonic guided wave imaging of soft biological tissues and rubber-like materials. The presented results can also be easily generalised, for example, to torsional or interfacial waves, thus providing a new way to characterise the material properties of such materials and identify damaged

tissues. Although the developed framework can be extended to compressible materials, the lack of fourth-order elastic constants coupled with the low elastic strain limit of ordinary stiff materials makes this option less attractive.

Finally, the theoretical results obtained form a foundation for the development of new experimental techniques for the evaluation of third-order elastic constants. These techniques can make use of the non-linear characteristic equations for Rayleigh and Lamb waves and can be potentially applied to non-homogeneous materials, the properties of which could be different due to fabrication processes or accumulated mechanical damage. An example of such a technique was presented in the current thesis in chapter 6.